

Hindcast of the wave climate in Öresund

- *Modeling of wave climate over 50 years using WAM with wind measurements input.*

Sara Schömer Ericsson

Laury Renac



Hindcast of the wave climate in Öresund

- *Modeling of wave climate over 50 years using WAM with wind measurements input.*

Sara Schömer Ericsson

Laury Renac

Acknowledgements

A thanks to DHI and the Engineering Geology Department at Lund University for providing us useful and needed wave data. Without SMHI's public accessible data about wind, it would have been more complicated to get hold on data and perform this thesis work.

We also would like to thank Robert Willander for his invaluable help and tips in regards to the WAM-model. A special thanks to Jonas Lindemann at LUNARC who has been of great help adapting and modifying the code of WAM model, transforming it into a more modern and usable version.

A great thanks to our examiner Magnus Larson who has always been there when guidance was needed. And finally we would like to thank Hans Hanson our supervisor at LTH and Sebastian Irminger Street at SWECO for their help, advice and counsel at all time.

Abstract

Öresund is a very dynamic economic area with numerous projects, there is a great need of a deeper understanding of the wave climate. The wave measurements currently available are scarce and they do not cover the whole area. For this reason, a modeled wave climate would be of interest and the results could be a starting point for different in depth analysis.

The objective of this study was to produce a wave climate over Öresund. The period considered was from 1961 to 2011, such a long period was chosen to be able to have reliable statistics on waves that can be expected at different locations in Öresund.

In order to produce the wave climates the WAM model was used with wind measurements from meteorological stations as an input. Once produced, the results of WAM were compared to actual wave measurements from Öresund to validate the model and parameters used. The conclusion of the validation was that the model has a good global estimation but tends to overestimate smaller waves.

The results showed that the significant wave height were in average around 0.5 m for coastal locations and presented a maximum of 2.5 m. The monthly averages of significant wave height were slightly lower during summer months in comparison to the winter ones. The same pattern is seen with the mean period of the waves.

The study of the return period lead to the conclusion that for most coastal locations a 1 year wave had a significant wave height of 1.3 m and a 50 years wave presented a H_s of 2.3 m. Also, a 2 m H_s wave had a return period of 10 years.

Monthly average run-up levels ranged from 0.15 to 0.62 m. A drop can be noticed in April and May, this due to the fairly low H_s and water levels during period. The direction of wave propagation also seem to be of importance in this process, during April south-eastern direction were stronger and lead to low run-up heights. The 10 year run-up were between 2 and 2.8 m (depending on the location), and the 1 year were between 1.4 and 1.8 m (respectively for Falsterbo and Landskrona).

In this study, the potential sediment transport along the Swedish coast was calculated and lead to the identification of potential accumulation and erosion areas. The potential areas of accumulation were located south of Helsingborg, in the center of Lundåkra bay and Lomma bay, at the horn of the bay outside of Vellinge and North of Falsterbo. Erosion could occur outside of Landskrona and Barsebäck, at a location situated between Malmö and Vellinge and in the bay of Höllviken.

A hypothetical scenario of climate change was tested in order to evaluate the impact of such a change on the wave climate of Öresund. The conclusion concerned more the behavior of the response than the actual values obtained. The wave climate in the region seemed to be more sensitive to a change in wind speed rather than wind direction, this could be due to the already limited fetch length in the strait. The wind direction affected the results as well but was more of an aggravating factor when coupled with a wind speed change.

Hindcasting wave climate is useful for many different applications, this thesis only explored some of the coastal processes. The results from it could give an indication about how the waves in the strait behave.

Acknowledgements	3
Abstract	5
1 Introduction.....	1
1.1 Background.....	1
1.2 Objective.....	1
1.3 Limitations.....	2
1.3.1 Project limitations	2
1.3.2 Other models.....	2
2 The Strait of Öresund	4
2.1 Geography	4
2.2 Bathymetry.....	5
2.3 Waves	5
2.4 Mean currents and stratification.....	5
2.5 Water level	6
2.6 Sediment transport	6
2.7 Wind	6
3 Numerical wave modeling.....	7
4 WAM model.....	9
5 Wind data	10
5.1 Analysis of the data	10
5.2 Area of influence	13
6 Sensitivity analysis.....	14
6.1 Time step.....	14
6.2 Wind speed.....	17
6.3 Strait of Helsingborg and Helsingör.....	20
6.4 Exclusion of Kattegat	21
6.5 Comparative results between Coarse grid, Fine grid and Measurements.....	23
6.5.1 Engineering Geology Department data vs WAM	23
6.5.2 Storm conditions test	24
7 Calibration and Validation	26
7.1 Bottom friction	26
7.2 Wind	27
7.2.1 Setup 1, 2 and 3.....	27
7.2.2 Helsingborg alone.....	27
7.2.3 Malmö and Helsingborg	27
7.2.4 Pre-modification of wind from Falsterbo.....	27

8 Results	30
8.1 Wave height and direction	30
8.2 Monthly averages	34
8.3 Run-up levels	35
8.3.1 Method	35
8.3.2 Results	36
8.4 Sediment transport	39
8.4.1 Method	39
8.4.2 Results	40
8.5 Climate change	42
8.5.1 Input	42
8.5.2 Results	44
9 Discussion and Conclusion	52
Reference list.....	I
Publications	I
Electronic sources.....	II
Appendix.....	I
Strait opening test	I
Calibration	II
Wave roses	V
Return period diagrams.....	VII
Potential sediment transport roses.....	IX
MatLab code:.....	XII
height_extract	XII
direction_extract	XIII
extract.....	XIV
direction_height_movie	XVIII
Fill_in	XIX
fort_extract.....	XX
run_up	XXIII
nearshore	XXV

1 Introduction

1.1 Background

In an engineering project a great concern has to be put on security and planning for different extreme scenarios that could damage structures or have an impact on the area. But also determining the everyday wear that the structures have to withstand.

A key part of coastal engineering is to predict the kind of waves that can be expected both for normal and extreme conditions.

Another aspect to consider when planning structures in coastal areas is erosion, specifically sediment transport, a process highly dependent on the wave climate. This has to be considered in everything from the stability of bridge foundations and choosing suitable location for building houses to planning of harbors.

It is usually difficult to find measurements with enough samples to be considered as a reliable source for planning. Thus engineers often use models to hindcast the wave climate produced by the wind, which is the only solution when no measurements are available. This method produces a reliable estimate of the wave climate in the area and a return period diagram for the waves.

Öresund is a key zone not only for Sweden and Denmark but also a strategic point between Scandinavia and the rest of Europe. Thus it is an extremely dynamic area both in terms of economical exchange and number of projects.

In Öresund there have been some measurements of wave from at least three locations during the 1980s-1990s, 1992-2000 and during the 2010s. The two first data sets only show significant wave height, i.e. the wave height representing the top one third highest waves, and the third include more information such as direction and period of the waves. These sets of data are indeed valuable, but they do not cover the whole area of Öresund and are only representing a short time period compared to the wind data available. If hindcasting with wind data over a 50 year period a more extensive analysis and a greater insight of the wave climate could be obtained.

This study of the wave climate in Öresund was performed to resolve this lack of data and with it gain more extensive insight in the wave climate.

1.2 Objective

The main aim of this thesis is to analyze the wave climate of Öresund by hindcasting waves over a period of 50 years, from 1961 to 2011. This has been done by using wind measurements from different meteorological stations along the Swedish coast as an input for the WAM model.

The secondary objective is to use the hindcasted wave climate for statistical analysis of the waves such as mean or maximum values, return period diagram for the significant wave height, the direction and the mean and peak period of the waves.

The data will also be used to examine coastal processes along the Swedish coast. Run-up height will be calculated and used to produce run-up levels at specific locations where water levels data are available or can be extrapolated. And a schematic overview of the potential sediment transport will be created.

Finally, a hypothetical scenario of climate change will be simulated in order to test how sensitive the wave climate is to changes in wind speeds and directions.

1.3 Limitations

1.3.1 Project limitations

In order to be able to complete the project, some limitations had to be set.

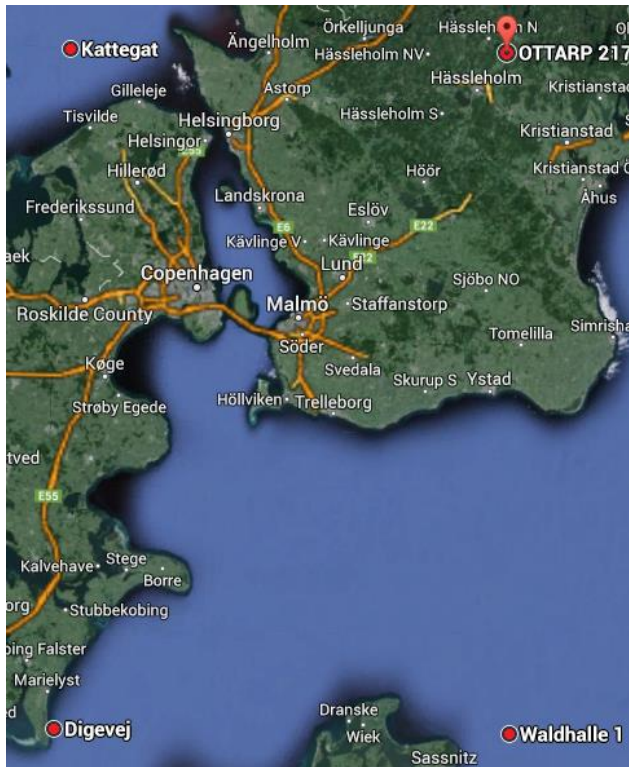


Figure 1. Area modeled delimited by the red dots.

One such limitation is the size and location of the grid. Increasing the size of the grid has a great impact on the computation time thus an optimum size/precision had to be found and the area modeled was set as shown in Figure 1. This area does not include Kattegat, which could have an effect on the waves coming in from the North and would mainly affect the area of Helsingborg/Helsingör. The influence of the exclusion will be discussed in Chapter 6.4.

The cell size used for the grid could also be a limiting factor for the precision of the model: the finer the grid the more accurate the model will be. But as in all modeling it might not benefit the result to have a very fine resolution since a trade of in the computation time, and finer grid does not always transfer into a great improvement of the results. This will be discussed in depth in Chapter 6.5.

The wind measurements used are from the time period of 1961 to 2011. During this period there are several gaps in the data. Missing wind data had to be extrapolated and this process will be explained in depth in Chapter 5. Due to these gaps the precision might be imperfect, but since the missing data only makes up a rather small part of the entire data set the effect can be considered negligible.

This study uses two stations located along the Swedish coast line. It would have been ideal to have more stations and data from the Danish coast to create a more accurate evaluation. Since the strait of Öresund is rather narrow and the total area included in the study is small the accuracy gain from including more stations might not be significant.

For this project ice coverage has been excluded, this is due to that all potential waves should be included and not be dampened by the ice. The ice would most likely have a negative effect on the evaluation of extreme events.

1.3.2 Other models

A few different models could have been used for this study, but only public models were considered as an alternative. Thus models such as Mike21, Delft or Telemac were disregarded.

SWAN is a third generation coastal wave modeling software (Link 1, 2014). It used to be specialized in the modeling of shallow water waves and breaking conditions. In this study, the focus was on a global wave climate of Öresund, not just on shore conditions. Due to these reasons, SWAN was

considered not as good as WAM for the study and thus was not chosen. Though, SWAN was considered as a possible solution for a more in depth analysis of the results. The output from WAM can be used as an input for SWAN to perform nested runs and get precise results for chosen coastal areas. However the use of SWAN for this type of analysis would have exceeded the time limit of the project. Instead, direct calculations for specific locations were performed since proofs were provided that these calculations would produce acceptable results (Larson et al., 2011).

WAVEWATCH III is also a third generation wave model. But it is mainly used for open seas conditions and oceanic wave modeling. In the past it has performed well on open water but not as good with shallow water conditions and with finer grid resolution. Öresund is a zone of mixed conditions of depth and fetch length, which makes WAVEWATCH III not optimal for this area (Link 2, 2014).

2 The Strait of Öresund

2.1 Geography

The strait of Öresund connects the Baltic Sea and the Atlantic Ocean. It also separates Denmark (isle of Zealand) from Sweden (region of Skåne).



Figure 2. The strait of Öresund.

The southernmost limit of the strait is Falsterbo (Sweden) / Stevns Klint (Denmark) and Kullen (Sweden) / Gilleleje (Denmark) is the northernmost limit (see Figure 2).

The two biggest cities of the area are Copenhagen - the capital of Denmark - and Malmö - the third biggest city in Sweden. They are connected by a bridge-tunnel. This bridge is a strategic link for economical exchange between the Scandinavian countries and the rest of Europe.

The economic dynamism of the area has given rise to a high density of structural project that would require wave data and statistics.

2.2 Bathymetry

The bathymetry of the area that will be used has been downloaded from the web site of IOW (Link 4, 2014), the compilation of the measurements was performed by the Leibniz Institute for Baltic Sea Research in Warnemünde.

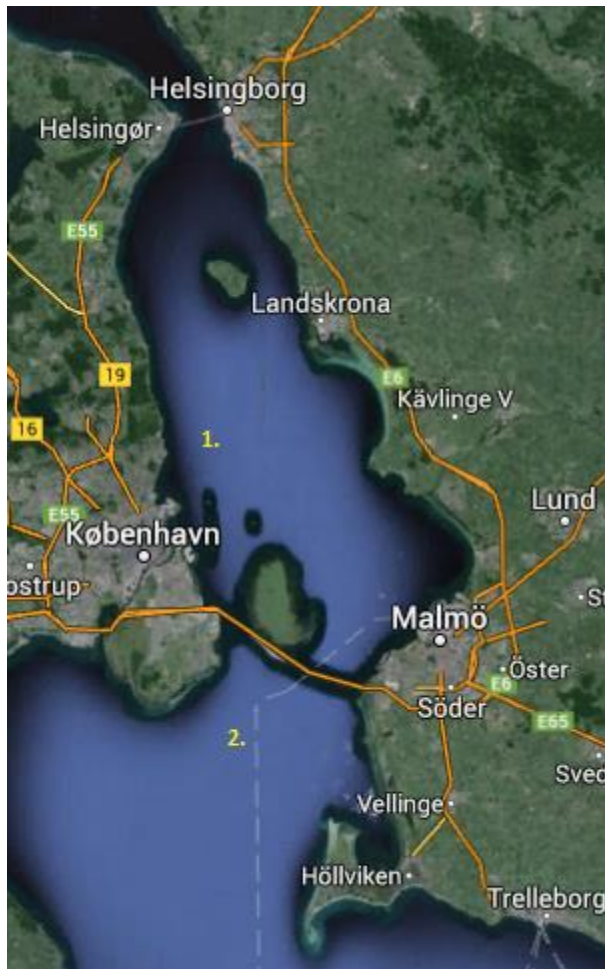


Figure 3. Map of the position of output locations used in the sensitivity analysis. Skovshoved is 1. and Drogden 2.

Over the whole calculation area, the maximum water depth is 58 m and the average water depth of sea points is 39 m. Whereas if looking only at the strait of Öresund, the maximum water depth is 36 m and the average water depth of sea points is 10.4 m.

2.3 Waves

Wave data was provided by DHI and the Engineering Geology Department at Lund University. The data from DHI covered the period from November 2013 to February 2014 at Skovshoved (see Figure 3). Wave data from the Geology department spanned from April 1992 to June 2000 and the measurements were made at Drogden, which is located in the waters outside of Copenhagen (See Figure 3). These data were used in this project to calibrate WAM. Several test runs were performed with different values for this parameter and the best fit was selected according to a linear fitting on a scatter plot.

2.4 Mean currents and stratification

The current through the strait is largely affected by the difference of water level between the sea of Kattegat and the area around Bornholm island, it is also, although limited, affected by tidal movements. The dominating direction of the current is towards the north, is partially due to persistent eastwards winds that creates a difference in the water level between the Baltic Sea and Kattegat Sea. The second most important factor for the northern moving current through the strait is the water from the catchment area of the Baltic Sea gives a higher surface level than in Kattegat (COWI/DHI/LIC, 1990). Reversed, southern current occurs when there is a low pressure in the west, Kattegat, and a parallel high pressure around the island of Bornholm, meaning that the water level in Kattegat is higher than in the Baltic Sea. Thus persistent westward winds subsequently means that colder and more saline, and thus higher density, water is pushed into the Baltic Sea (SMHI, 2014). This is an important factor for the increase of oxygen concentration in the deeper parts of the Baltic Sea (Den svenska Öresundsdelegationen, 1987). This is of significant value for the biota, for instance

for the cod, an economically important fish for the region (Den svenska Öresundsdelegationen 1987), which lay their eggs at depths with specific salinity concentration (Miljöförvaltningen Landskrona kommun / Toxicon AB, 1998).

2.5 Water level

The water-levels in Öresund are depending on wind blowing in the area, air pressure but also on the water exchange between Kattegat and the Baltic Sea (see Chapter 2.5). Calculating wave heights and run-up levels one can encounter any kind of combination e.g. large wave height and low water-level or the opposite. Though, south of the bridge (which is built on a natural threshold) a general tendency can be noticed: high wave heights are often associated with low water levels. In depth information about water-levels and run-ups will be discussed in Chapter 8.3.

2.6 Sediment transport

Different hydrodynamic processes affect the sediment transport in coastal areas. Wind generated waves, surges and wind driven currents all affect sediment transport in coastal areas. Wind is the driving force of these phenomenon and they were thus dependent on the direction (i.e. fetch length) and speed of the wind, i.e. how much energy have been transferred from the air to the water (CEM, 2006).

As the wave moves towards the shore the entry angle will be changed due to refraction as the water becomes shallower. The refraction when the wave crosses the bottom contours is caused by dissimilarity in water depth along the crest of the wave, the effect is a difference of wave speed. This affects the sediment transport rate since it causes the wave energy to diminish (Komar, 1998).

The net direction of the current, i.e. mean flux of the water, can vary from perpendicular to parallel but can also be a mixture of those two. For sediment transport in coastal areas an important type of current is undertow, which acts perpendicular to the shore. While the breaking of waves in the surf zone contributes to the suspension of sediment, the undertow contributes to the process of redistributing suspended sediment by transporting it outward from the shore (Komar, 1998), which is seen as a cross-shore sediment transport process. When the entrance angle of the wave diverge significantly from 90° it will generate a more prominent alongshore current and with that sediment transport along the shore. If the entrance angle is close to 90° the waves will give rise to a combination of alongshore and cross-shore current, i.e. rip current (CEM, 2003).

The suspension and transport of sediment are also dependent on the grain density, volume concentration, angle of repose and fall velocity, although the grain size is commonly the most essential characteristics (CEM, 2002a).

2.7 Wind

Winds over Öresund were studied through data from SMHI (Sveriges Meteorologiska och Hydrologiska Institut) and the stations used in this study were located in Helsingborg, Malmö and Falsterbo. The main directions for the winds blowing over Öresund were found to be from South to West. In the data, these directions alone represent 50% of the values. The average wind speed in Öresund is around 5 m/s and a maximum of 28 m/s was measured in Falsterbo.

More in depth information about the wind data used in the study will be presented in Chapter 5.

3 Numerical wave modeling

The main objective of a model is to give a mathematical description of the world in a simplified way. The wind generated waves are caused by the friction of wind blowing over the water surface. The drag force produced by the wind can be modeled with fairly high accuracy and other processes involved in the wave generation can also be translated into mathematical equations.

In order to use a numerical model of any sort, one must first discretize the area and time studied. Spatially, the modeler has to create a grid, composed of cells. Each cell of the grid represent a part of the total area and inside each cell all the parameters and variables were spatially constant. The discretization of time works the same: the modeler will choose a time step length and all the variable of the system will be considered as constant over one time step. Thanks to this method, a computer can handle the calculation for each cell and time. Moving from one cell to another and from a time step to the next, the variables for the whole area and time period will be calculated.

The basis of wave modeling is the wave energy spectrum introduced by Pierson in 1957. From this spectrum one can extract numerous information about the wave, e.g. significant wave height, wavelength, period...etc.

The energy spectrum represents the amount of energy in a wave depending on its frequency and direction. Thanks to the spectrum, one can determine of which frequencies and directions of propagation for the waves contain the highest energy (CEM, 2002b).

Since frequency and period were inversed proportional, it is easy to deduce the dominant period from the spectrum. Then, the wave height and other interesting output can also be extracted using statistical tools (CEM, 2002b).

Thus, the challenge for the modeler is to describe the evolution of this spectrum by using an equation that can be computed.

The equation below known as the transport equation (TE) comes from the conservations laws applied to wave energy in the ocean and is the main equation of wave models.

$$\frac{\partial F}{\partial t} + \nabla \cdot (C_g F) = S_w + S_f + S_{NL} \tag{1}$$

- F is the two-dimensional ocean wave spectrum with respect to frequency f and direction (measured clockwise relative to true north) at each grid point.

- C_g is the group wave velocity.

- S_w is the wind input source term.

- S_f represents the dissipation of energy by friction.

- S_{NL} represents the nonlinear energy interactions.

Different ways of describing the source/sink terms have been used throughout the years and the differences classify the models into 3 generations of wave models (Gunther et al., 1992).

The interaction term is of great importance, indeed if it didn't exist the waves produced would only be short surface waves. The interaction between waves allows the longer waves to take energy from the short wind waves, this process produces waves with bigger amplitude and wave length.

The older models can produce good local results, but they need tuning of constants in order to compensate for not including an explicit calculation of the non-linear interactions between waves (Hasselmann, 1962). Though significantly better than the previous generation at hindcasting waves, the 3rd generation models are still perfectible. They respond well to a persistent wind input, but in case of highly changing winds the results are deviating from measurements (Van Vledder and Holthuijsen, 1993, WMO, 1995). Thus further research and improvements are still to be done to consider these models good for all potential conditions (WMO, 1995).

4 WAM model

In the late 80's, oldest version of WAM model was developed and was the first to be considered as a third generation model. It has been used successfully for both hindcasting, using wind measurements; and forecasting, using meteorological models to estimate wind conditions (Arduin et al., 1999).

WAM uses a 2 dimensional wave energy spectrum and, as most of the models, it is based on the Transport Equation to predict the evolution of the spectrum. It is a third generation model, which means that the nonlinear energy interactions source/sink term (S_{nl}) is explicitly calculated.

An in depth description of the model governing equations will not be presented here, but can be found in the paper written by WAMDI Group (1988).

A few parameters need to be set in the model, such as the number of bins, the spatial grid or the time step.

The number of directional bins (respectively frequency bins) define the number of possible directions of propagation (respectively frequencies) for the waves in the model. This discretization is then used by WAM to generate the energy density spectrum. The more bins, the more precise the model will be, but on the other hand, the calculation time will increase as well.

As mentioned in Chapter 3, a spatial and a time discretization were needed. Here again the precision of the grid influence the calculation speed and one must know that to avoid stability problems during the computation, the time step has to be adapted to the spatial grid set up e.g. if a 0.05×0.05 degrees (given as decimal degrees) is used for the grid cell size, the time step must be lower than 180 second. A change in the grid cell size can lead to a much greater change in the computational time: if one divides by a factor of 2 the cell size, the time step must be divided as well and the final calculation time can be multiplied by a factor of 12.

5 Wind data

5.1 Analysis of the data

To produce a wave climate with WAM, wind data must be supplied. Two main possibilities can be considered for the input: the output of a meteorological model, or meteorological stations measurements.

In this thesis the input for wind and direction were from meteorological observations stations. This decision was based on that the amount of data available for the area were sufficient for generating reasonable results. The other possible approach using wind models was tested by Arduina et. al. (2007) and was considered a less accurate representation with respect to real wind data. Blomgren, et al. (2001), and Iriminger-Street (2011) both showed that the wave climate can be modeled with accuracy by using wind measurements.

For this study, wind data from meteorological stations in Falsterbo, Helsingborg and Malmö were considered.

The data materials were missing some periods. Compensating for shorter periods, e.g. one day, an average was taken from the closest available data for that location. This kind of missing value was the most common and was due to the lack of human resources in the early days of measurements; they often occurred during nights. Thus these gaps are not influencing significantly the precision of the model in a negative way. In some isolated cases, longer periods were missing, e.g. varying from several days to, in rare cases, months. The assumption was made that the other stations were the most accurate representation over that period. That might not be completely true since it frequently happens that wind speed and direction differs significantly between the locations of the measuring stations. This assumption could be seen as especially misleading for storms, thus generating waves in the model that would not be similar to the reality but were still considered to be precise estimations. No storms seems to have occurred during those periods thus even if some values are faulty, they will not influence the quality of the results.

The majority of the data material is reasonably intact and there were plenty of storms to provide reasonable representation, in the model, for what waves can be expected during these situations.

Although wind data were available from an observation station in Malmö, they were disregarded since there were several long periods with missing data. The data from Falsterbo were considered to be reasonable representation for the area, this partially because of how close they were located. But also due to that Falsterbo is located on a small peninsula and the Malmö location is more sheltered in comparison. Wind data from Germany and Denmark were available but not for the whole simulation period and was thus excluded.

Data used for the study are presented in the following graphs and charts (see Table 1 and Figure 4 to Figure 6).

Table 1. Wind statistics for Helsingborg and Falsterbo.

Station name	Max speed (m/s)	Mean speed (m/s)	Number of available measurements	Extrapolated values	Total number of values
--------------	-----------------	------------------	----------------------------------	---------------------	------------------------

Helsingborg	26	4,14	106155	42860	149015
Falsterbo	28	6,61	138970	10045	149015

From Table 1 and Figure 4 it can be seen that the wind distribution was similar for Falsterbo and Helsingborg. The extrapolation of the values in Table 1 is described above.

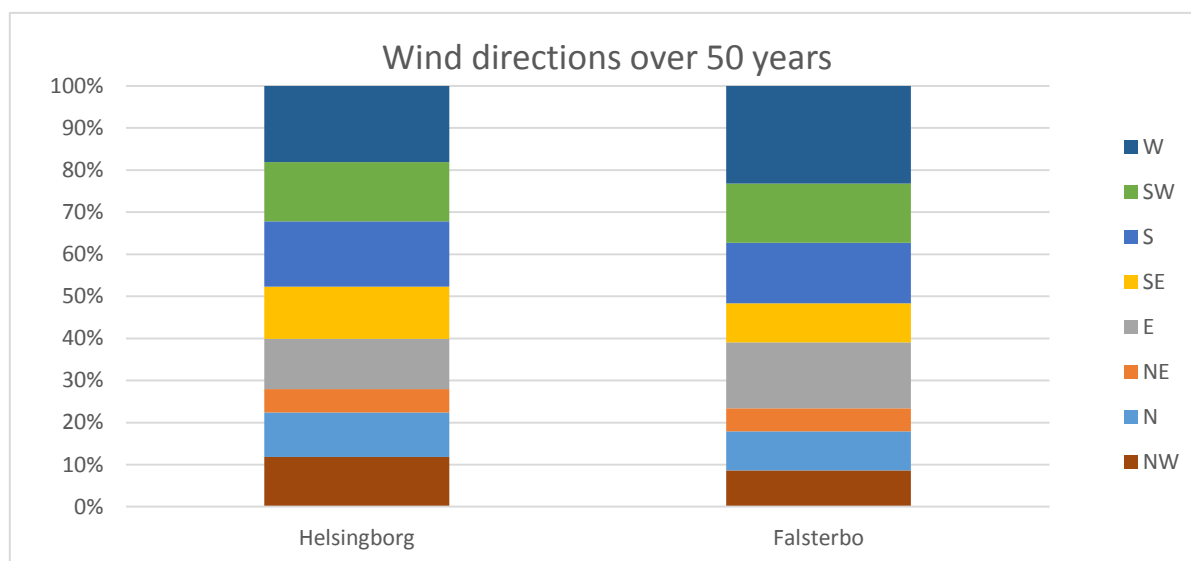


Figure 4. Wind direction distribution for Helsingborg and Falsterbo.

If the wind direction were equally distributed, south, south west and west directions would represent 37.5% of the observed values instead they represent approximately 50%, which can be seen in Figure 4. The main wind directions were South to West.

The mean wind speed for Helsingborg and Falsterbo were respectively 4.14 and 6.61 m/s, while maximum wind speed were 26 and 28 m/s (Table 1). The higher values for Falsterbo could be due to the more exposed location of the meteorological station and the difference in wind characteristic; the wind is mostly coming from west to south, directions where Falsterbo is exposed to open sea.

Figure 5 shows the average wind speed for each different direction. It can be concluded from Figure 4 and Figure 5, that the wind directions were mainly from the West/South-West but also the winds from these directions were stronger on average.

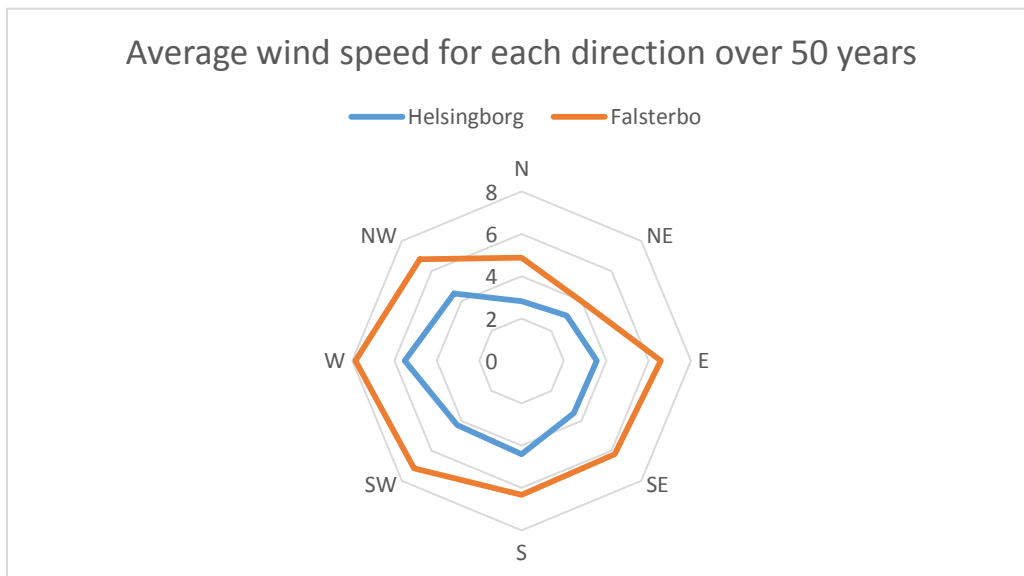


Figure 5. Average mean speed (m/s) per direction for Helsingborg and Falsterbo.

Figure 6 presents wind roses for Falsterbo and Helsingborg. It shows the percentage of winds per direction and for each direction the percentage of winds being below a certain wind speed. As seen in Figure 4 and Figure 5, the west direction is the most represented and the one containing the strongest winds. This is also confirmed by Figure 7 where the strongest are shown alone.

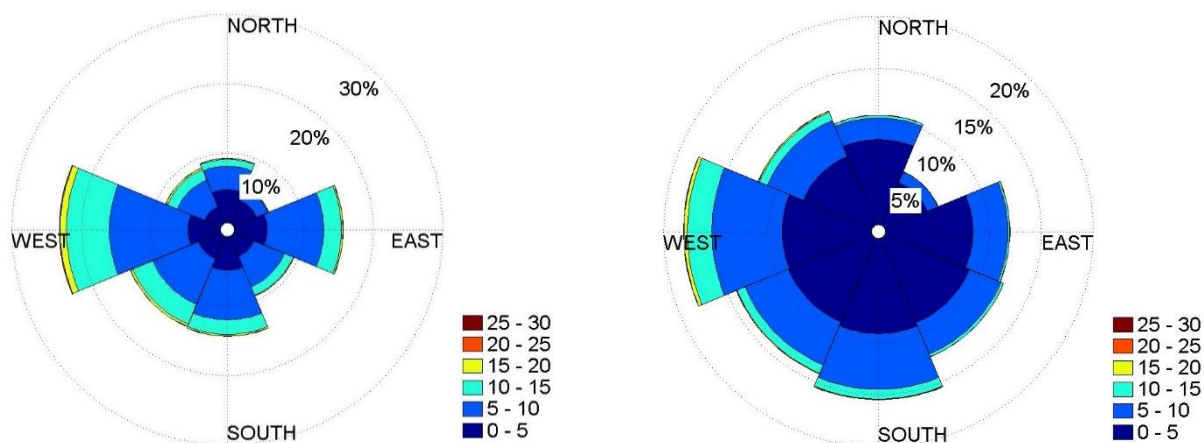


Figure 6. Wind roses over 50 years (1961 to 2011) in Falsterbo (left) and Helsingborg (right). The scale is in m/s.

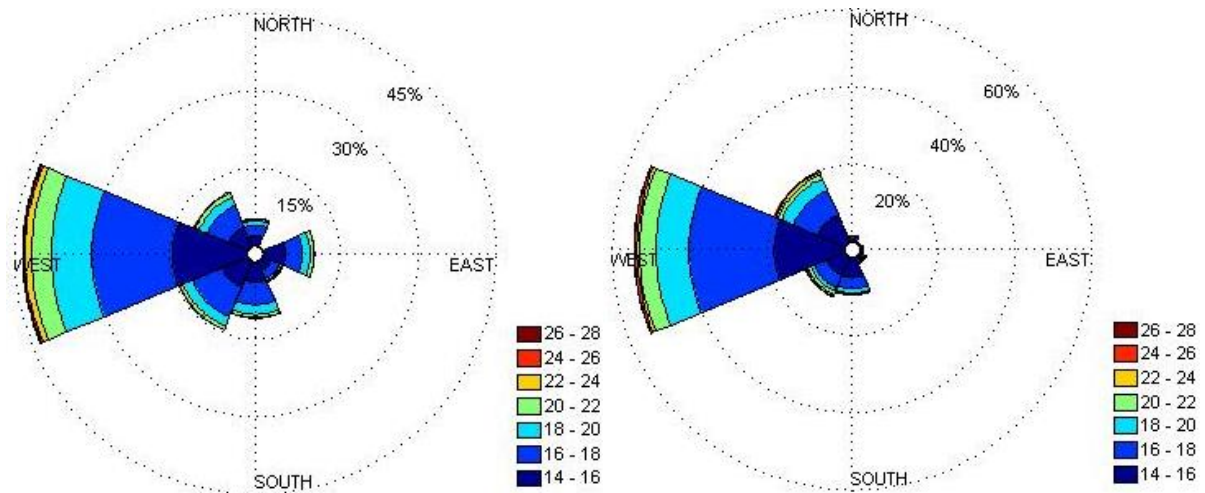


Figure 7. Wind roses over 50 years (1961 to 2011) in Falsterbo (left) and Helsingborg (right), including only winds over 15m/s. The scale is in m/s.

To be used as an input for WAM the wind data must be modified. A few different setups were possible and described in CEM (2006) and by Irmingier-Street (2011). Based on this study and because the studied areas were very similar, it was tested and concluded that the best option for this modeling was to use the setup that includes a logarithmic growth of the wind, referred to as setup 3 in Irmingier-Street (2011). This setup modifies the wind speed with a logarithmic relation: each wind speed is increased in respect to this relation. The modification is necessary because of the difference between the wind speed measured and the actual wind speed blowing over the water surface, i.e. to compensate for the height at which the measurements are taken.

5.2 Area of influence

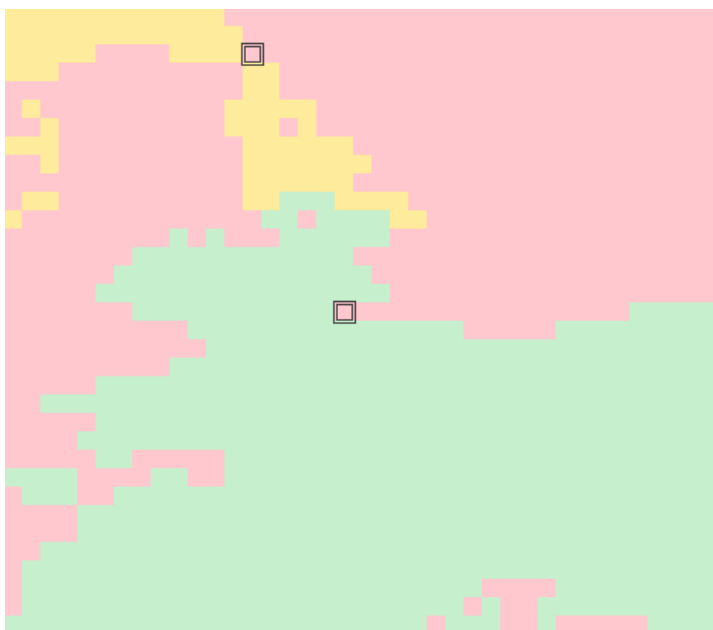


Figure 8. Area of influence used.

The area of influence for the two meteorological stations, Helsingborg and Falsterbo, was determined by taking the midpoint between them in the strait and assigning the northern part to Helsingborg and the southern part to Falsterbo. The Figure 8 presents the area of influence.

6 Sensitivity analysis

In this Chapter the sensitivity of the WAM model was tested, these tests were made in order to gain knowledge of how the model responds to various changes in models parameters and or set ups. The tests performed were in regards of calculation time step, wind speed, the grid response at the strait of Helsingborg and Helsingör, the effect of Kattegat and lastly the a side by side comparison between a coarse and fin grid. For all tests the cells in the grid used for the runs were set to 0.050 degrees. Four different locations in the strait was selected in order to get a good representation of how the changes tested effects the strait. The locations were Helsingborg, Copenhagen, Malmö and the southern midpoint of Öresund (see Figure 9).

6.1 Time step

The sensitivity of the model in respect to the calculation time step was tested by performing and comparing three runs with three different time steps (respectively 60, 120 and 180 seconds). The results were extracted from four locations corresponding to Helsingborg, Copenhagen, Malmö and the southern midpoint of Öresund. The simulation was run for one day, during which the wind speed was set to 10 m/s and the wind direction moved from 0 to 315 degrees. The chosen parameters to observe the sensitivity were the direction of propagation of waves and the wave height.

It was observed that the wind direction is not affected significantly by a change in the time step used. And that the direction of propagation of the waves follows the wind direction changes with a latency of a few hours.

The maximum change in wave height due to a time step change is about 2 cm, which is negligible. Though, the wind direction affects the wave height. This is due to the fact that wave height is directly linked to fetch length and that a rotating wind will generates varying fetch length.

The conclusion of this test was that the time step was not a significant factor for the precision of the model. Thus in order to minimize the computational time, a time step of 180 seconds was chosen for this case study. The figures can be found in Appendix.

Figure 9 is depicting the locations used during the sensitivity analysis. Helsingborg is 1, Malmö 2, Copenhagen 3 and Southern midpoint 4. These locations were chosen because of the different conditions they were representing.

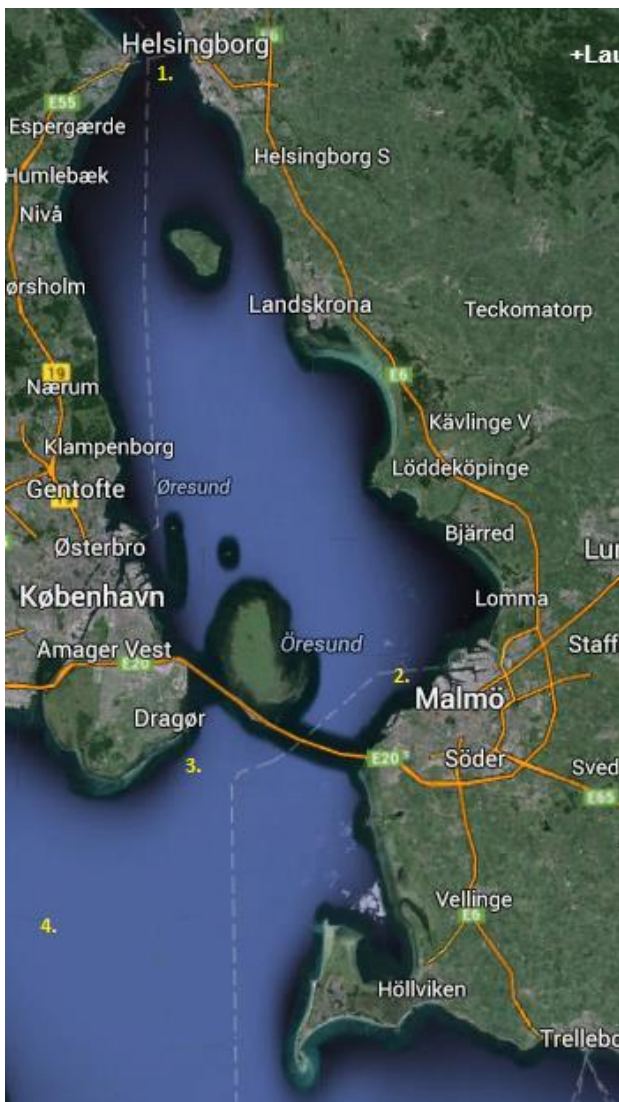


Figure 9. Map of the position of output locations used in the sensitivity analysis. Helsingborg is 1, Malmö 2, Copenhagen 3 and Southern midpoint 4.

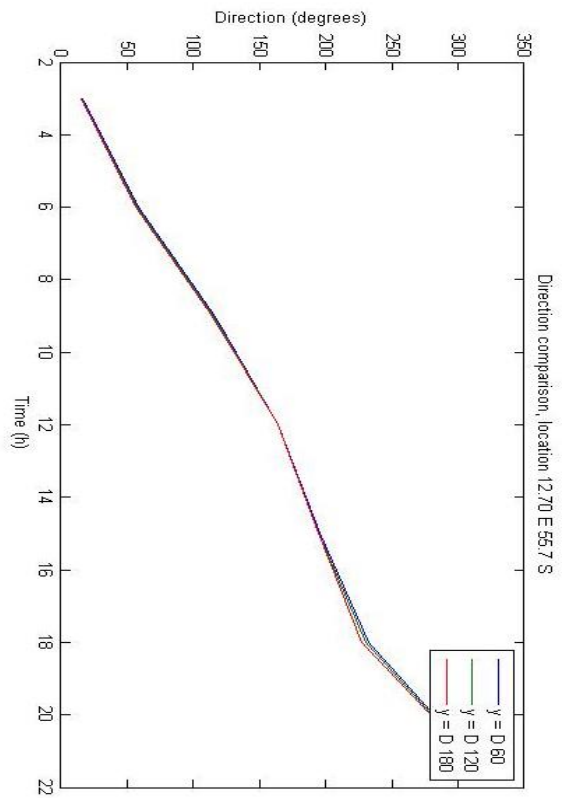
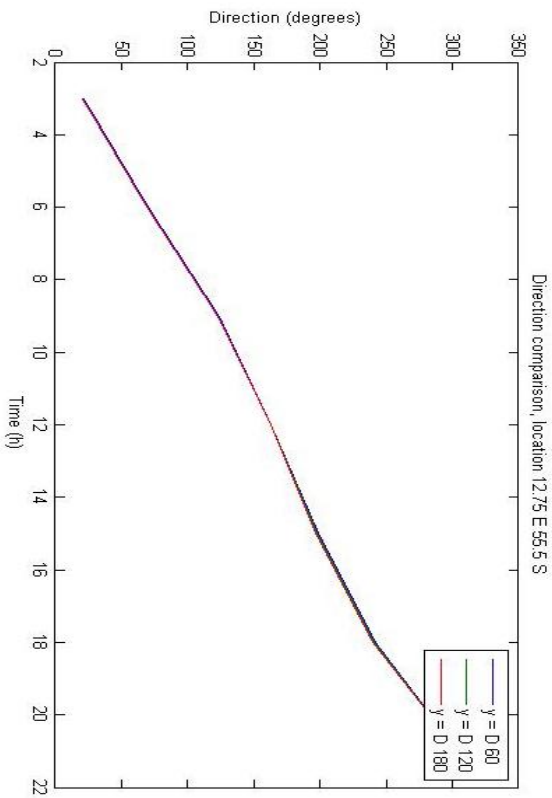
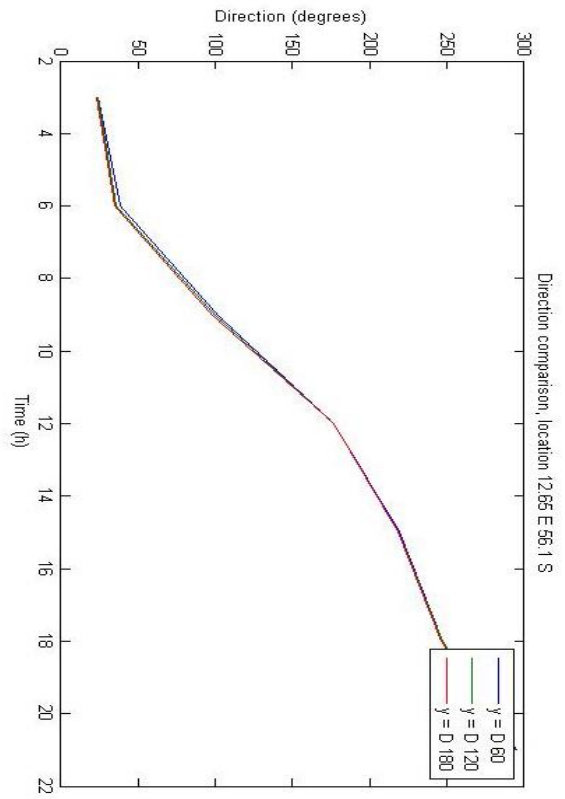
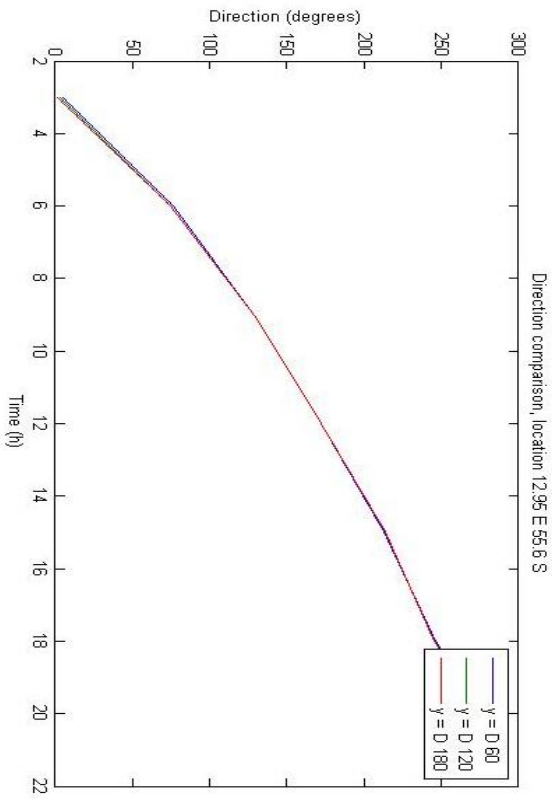


Figure 10. Wave direction of propagation against time for the three different setups. In top right corner: Helsingborg, bottom right: Copenhagen, top left: Malmö, bottom left: Southern midpoint.

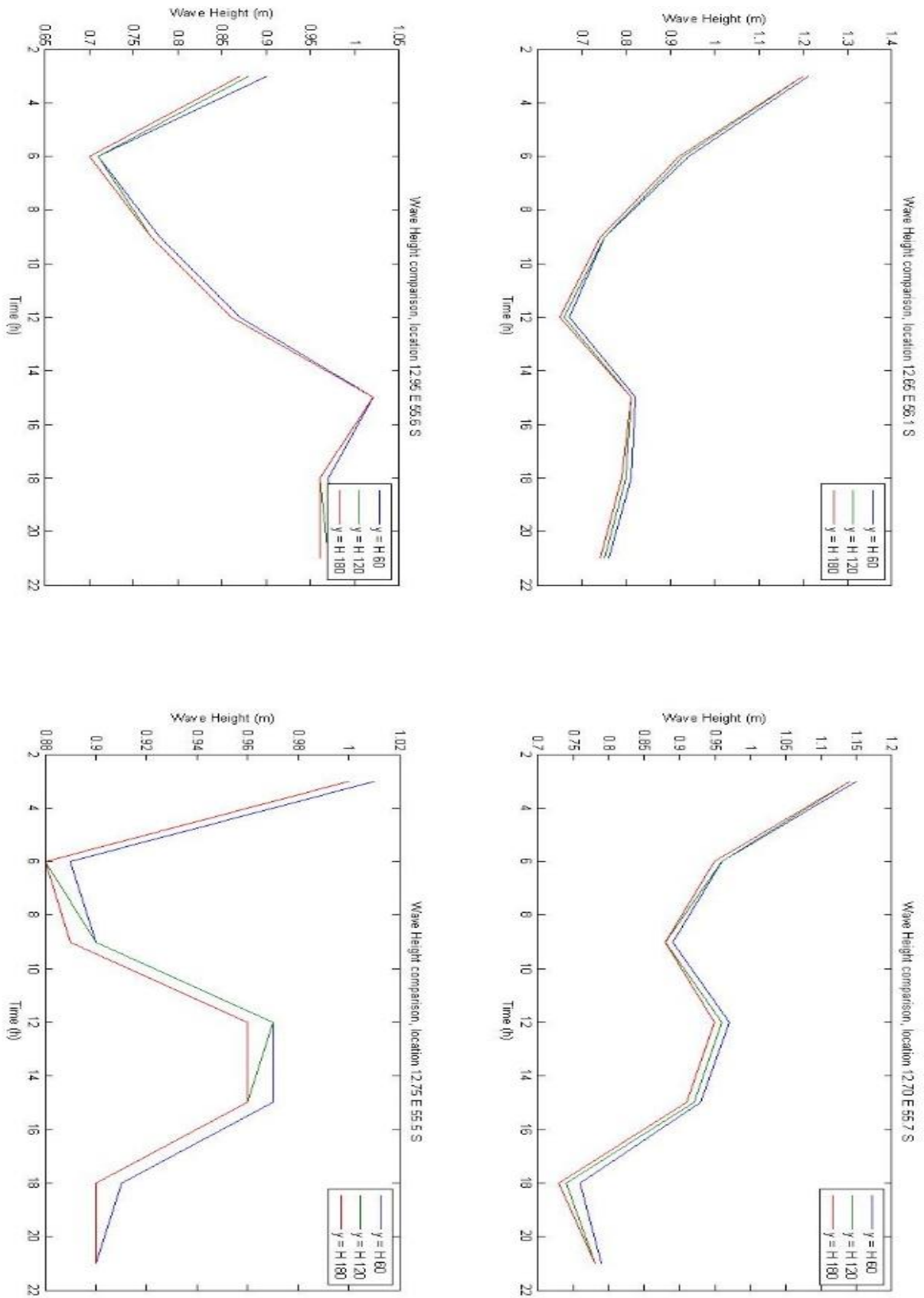


Figure 11. Significant wave height (m) against time for the three different setups. In top right corner: Helsingborg, bottom right: Copenhagen, top left: Malmö, bottom left: Southern midpoint.

6.2 Wind speed

The effect of the wind speed on the wave generation was also studied. A steady wind was used to generate waves until the wave height reached a stable level. Then the final wave heights for different wind speed were plotted. The locations used for this test were Helsingborg, Copenhagen, Malmö and Southern midpoint. Four wind speeds were used: 5, 10, 15 and 20 m/s. And the direction of the wind was South-West, this choice was based on the statistical study of the wind direction: this direction was the most common for the studied region.

The only parameter analyzed here was the final wave height (after stabilization), the wave direction of propagation did not seem to be relevant for this test. The stabilized wave heights were then normalized by dividing with the stabilized wave height at the wind speed 5 m/s, a side by side comparison between the normalized and the non-normalized wave height can be found in Table 2.

The difference in wave height between the four locations was most likely due to the difference in fetch length, e.g. the largest waves were found at the Malmö location, which was the one with the longest fetch length for a wind coming from South-West.

Table 2. Significant wave height as normalized and non-normalized (m) depending on wind speed.

	Helsingborg		Copenhagen		Malmö		Southern midpoint	
Wind speed (m/s)	Normalized	Non-normalized	Normalized	Non-normalized	Normalized	Non-normalized	Normalized	Non-normalized
5	1	0.37	1	0.36	1	0.43	1	0.4
10	1.2973	0.96	1.3611	0.98	1.3837	1.19	1.3	1.04
15	1.6577	1.84	1.8148	1.96	1.814	2.34	1.6833	2.02
20	1.9392	2.87	2.1597	3.11	2.1744	3.74	1.9875	3.18

Table 3. Linear factor of wave heights for the different wind speeds used.

	Helsingborg	Copenhagen	Malmö	Southern midpoint
H10-5	0.118	0.124	0.152	0.128
H15-10	0.176	0.196	0.23	0.196
H20-15	0.206	0.23	0.28	0.232

Table 2 and Table 3 present two ways of analyzing the results from the wind speed test. Table 2 consists of final wave heights for each wind speed normalized in respect to the 5 m/s generated wave height. This ratio was then divided by the ratio of the corresponding wind speeds:

$$R = \frac{H_i/H_5}{U_i/U_5} \quad (2)$$

Values in Table 3 correspond to the linear factors of two consecutive points:

$$R_2 = \frac{H_{i+1} - H_i}{U_{i+1} - U_i} \quad (3)$$

Where H was the wave height after stabilization and U the input wind speed.

These ratios were calculated to compare the influence on the wave height of different increases of the wind speed. In Table 2 and Table 3, it can be seen that the growth of the wave height in respect to wind speed was not linear. The stronger the wind, the greater the increase of the wave height. The growth seems to be exponential:

$$f = a * e^b \quad (4)$$

With $a = 0.31 - 0.37$; $b = 0.56 - 0.58$

These results were indicating that storms conditions can create larger waves than one could have expected from a linear relation (which is the most intuitive relation) between wind speed and wave height. This behavior is confirmed by the results shown in Figure 12. According to SPM this relationship is cubical.

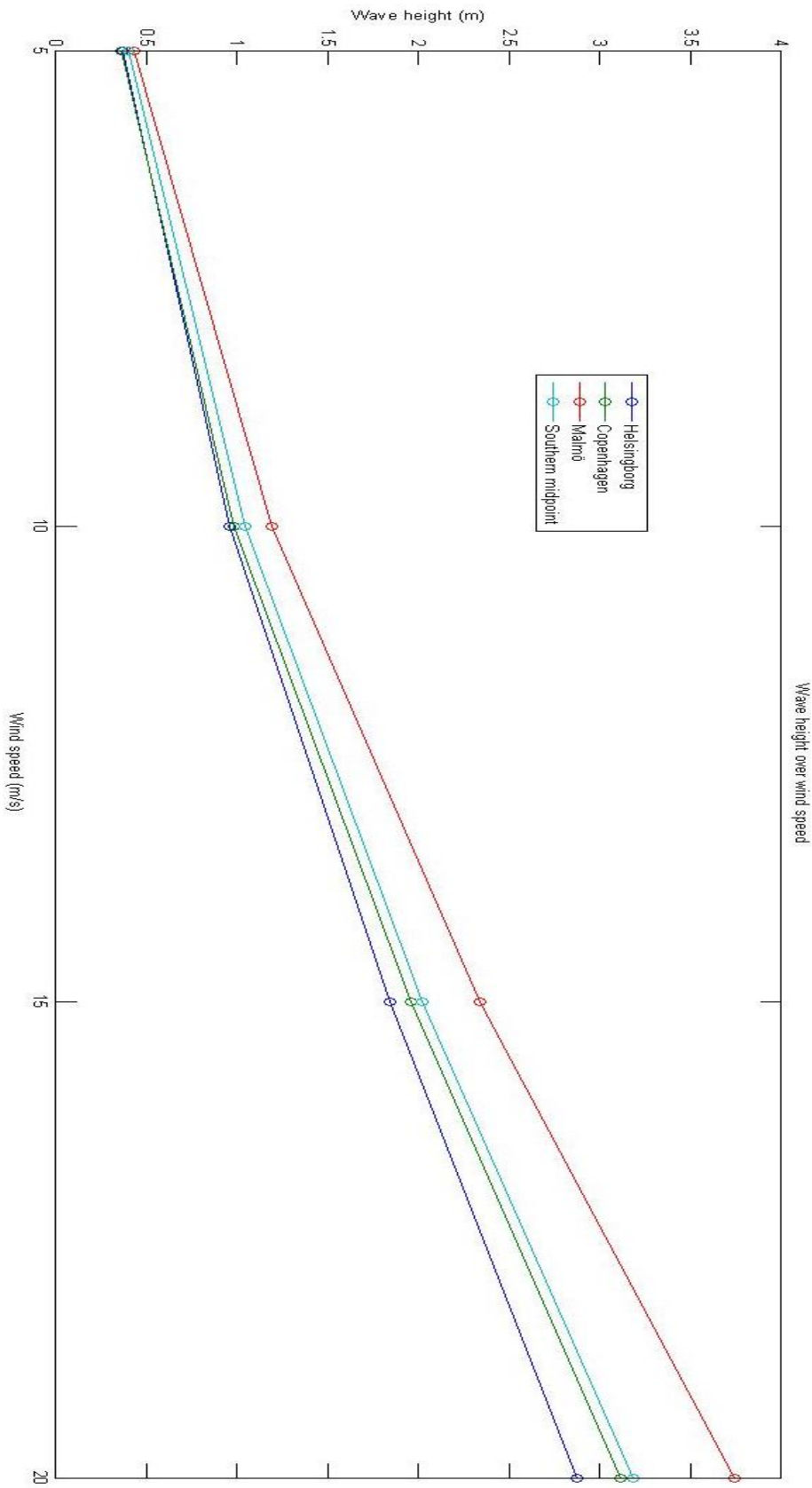


Figure 12. Significant wave height (m) reached for different steady winds.

6.3 Strait of Helsingborg and Helsingör

In figure 8 is presented the grid used for this tests, the pink represent land, the yellow and green represents the sea area set to wind values from the Helsingborg and Faltserbo metrological station, respectively.

The precision of the spatial grid used seems to close the strait between Helsingborg and Helsingör (see Figure 13 for closed condition and Figure 14 for opened). In order to test the influence of an opening of this strait, a run was performed with a modified grid where the Helsingör cell was converted from land into an ocean area. Two main reasons can be linked to a great difference of the wave climates, and they were: waves coming from Kattegat can change the wave climate around Helsingborg; the waves going north were trapped because of the closed strait between Helsingborg and Helsingör.

Figure 15 and Figure 16 show the comparison between wave height and direction respectively, produced by the original grid and modified grid run.

No significant difference can be seen between the results from the two runs. Even if the area outside of the strait was rather small, it was believed that an opening of the strait from a closed state would have produced a larger difference in the results. The R^2 in both Figure 15 and Figure 16 were above 0.95, which indicates that the results were not affected by the opening of the strait. Also, the constant for the linear fitting were both around 0.99 which also gives a strong indication that the results from the non-modified grid were trustworthy.

Results from other location than Helsingborg were analyzed: Copenhagen, Malmö and the Southern midpoint of Öresund. They all gave R^2 value of at least 0.999 and $k = 0.99$, indicating that the opening had no impact at all on the rest of Öresund. The figures used to analyze these locations can be found in the appendix, page II.

Such a small difference was unexpected, since trapped waves should have had a greater influence. A possible explanation for this lack of influence is that the strait was actually opened according to WAM. Probably waves can pass through the touching corners of two cells and the extremely small differences between the two runs seemed to be explicable by the change of one single cell.

A deeper analysis of the code and how WAM handle the equations gave the same conclusions about this problem.

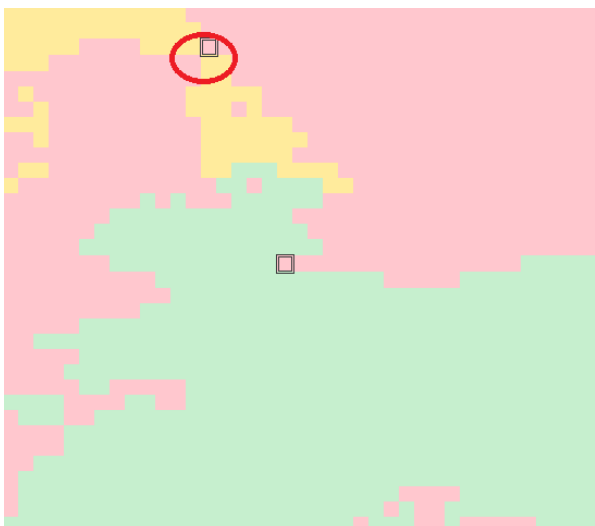


Figure 13. The grid before the opening.

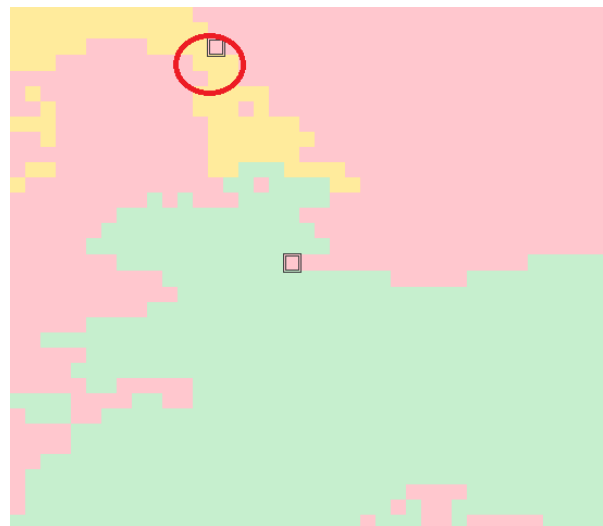


Figure 14. The grid after opening.

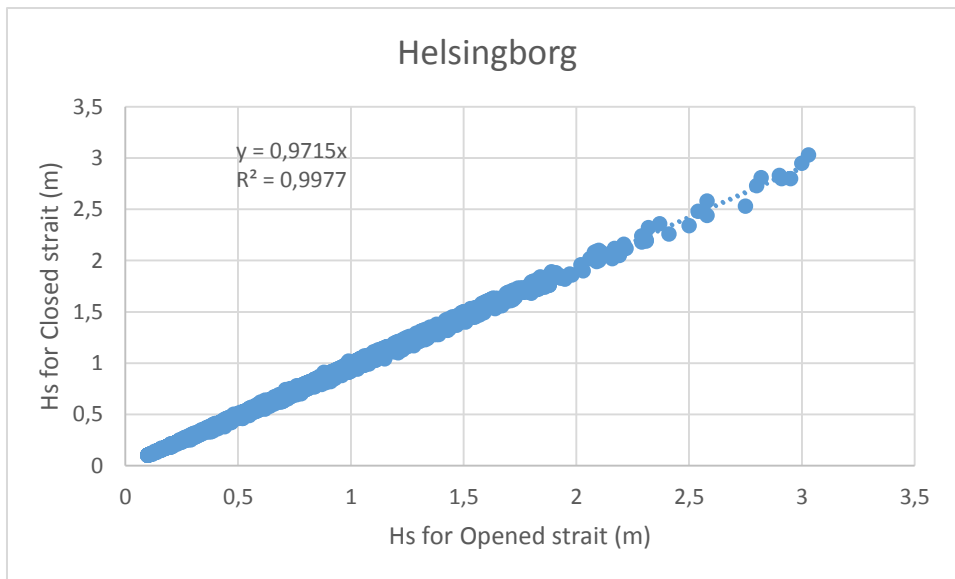


Figure 15. Significant wave height (m) comparison, location Helsingborg.

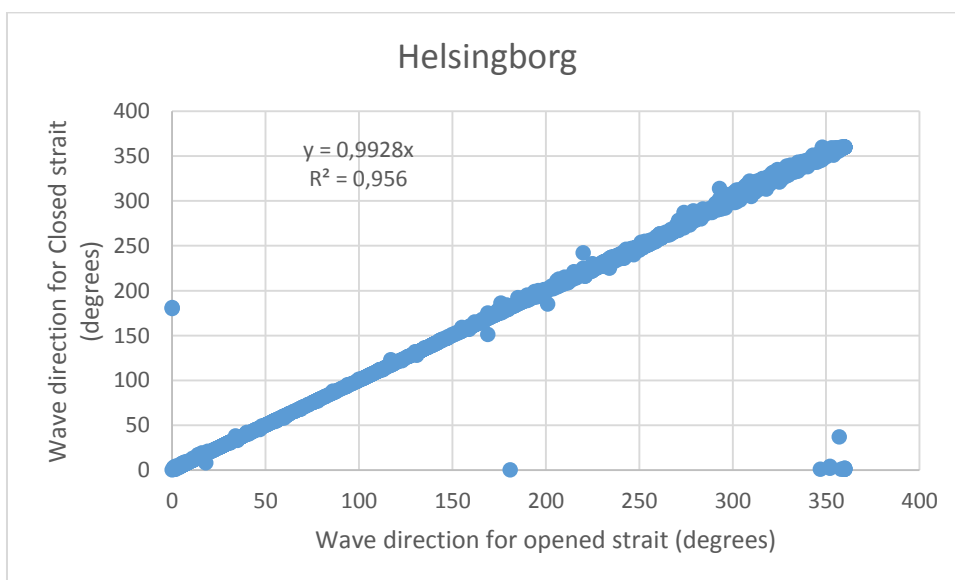


Figure 16. Wave direction of propagation comparison, location Helsingborg.

Scatter plots for other locations can be found in the appendix, page I.

6.4 Exclusion of Kattegat

In order to test if excluding the fetch of Kattegat would have had an impact on the results, two different setups were tested. One is including Kattegat, one excluding it. The whole Kattegat was still not included but it was assumed that the area included was large enough to have a significant effect on the results. Since waves coming from the North would be the main influence on this exclusion, a period presenting such winds was selected: 1999-12-12 to 1999-12-21.

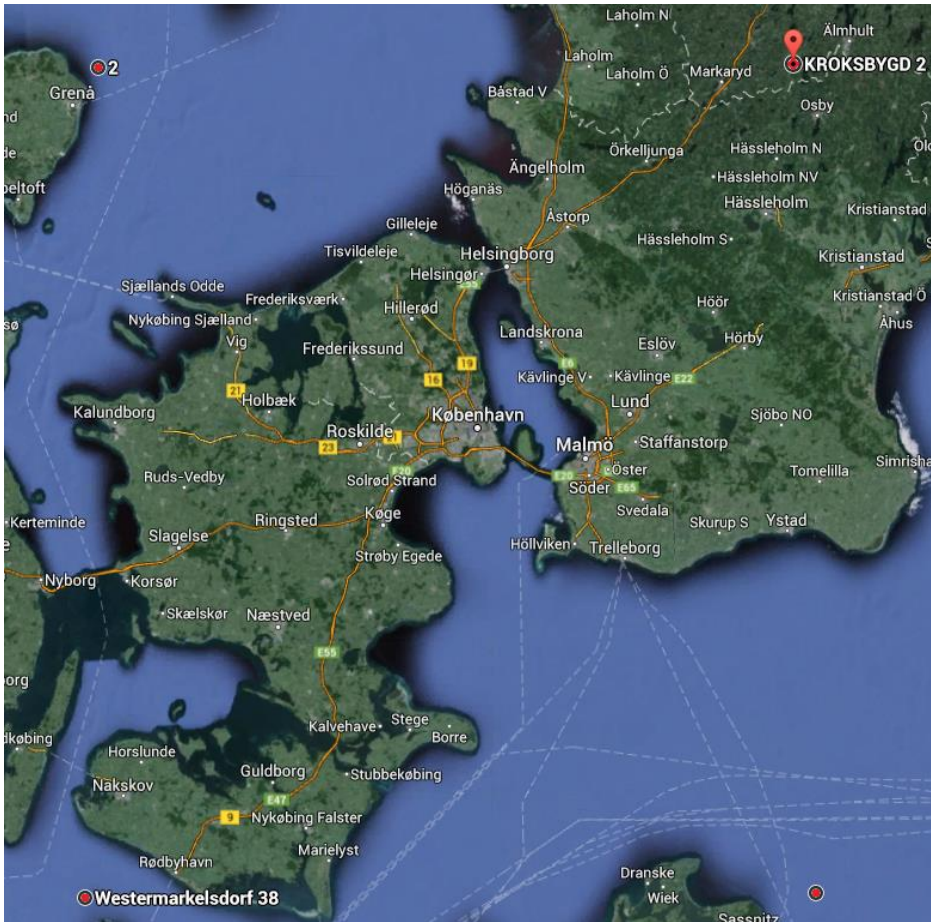


Figure 17. Map of the area used to simulate the inclusion of Kattegat. The four corners of the grid used are the four red dots. Latitudes from 54.6 to 56.5, Longitudes from 11 to 13.9.

In Figure 18 the scatter plot of the run with Kattegat versus the run without is shown.

From the trend line equation it was concluded that the influence of the exclusion of Kattegat did not have a significant impact on the wave climate, since Helsingborg was marginally affected.

Thus it was decided to use the setup excluding Kattegat for the remaining runs.

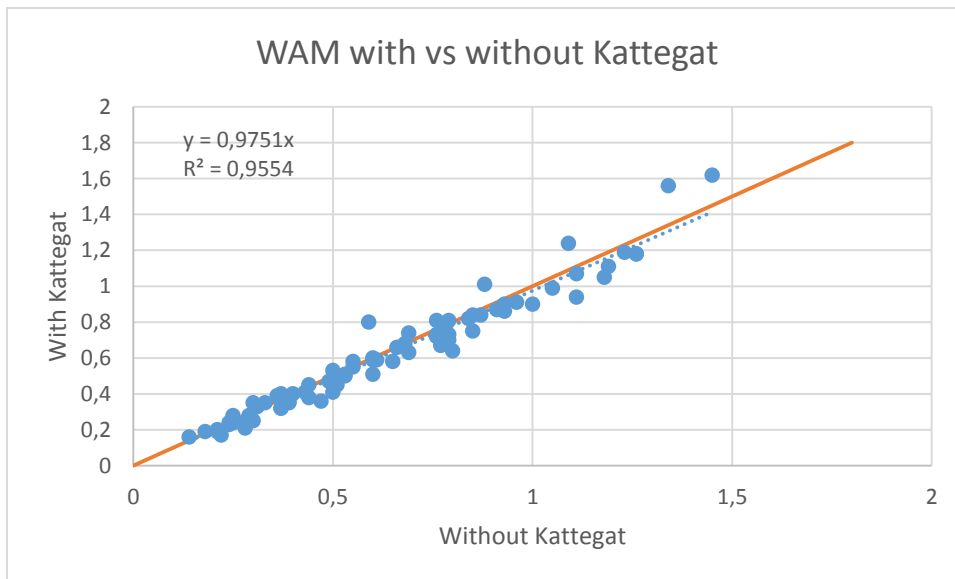


Figure 18. Significant wave height comparison between runs with and without Kattegat. In Helsingborg for the period 1999-12-12 to 1999-12-21. The 1-1 line is in orange.

6.5 Comparative results between Coarse grid, Fine grid and Measurements

From Figure 19 to Figure 21 presents the results from simulation test runs for 1999 in Öresund at the location Drogden. This point was chosen because it is the location of the wave data provided by the Geological Department at Lund University.

Two different setups were tested for WAM, a fine grid 0.025×0.025 and a coarse grid 0.05×0.05 (in decimal degrees).

All other parameters for WAM (wind setup, bottom friction coefficient) were set to be best according to the tests that will be presented later on in Chapter 7. Thus a back and forth process has been used to perform these test runs at optimum conditions.

6.5.1 Engineering Geology Department data vs WAM

Figure 19 shows the significant wave height correlation between the Engineering Geology Department (EGD) and WAM with the fine and the coarse grid. From the multiplying factor of the trend line equation, it can be seen that WAM has the same behavior with coarse or fine grid and model correctly the wave height. The R^2 values in

Figure 19 are almost indistinguishable from one another, which means that the fine grid does not increase the precision significantly. They both show that there is a good correlation between

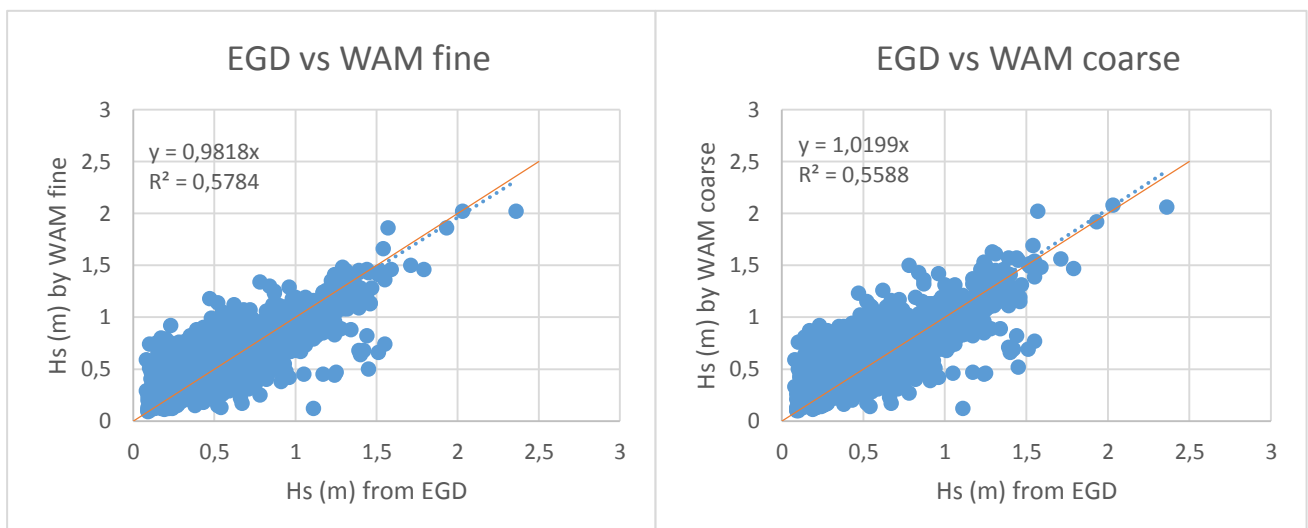


Figure 19. Scatter plot of Hs (m) from EGD data against WAM results using a fine grid (left) and a coarse grid (right). The 1-1 line is in orange.

measured data and simulated results. The R^2 seen in Figure 19 are acceptable but they indicate that the results are not optimal for this period.

6.5.2 Storm conditions test

In order to test the similarities between fine and coarse grid in extreme conditions a run was performed over a period which included severe storm conditions. During the late part of 1973, winds over Öresund reached a peak value of 28 m/s, which was the largest recorded wind speed between 1962 and 2011 by the meteorological stations used in this study.

Figure 20 and Figure 21 respectively display the wave height and direction comparison between a coarse and a fine grid run. The locations used were Helsingborg, Copenhagen, Malmö and the southern midpoint of Öresund.

All locations in Figure 20 and Figure 21 except Malmö showed extremely good correlation for both wave heights and directions. In the case of Malmö, the wave height comparison was as good as for the other locations, but the direction of propagation of the waves did not seem to indicate a perfect fit between the coarse and fine grid runs. Still, the results were acceptable and showed a rather good correspondence of the results from the two runs.

The reason behind numerous outliers was due to the circular nature of the directional system e.g. 358 and 3 degrees were almost the same but completely opposite in the graphs.

These results confirm that the coarse and the fine grid generate highly similar results, even during storms.

The conclusion was that the coarse grid can be used in order to reduce computational time without compromising the quality of the results.

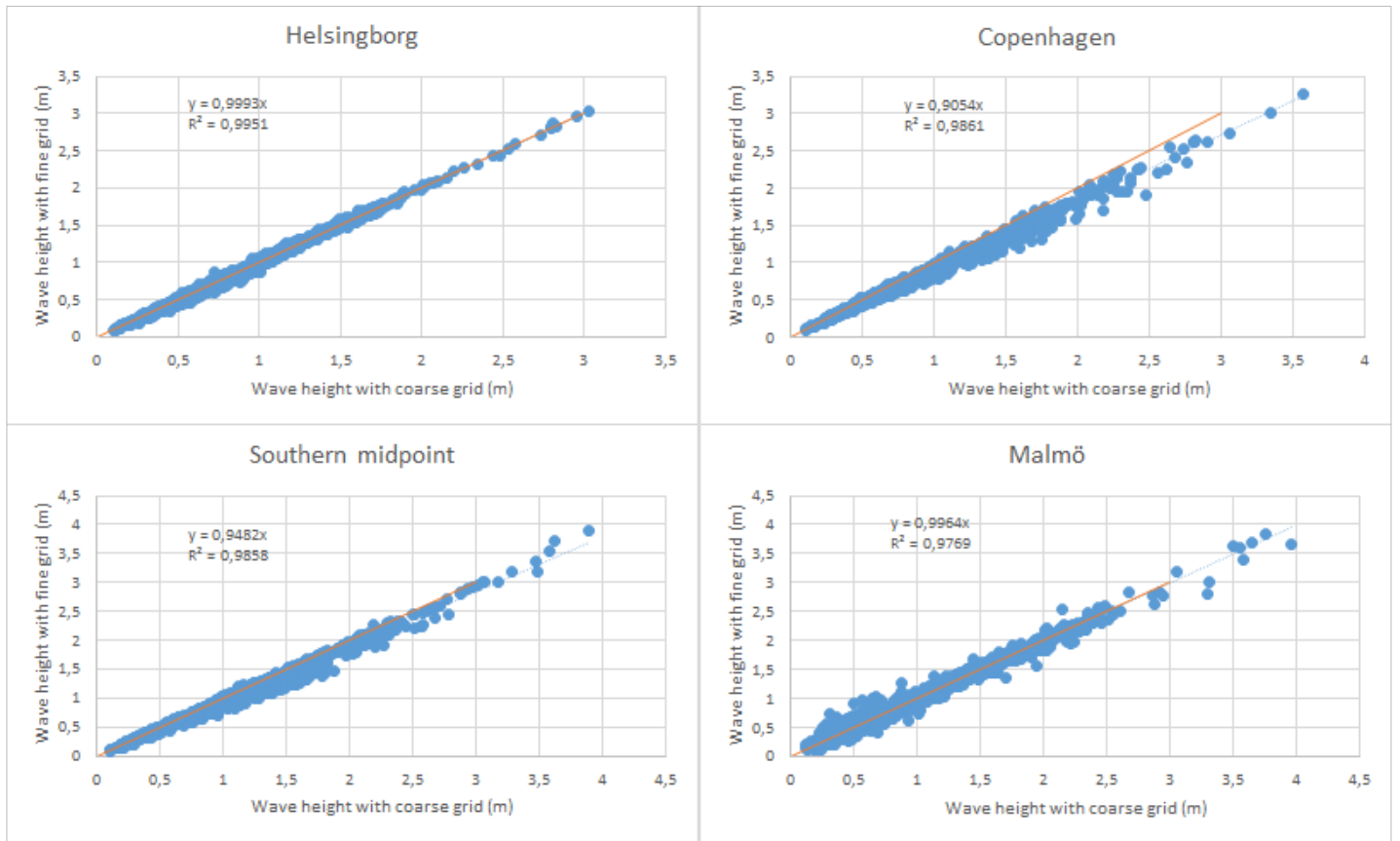


Figure 20. Significant wave height (m) comparison between runs performed with a coarse and a fine grid. Sept to Dec 1973. The 1-1 line is in orange.

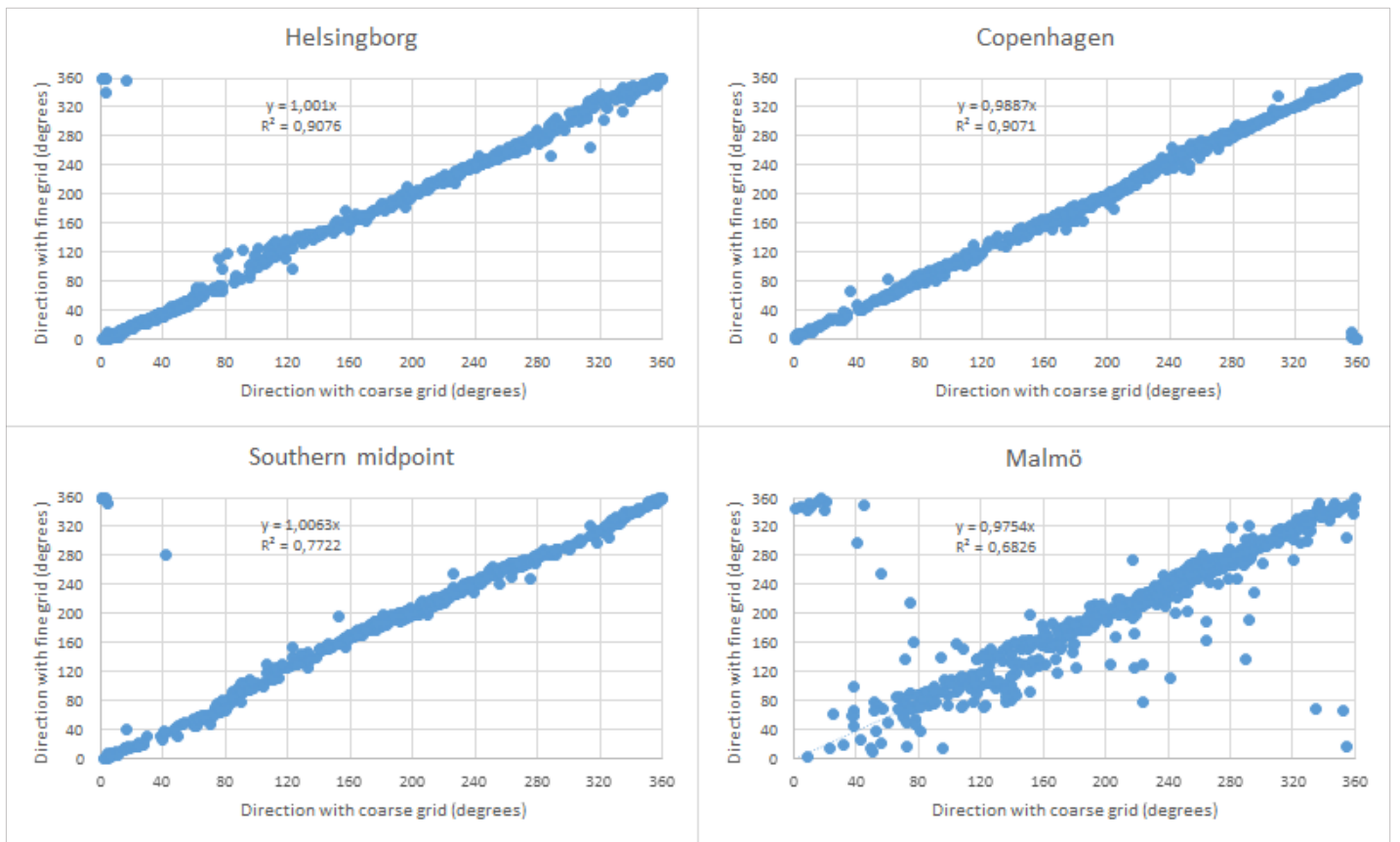


Figure 21. Wave direction of propagation (degrees) comparison between runs performed with a coarse and a fine grid. Sept to Dec 1973.

7 Calibration and Validation

In this chapter will be presented the different setups that have been tested in order to produce the best results possible. The time period used for these tests was December 1999 because it includes both a storm and calm periods. The parameter tested have been:

- the bottom friction coefficient
- the modification of the wind used, i.e. how the wind speed was adapted from the measured value to the value used in the equation
- the wind station used
- the pre-modification of the wind data from Falsterbo.

For the final test, the whole year of 1999 was simulated and a few other arbitrary periods were selected.

The wave measurements used as a comparison were provided by the Engineering Geology Department at of Lund University and DHI. These measurements came respectively from Drogden and Skovshoved, see Figure 22. Due to the amount of work needed to extract values from the



provided data, only one year has been used to perform these tests. It was believed that a full year of comparison was sufficient to perform a reliable calibration and validation.

The set up used for the calibration and validation was as follows:

- Two metrological stations, Helsingborg and Falsterbo
- The Falsterbo wind speed data were divided by the constant 1.5 (before any other modifications)
- logarithmic increase of all wind speeds
- the grid cell size was set to 0.05x0.05 (decimal) degrees
- the grid consisted of a 34x39 cell square (see Figure 8).

Figure 22. Map of the location of the measurements.

7.1 Bottom friction

The model was set to shallow water mode since the conditions in Öresund can be assumed to be predominantly shallow. At shallow conditions the bottom friction coefficient has a greater effect on the wave development (Komen et al, 1994).

Different values on the bottom friction coefficient were tested in order to examine its effects on wave height. The bottom friction coefficient was multiplied by a factor: 1, 4, 40 or 400, respectively. The impact that this modification had on the waves was the opposite of what was desired, i.e. the larger waves decreased and the smaller waves were almost unaffected. It is also worth mentioning that for the factor increase of 400 there were a reduction of the height of the smaller waves, but since this extreme increase of the coefficient is not reasonable it was not considered as an option. The results can be found in appendix pages II to IV.

7.2 Wind

The wind statistics for the different stations were compared over the time period of 1962-2011. The average wind speed in Falsterbo was 50% higher than in Malmö and 60% higher than Helsingborg. This is most likely due to the unprotected location of the Falsterbo meteorological station and does not correspond well to the conditions in the strait. Thus a few tests were performed in order to gain an understanding of how the wind speed might be affecting the wave conditions in the strait.

In the following sub-chapters these tests will be described more in depth.

7.2.1 Setup 1, 2 and 3

For setup 1 the wind measurements were used without any modifications. Setup 2 used an increase of 20% for all the wind speeds and Setup 3 used a logarithmic increase of the wind speeds (Irminger-Street, 2011).

Tested with other parameters unchanged, the best results were obtained with Setup 3, thus in the following tests this setup was used.

7.2.2 Helsingborg alone

A test run using only winds from Helsingborg meteorological station was performed to avoid the influence of the stronger winds from Falsterbo. By using this method, the decrease in wave height was too strong. The multiplying factor of the trend line drop down to $k=0.81$ which seems too low since the focus of this study is more on the larger waves. It is thus preferable to slightly overestimate than underestimate the wave heights.

7.2.3 Malmö and Helsingborg

Another option tested was to use winds from Helsingborg and Malmö and fix the missing the values in Malmö with corrected values from Falsterbo.

The results from this test are similar to the ones using only Helsingborg and this option was disregarded due to, again, underestimation of the wave heights.

7.2.4 Pre-modification of wind from Falsterbo

In order to correct the wind measurements from Falsterbo, the wind speeds from this station were divided by 1.5 before applying the logarithmic increase to the wind speed. This was done in order to match the average wind speed in Falsterbo to the one in Malmö. In Figure 23 are presented the results from this test together with a Setup 3 run without pre-modification of Falsterbo wind speed.

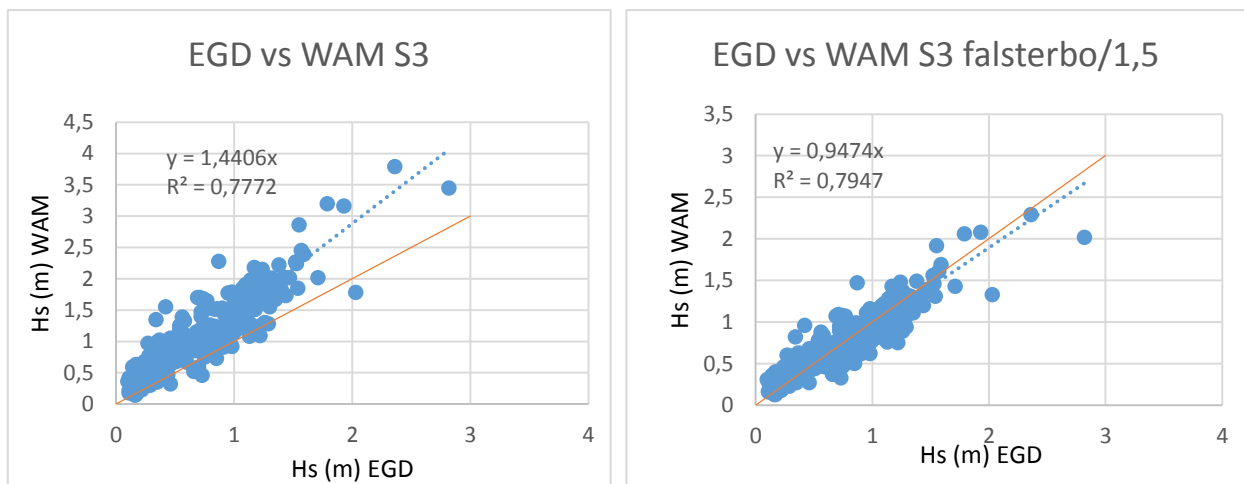


Figure 23. Scatter plot of data from Engineering Geology Department at Lund University against setup 3 with and without pre-modification of wind speed in Falsterbo.

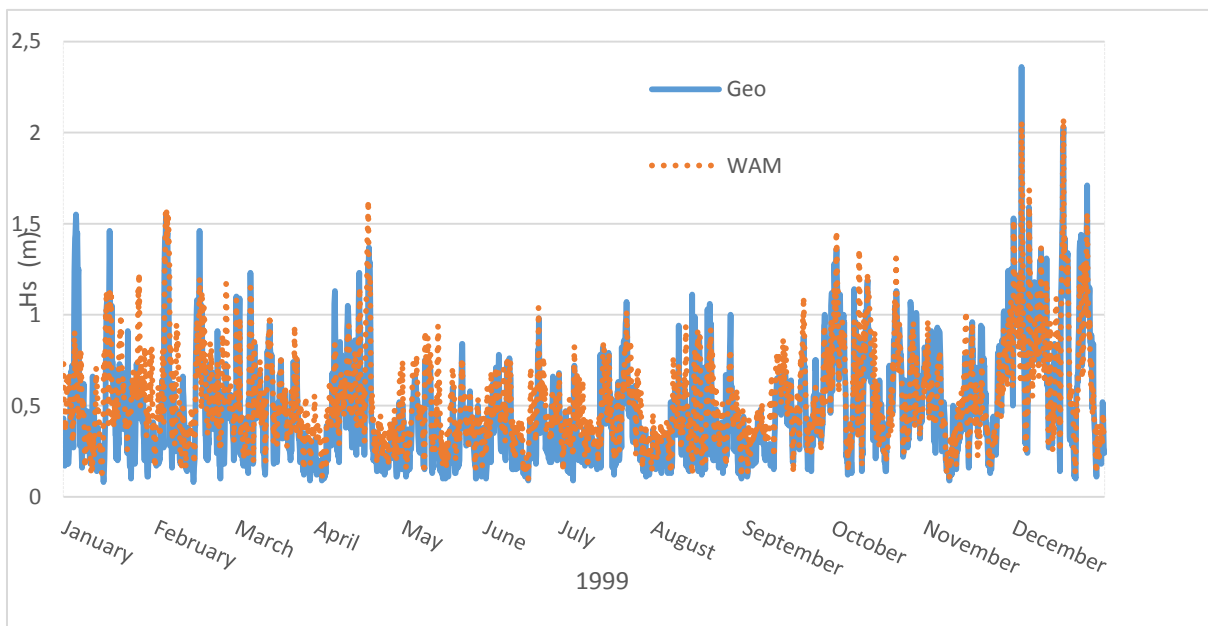


Figure 24. Measured (blue) and modeled (orange) significant wave height (m) in Drogden in 1999.

The point of the pre-modification was to reduce the wave height on the assumption that Falsterbo winds were too strong to be valid for the strait. The results show that this assumption was valid since the multiplying factor of the trend line is much better with the pre-modification: $k_1=1.44$, $k_2=0.95$.

The R^2 is marginally improving when dividing Falsterbo wind speeds, from $R_1=0.78$ to $R_2=0.79$.

Figure 24 is a timeserie of the significant wave height over the year 1999 in Drogden. Here, the tendency of WAM to overestimate smaller waves is clear, this tendency can also be observed in

Figure 23. But from these two figures the conclusion can be drawn that WAM models the majority of the waves with fairly good precision, in terms of wave height.

This assumption is confirmed by the Figure 25 that displays wave roses for another time period (November 2013 to January 2014) and another place, Skovshoved. The left wave rose represents the results from WAM while the right is based on measured data from DHI. On these wave roses, the direction of the wave is included as well and indicates that WAM is also reasonably reliable in terms of direction of propagation of the waves. Though, the wave height is slightly higher with WAM. That could be partially due to the water depth at the location, which is too shallow (6 meters deep) to be considered as optimum modeling conditions for WAM.

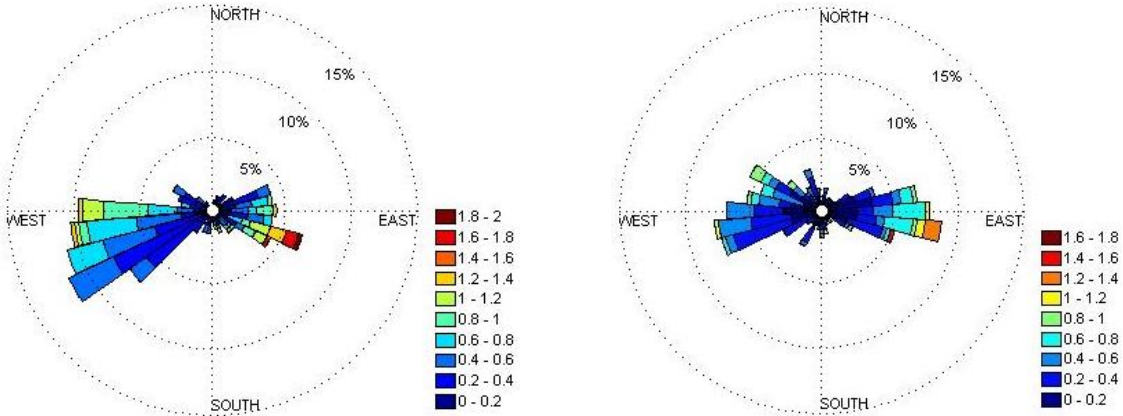


Figure 25. Wave roses from Skovshoved in December 2013. WAM results (left), DHI data (right). The scale is in meters

8 Results

In this chapter the results from the final runs are presented; an examination of the significant wave height and direction, monthly averages of significant wave height and run-up levels, sediment transport and a climate change scenario. A more in depth description of each results set ups and runs will be described in the following sub-chapters.

8.1 Wave height and direction

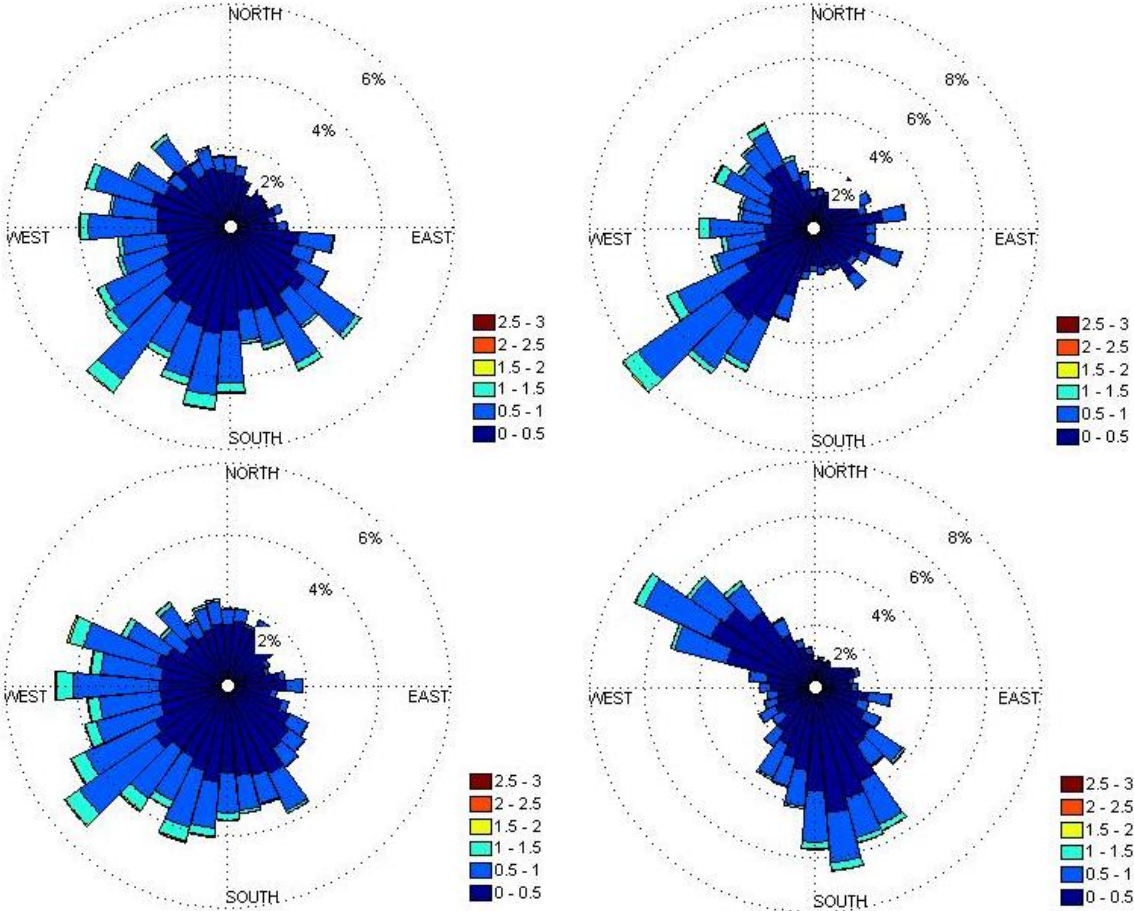


Figure 26. Wave roses at Falsterbo (top left), Malmö (top right), Landskrona (bottom left), Helsingborg (bottom right). The scale is in meters.

Figure 26 displays the wave roses for the waves from Falsterbo, Malmö, Landskrona and Helsingborg. The direction shown in the wave roses are the direction of propagation of the waves.

For each location the effect of nearby land is clearly represented, especially for Helsingborg where the North-East and South-West directions are almost non existent. Also, the influence of the island Ven is visible in the Landskrona wave rose; north-western waves seem to be reduced.

Wave roses for some other locations can be found in the appendix, pages V and VI.

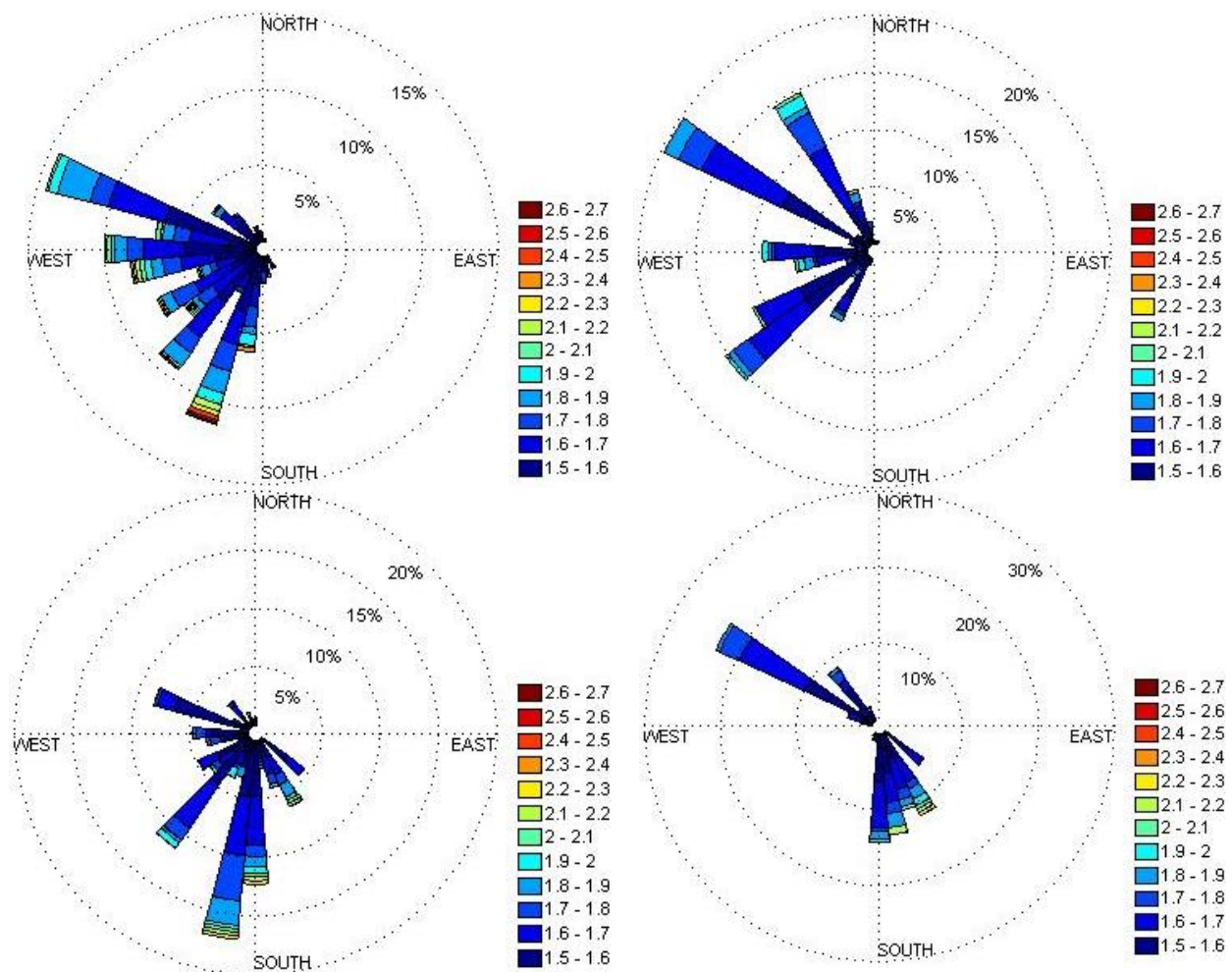


Figure 27. Wave roses for waves higher than 1.5m at Falsterbo (top left), Malmö (top right), Landskrona (bottom left), Helsingborg (bottom right). The scale is in meters.

It is also noticeable that the waves in the Northern part the strait have a larger proportion of smaller waves in comparison to the Southern part of the strait. This is confirmed by the results shown in Figure 27 where the waves higher than 1.5 m are presented alone. This tendency is also noticeable in Table 4, both the mean and maximum values of H_s are decreasing from South to North. Falsterbo has a maximum H_s of 2.68 m while the maximum in Helsingborg is only 2.22 m.

Table 4. Mean and maximum values of H_s (m), and depth (m) at the four locations.

	Mean Values	Max values	Depth at locations
Falsterbo	0,49	2,68	7
Malmö	0,47	2,28	10
Landskrona	0,47	2,23	24
Helsingborg	0,43	2,22	13

Figure 28 illustrates the accumulative probability of H_s (m), from the figure it can be concluded that more than 60% of the significant wave height were lower than 0.50 m. Worth noting is also that the wave heights in Malmö and Landskrona were almost identical. The probability curve for Helsingborg is shifted upwards and left in the figure, meaning that the probability of measuring larger waves are on average smaller there. In this figure, for each point on a curve, the y-axis value is the percentage of

waves smaller than the x-axis value in meter. So the higher the curve is, the smaller the percentage of large waves is. As expected the probability curve for Falsterbo is downward and to the right in Figure 28, indicating a higher probability of larger waves.

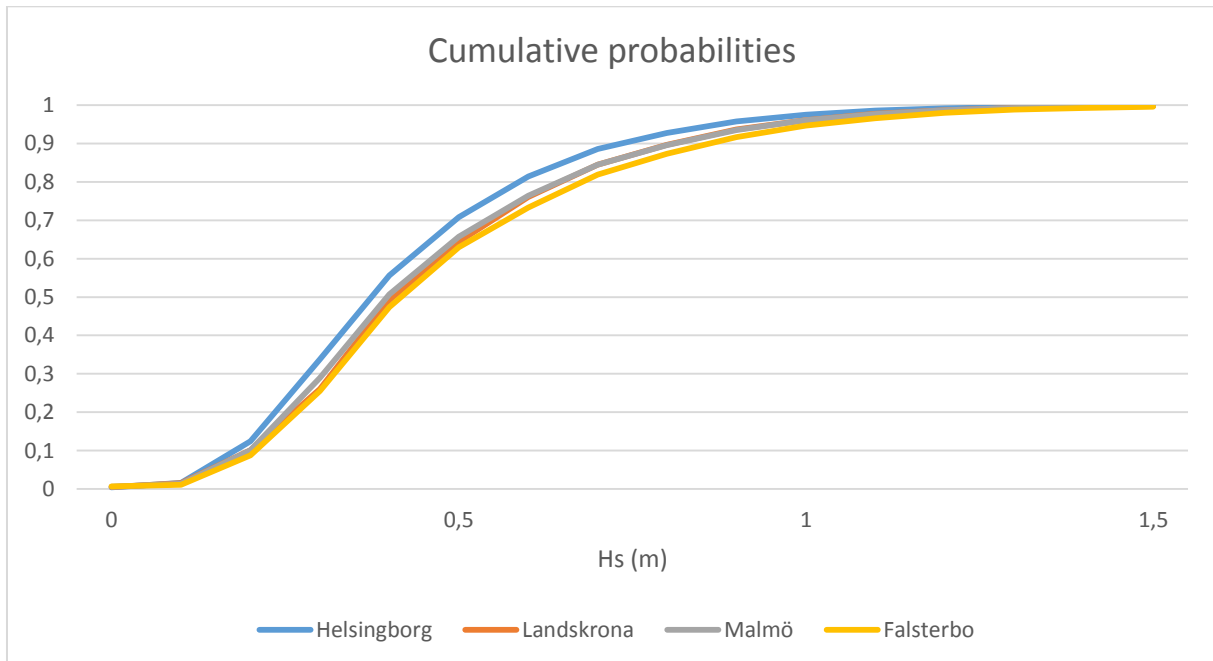


Figure 28. Cumulative probabilities of Hs (m) occurrence.

Figure 29 shows the same trends but focus is more on the importance of each 10 cm interval.

Results from all locations seem rather similar with this kind of graph, but similar trends as in Figure 28 can be observed i.e. slightly larger waves in Falsterbo than in Helsingborg. The main conclusion

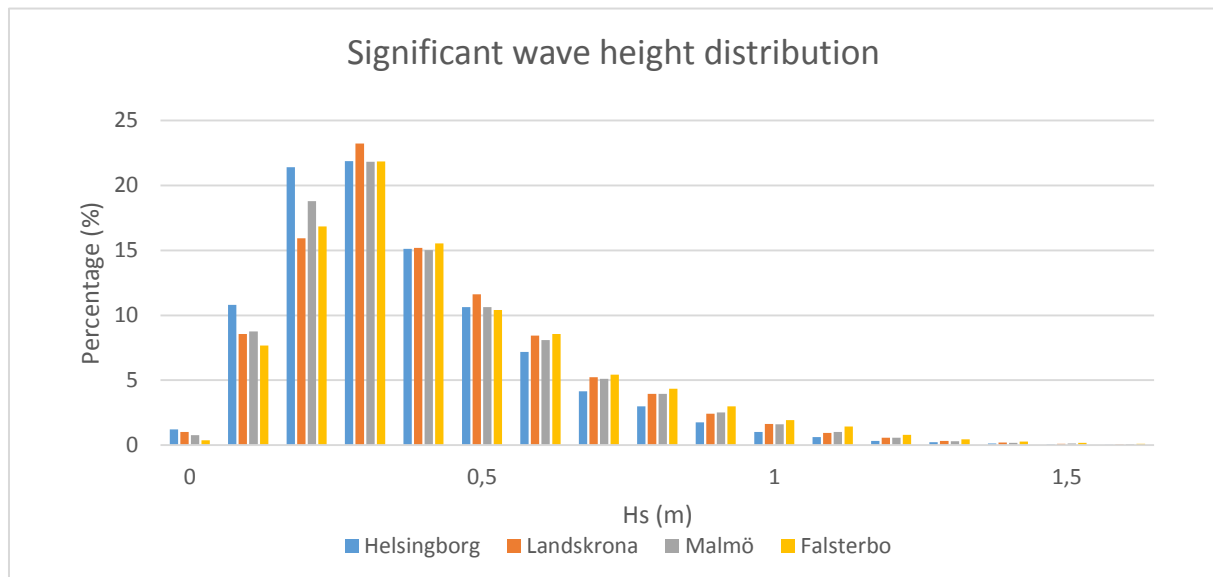


Figure 29. Percentage of Hs (m) per 10cm interval.

that can be drawn from Figure 25 is that, most of the wave heights are included in the interval 0.2 and 0.5 m, with a peak for 0.3 m waves.

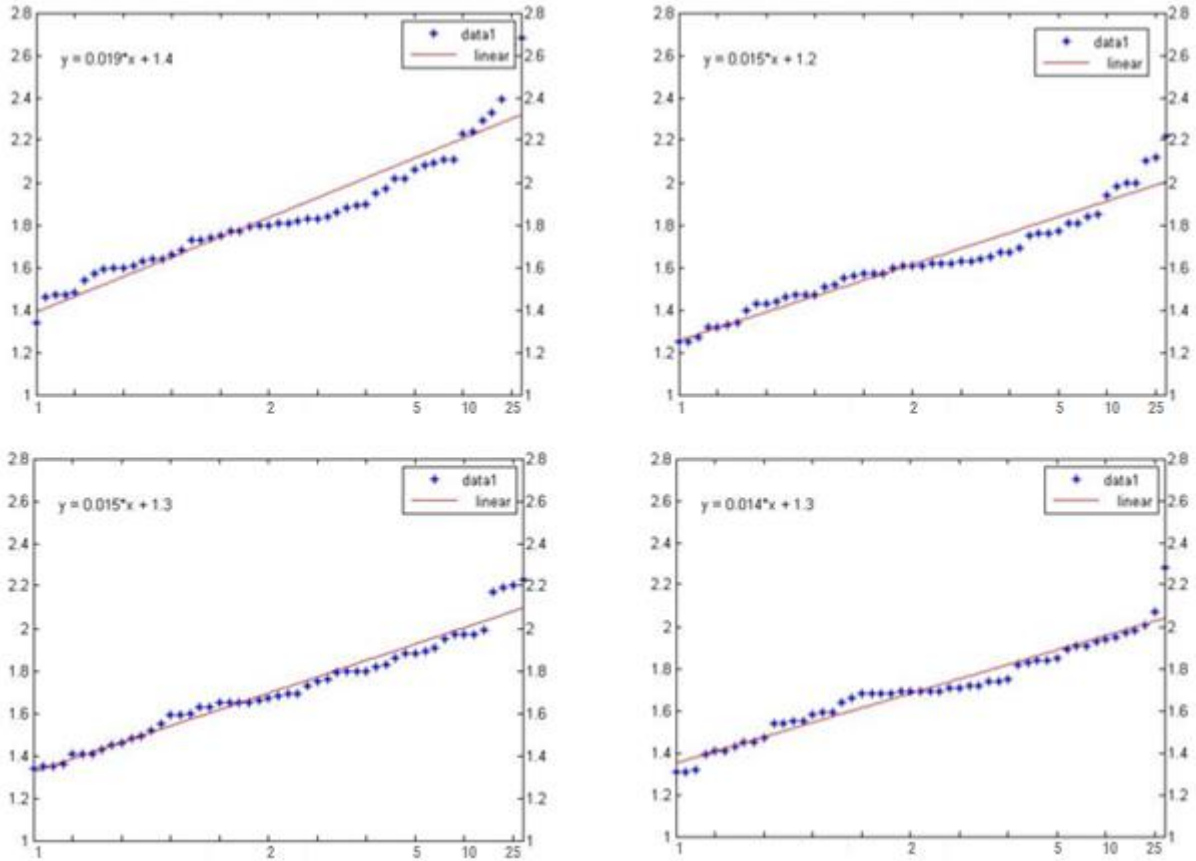


Figure 30. Significant wave height (m) return period diagram over 50 years. The locations are Falsterbo (top left), Malmö (top right), Landskrona (bottom left) and Helsingborg (bottom right).

Figure 30 displays the return period diagram for significant wave height using the Gumble method as a linearization, over the time period from 1961 to 2011. All four locations seem to have a reasonably good fit, except for the 50 year values which are slightly above the trendline. This is not uncommon and implies that these extreme are not following the Gumble linearization. This also means that these results might not be suitable for an extrapolation of extreme waves with a return period of 100 years or more.

Table 5. The statistical return period values for the significant wave height (m).

Return period (years)	Falsterbo	Malmö	Landskrona	Helsingborg
1	1,34	1,31	1,34	1,25
2	1,8	1,69	1,67	1,61
5	2,08	1,89	1,89	1,81
10	2,24	1,95	1,97	1,98
25	2,65	2,07	2,2	2,12
50	2,68	2,28	2,23	2,22

This information, in regards to the extreme values, might be of interest when planing or dimentioning structures, as a first step when examining the conditions in the area. Although these results should not be the sole investigation in such cases.

Table 5 contains the statistical values of the return period for the significant wave height. Apart from Falsterbo which tends to give slightly higher values, the different locations have similar results.

Return period diagrams for all locations can be found in the appendix, pages VII and VIII.

8.2 Monthly averages

In Figure 321 to Figure 33 are displayed the monthly averages of significant wave height, mean period and peak period, over the period 1961 to 2011, at the locations Helsingborg, Landskrona, Malmö and Falsterbo. The winter months have higher average significant wave height than rest of the year, this was expected considering that the wind was stronger for this part of the year. Similar tendencies can be observed for average mean period, see Figure 31. For peak period (Figure 33) the tendencies are not as obvious, but small differences can be observed between summer and winter

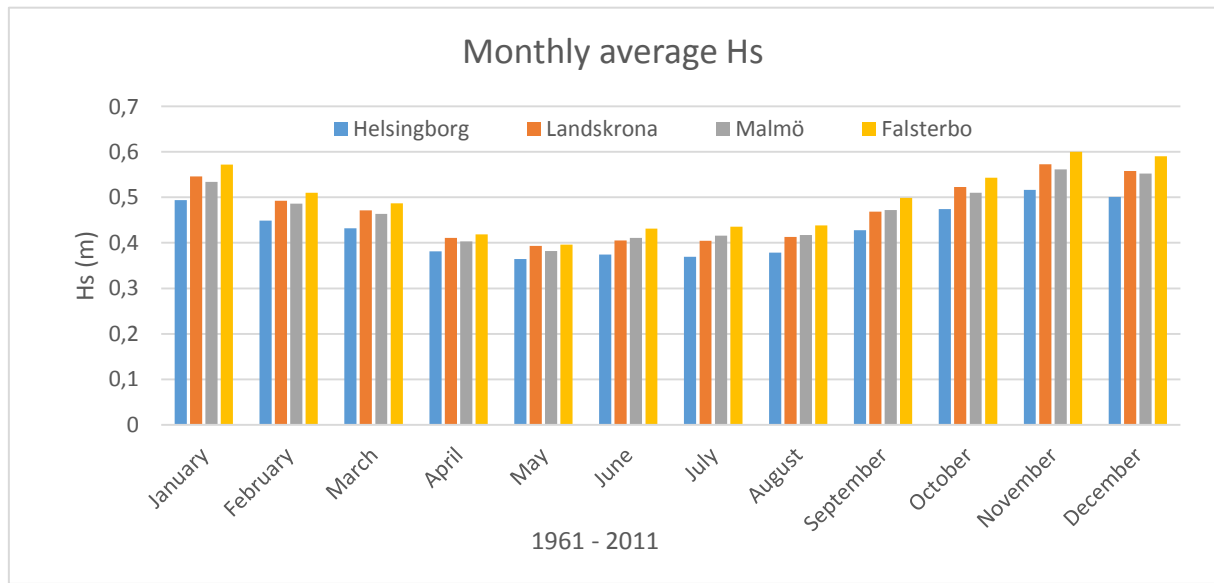


Figure 32. Monthly averages of significant wave height (m) over the period 1961 to 2011, at the locations Helsingborg, Landskrona, Malmö and Falsterbo.

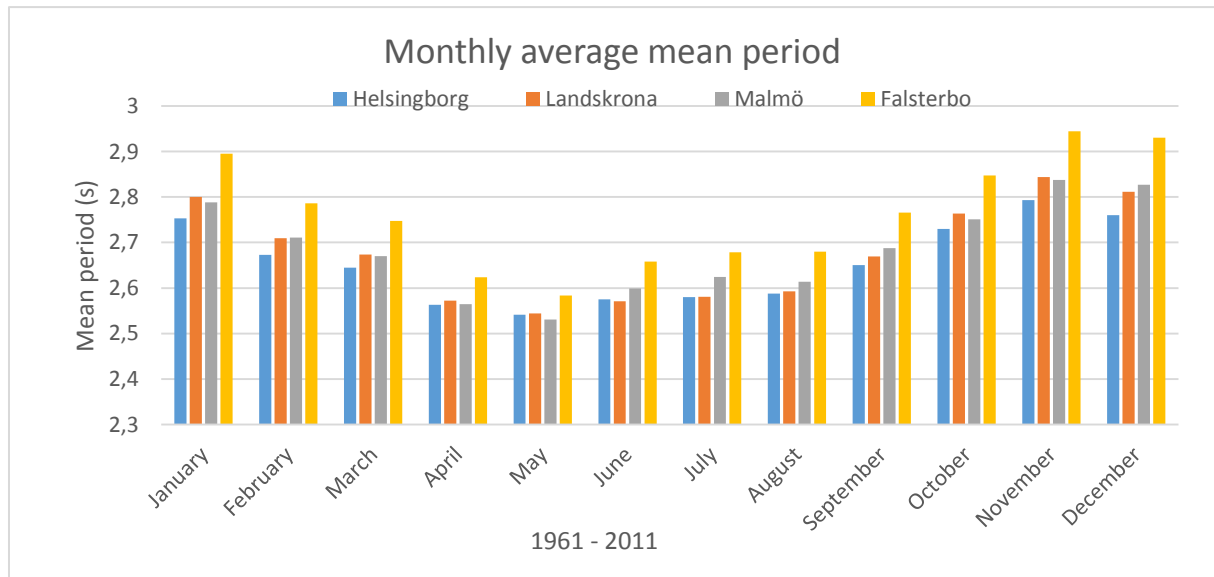


Figure 31. Monthly averages of mean period (s) over the period 1961 to 2011, at the locations Helsingborg, Landskrona, Malmö and Falsterbo.

months.

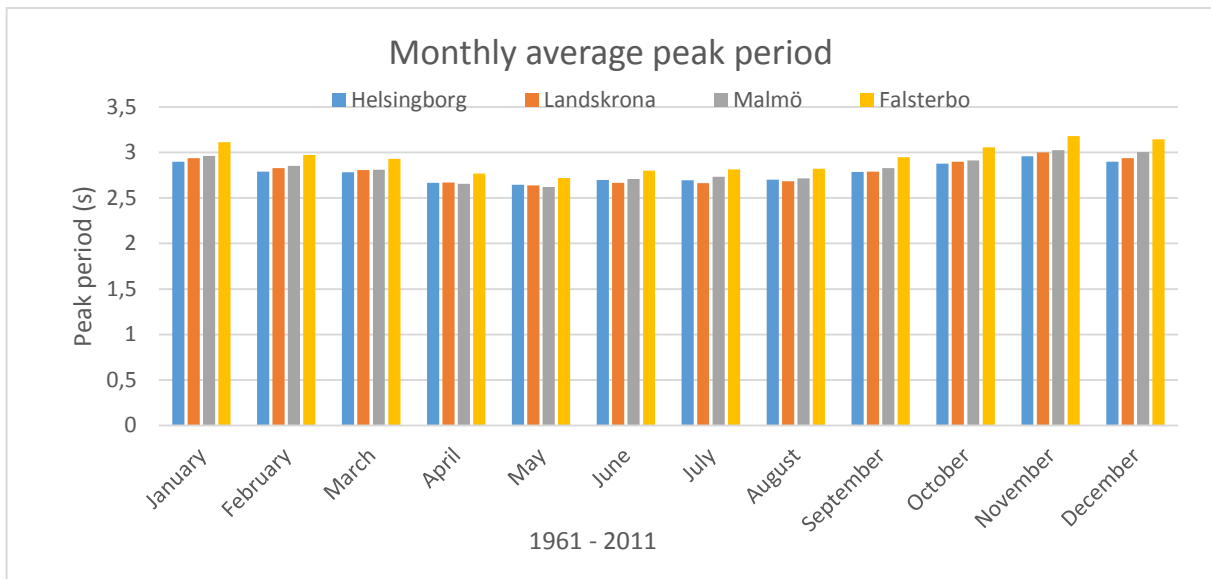


Figure 33. Monthly averages of peak period (s) over the period 1961 to 2011, at the locations Helsingborg, Landskrona, Malmö and Falsterbo.

8.3 Run-up levels

8.3.1 Method

With the results of significant wave height and direction of propagation, the run-up height was calculated for four locations: Helsingborg, Landskrona, Malmö and Falsterbo.

With additional water levels data from SMHI, the water levels at these locations were extrapolated using a linear regression. This extrapolation was not conducted across the bridge due the presence of a threshold that creates two separates zones for the water level.

The water levels data used were from Falsterbo, Barsebäck and Viken and covered the time period from January 2001 to December 2011 (Link 5, 2014).

The extrapolated values were added to the calculated run-up height in order to get the total run-up levels.

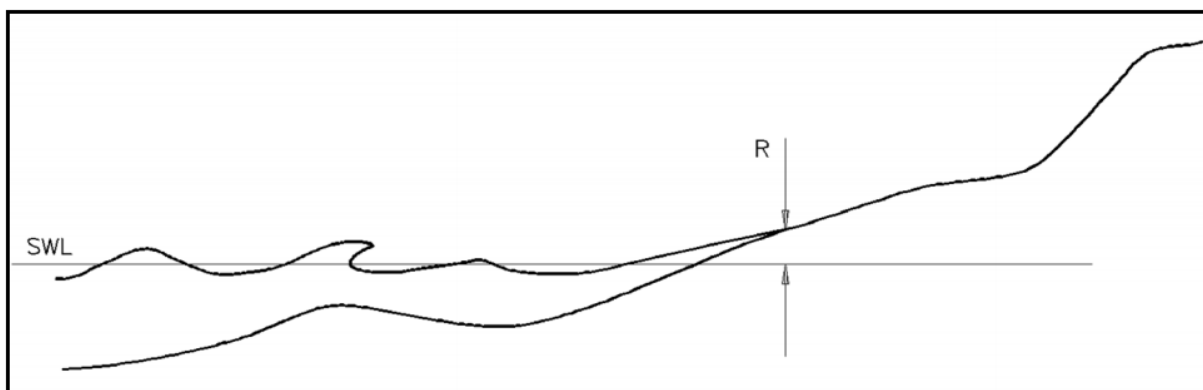


Figure 34. Schematic representation of the run-up height (R). SWL means still water level. The figure is from CEM, 2003.

To compute the run-up heights (see Figure 34), the Hunts formula was used:

$$R = H_0 * \frac{\tan \beta}{\sqrt{H_0/L_0}} \quad (5)$$

Where R is the run-up height, H_0 the wave height, L_0 the wave length and $\tan\beta$ the bottom slope angle. A typical arbitrary bottom slope angle of the locations studied was chosen:

$$\tan \beta = 0.15. \quad (6)$$

The use of an arbitrary value for the bottom slope results in that run-up values easier can be compared between different locations. This means that the total run-up levels might be lower than what the calculated values indicate, since the beach profile usually has a moderate slope the first few meters (corresponding to the $\tan\beta = 0.15$) and then the steepness increased. The Hunts formula uses H_0 as if the direction of propagation of the waves was perpendicular to the shoreline. Here it was not the case so a correction had to be made. According to Hanson and Larson (2008) an acceptable estimate of the wave correction can be obtained by using:

$$H'_0 = \sqrt{\cos \theta_0} * H_0 \quad (7)$$

Where H_0 is the original wave height, H'_0 is the corrected wave height and θ_0 the angle difference between the direction of propagation of the waves and the shoreline.

8.3.2 Results

Before analyzing the results, the difference between terms that will be used has to be made clear. The water level is the variation of the still water level from an origin position. The run-up height is the run-up produced by the waves. The run-up level is the sum of the water level and the run-up height.

Table 6 presents the mean and maximum values of run-up levels for the whole studied period, the highest run-up level in Helsingborg, Landskrona, Malmö and Falsterbo were 2.76 m, 2.89, 2.48 and 1.99 respectively. Considering the significant wave height at these locations (see Chapter 8.1), it could have been expected that Falsterbo would present the largest run-up levels. But here the angle of the shoreline has a key role together with the direction of propagation of the waves. Coupled, these factors make Landskrona the location with the most extreme results. That is easily explained looking at Figure 39; the line used in Landskrona is perpendicular to the direction of propagation of the strongest waves: coming from the South-West.

Table 6. Average and maximum run-up level (m).

	Mean Values (m)	Max values (m)
Helsingborg	0,36	2,76
Landskrona	0,49	2,89
Malmö	0,38	2,48
Falsterbo	0,44	1,99

Figure 35 to Figure 36 are the monthly averages of respectively the run-up levels, run-up heights, and water-levels.

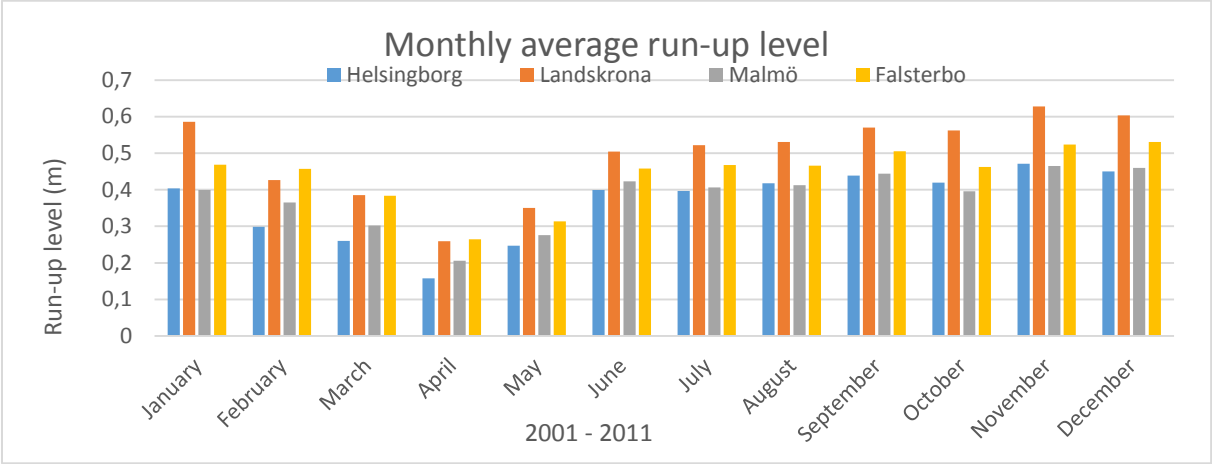


Figure 35. Monthly averages of run-up levels (run-up height, based on peak period, plus water level, in meters) over the period 2001 to 2011, at the locations Helsingborg, Landskrona, Malmö and Falsterbo.

The monthly run-up levels for Helsingborg varies between 0.16 and 0.47, Landskrona varies between 0.26 and 0.62 m, Malmö varies between 0.21 and 0.46 m, and Falsterbo varies between 0.26 and 0.53 m (see Figure 35). In Figure 36 the monthly average water levels are presented, for Helsingborg average water level varies between 0.02 and 0.16 m, for Landskrona the levels varies between 0 and 0.16 m, for Malmö the levels varies between 0.03 and 0.21 m, and for Falsterbo the levels varies between 0.07 and 0.22 m. As seen in Figure 36, the water levels present a dramatic decrease in April, for all locations. That explains the substantial drop of the run-up levels observed in Figure 35. It can also be noticed that the water levels in Falsterbo compensate for the low run-up heights whereas the opposite is seen in Landskrona.

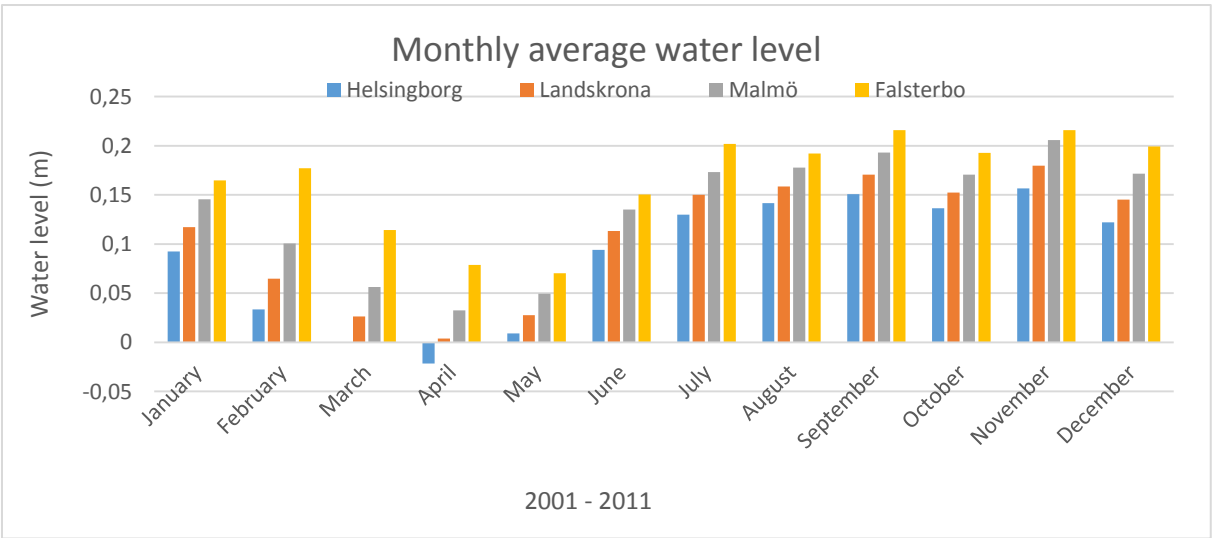


Figure 36. Monthly averages of water levels (m) over the period 2001 to 2011, at the locations Helsingborg, Landskrona, Malmö and Falsterbo.

When analyzing the wind statistics, one can notice that the most common wind direction changes over the months. In April the winds seemed to come from the east more than during the other months. The effect can be seen in Figure 37. Then from May to winter months, the run-up heights

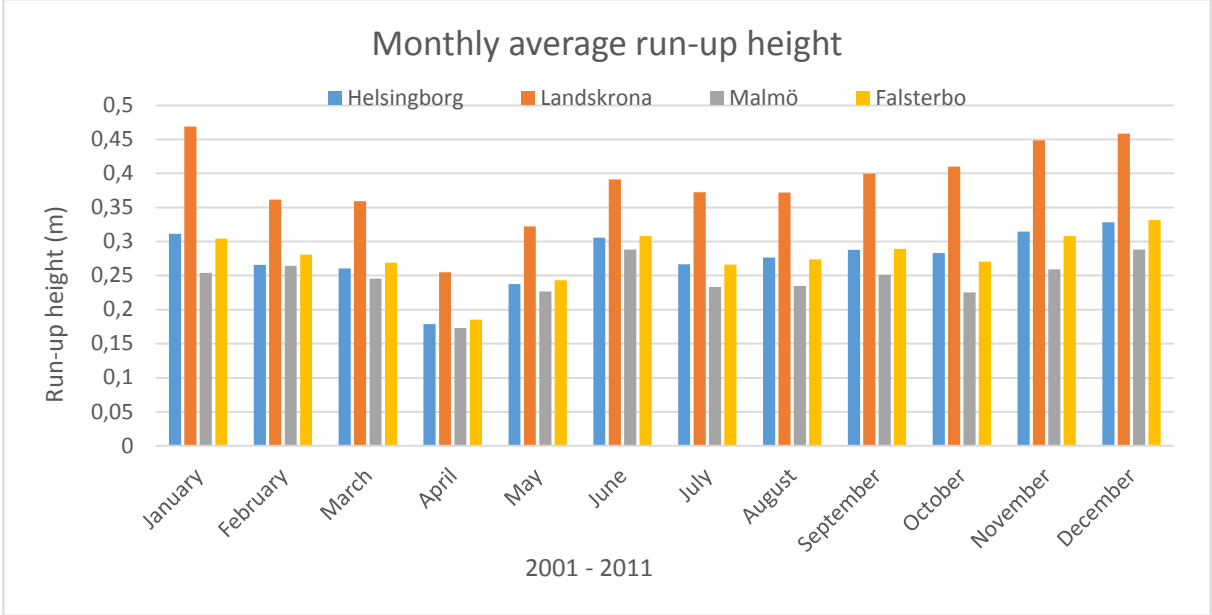


Figure 37. Monthly averages of run-up height (m) over the period 2001 to 2011, at the locations Helsingborg, Landskrona, Malmö and Falsterbo.

are slowly growing whereas this growth only starts in August for the significant wave heights.

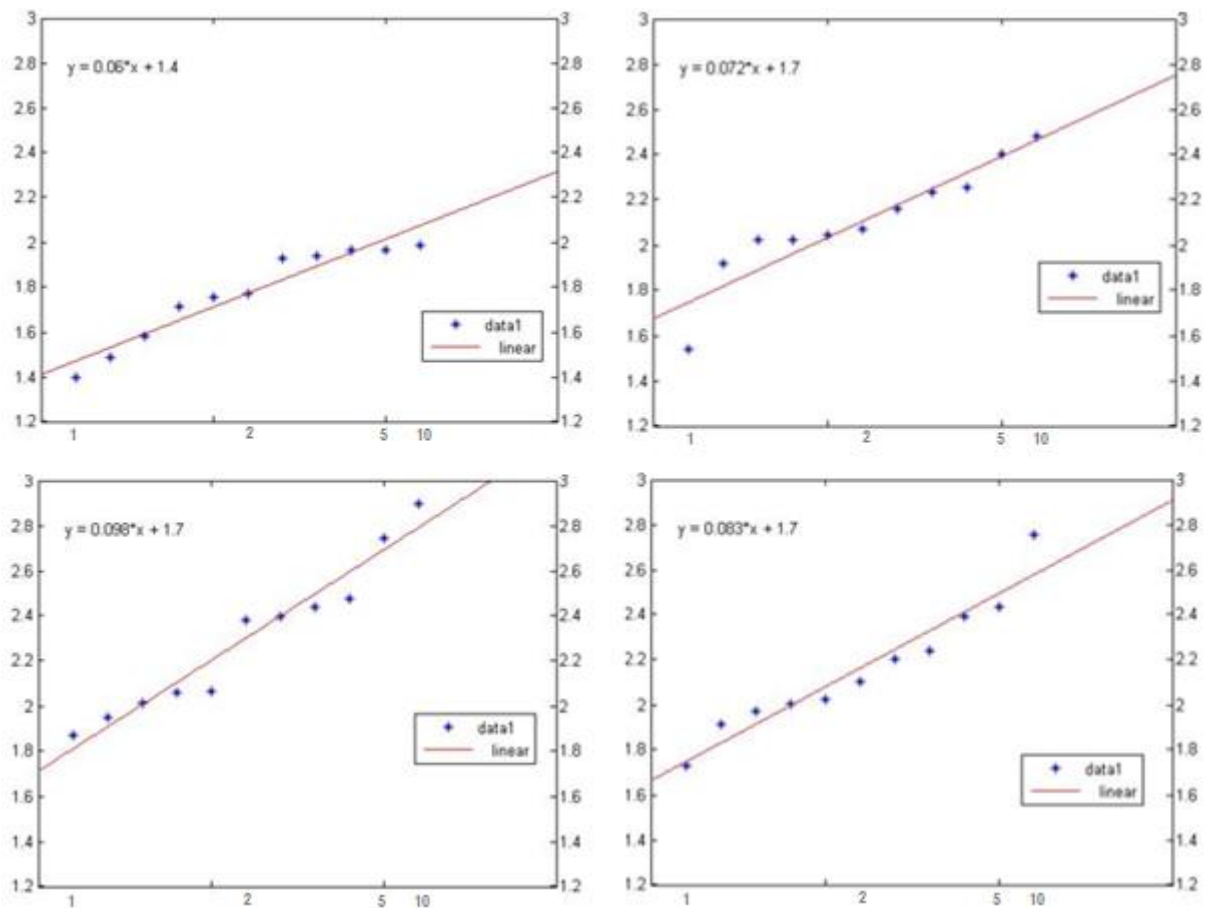


Figure 38. Return period of run-up level (m) over the period 2001 to 2011, at the locations Falsterbo (top left), Malmö (top right), Landskrona (bottom left), and Helsingborg (bottom right).

In Figure 38 are displayed the return period diagrams of the four locations for the run-up levels. The linear regressions, i.e. in these cases the Gumbel distribution, seems to be a good approximation for all of them and a 15 year value can be estimated, but more data would be needed if a long extrapolation of the results was to be produced (due to time constraints, this was not possible). In fact, a small deviation of the trend line would lead to a great difference in the results if longer return periods are to be estimated.

8.4 Sediment transport

8.4.1 Method

As mentioned in Chapter 2.7 sediment transport may affect coastal areas and structures, thus it is of interest to evaluate the potential sediment transport. From the significant wave heights and wave directions one can compute the effect of the waves on the shore. Some other variables would be needed if precise values were wanted, but here the sediment has been assumed to be sand all along the Swedish coast. This assumption led to the calculation of a potential long-shore sediment transport that can give an idea of the erosion and accumulation areas. In this thesis an empirical formula, developed by Larson et al. (2011), has been used in order to directly compute the breaking wave height and angle. One should note that the formula does only take the long-shore sediment transport into account, thus it might mean that the actual cross-shore sediment transport would give a different result.

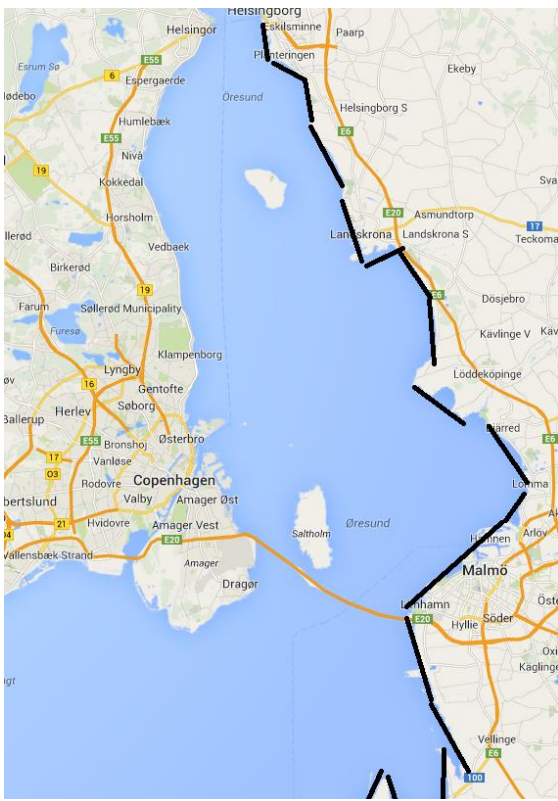


Figure 39. Lines used as an approximation of the shore.

Figure 39 displays the lines used as an approximation of the shore for the sediment transport calculations. These lines are of importance because they impact directly on the angles used in the calculations.

Below are the equations used:

$$h_b = \lambda * \frac{c^2}{g} \quad (8), \quad H_b = \gamma * h_b \quad (9)$$

$$\theta_b = \sin^{-1}(\sin(\theta_0) * \sqrt{\lambda}) \quad (10).$$

Where h_b is the water depth at breaking, c the wave velocity, g the gravitational acceleration, H_b the wave height at breaking, θ_b the angle at breaking, θ_0 the deep-water wave angle and γ is an arbitrary coefficient set to 0.78 (according to standards).

λ is calculated by using the equation below:

$$\lambda = \delta * \lambda_a \quad (11), \quad \lambda_a = \left(\frac{\cos \theta_0}{\alpha}\right)^{2/5} \quad (12), \quad \alpha = \left(\frac{c}{\sqrt{g * H_0}}\right)^4 * \frac{c}{c_g} * \gamma^2 \quad (13).$$

Where H_0 is the wave height at deep-water conditions, c_g the group velocity and δ is calculated with the following equation:

$$\delta = 1 + 0.1649 * \varepsilon + 0.5948 * \varepsilon^2 - 1.6787 * \varepsilon^3 + 2.8573 * \varepsilon^4 \quad (14),$$

$$\text{with} \quad \varepsilon = \lambda_a * (\sin \theta_0)^2, \quad 0 \leq \varepsilon \leq 0.5 \quad (15).$$

Once breaking wave height and angle are obtained, one can use the CERC formula (SPM, 1984) to find the potential sediment transport:

$$Q = \frac{0.023 * \sqrt{g}}{s-1} * H_b^{5/2} * \sin(2 * \theta_b) \quad (16).$$

Where s is the ratio between the material density and the density of the medium, in this case sand is the material and water is the medium (which gives $s = 2.65$).

From this formula it is understood that grain size is not taken into account, which means that this formula only evaluates potential sediment transport of sand. Depending on the area, the calculated transport may not be correct, due to this assumption. The formula does not either take the porosity of the sand mass into account which may lead to further decrease of the accuracy of the results. However it gives a relative insight on the forces that are affecting the coastal area.

8.4.2 Results

In order to use this method, the Swedish coastline of Öresund has been segmented into eighteen sections each represented by a straight line. In Figure 40 the average sediment transport calculated from the full 50 years are displayed for the eighteen sections of the Swedish coast. A positive number means that the transport is northward and southward transport corresponds to negative values.

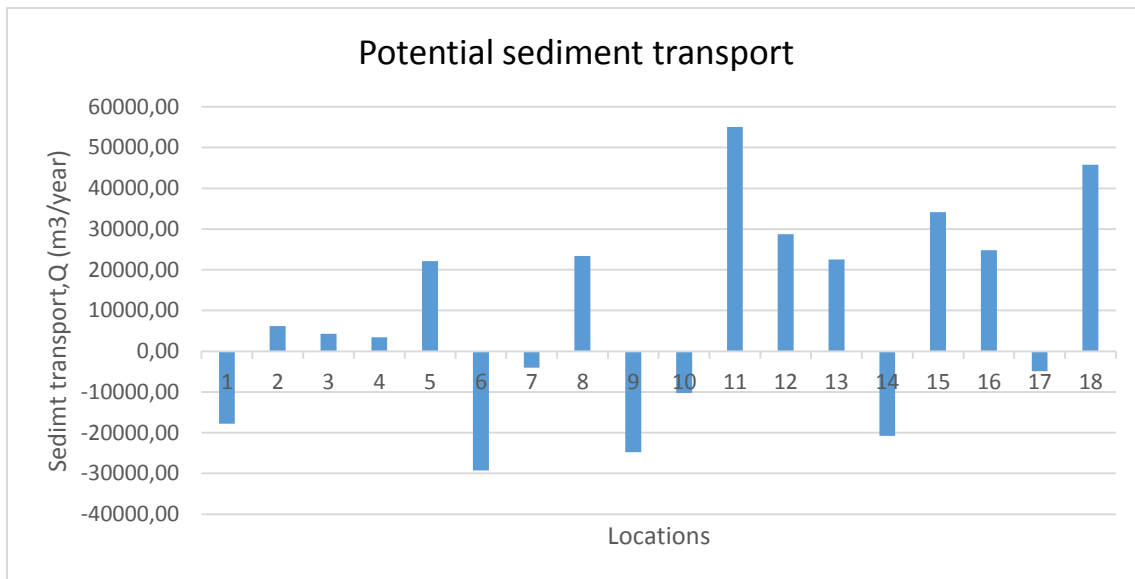


Figure 40. Average potential sediment transport ($m^3/year$). Calculated from 1961 to 2011.

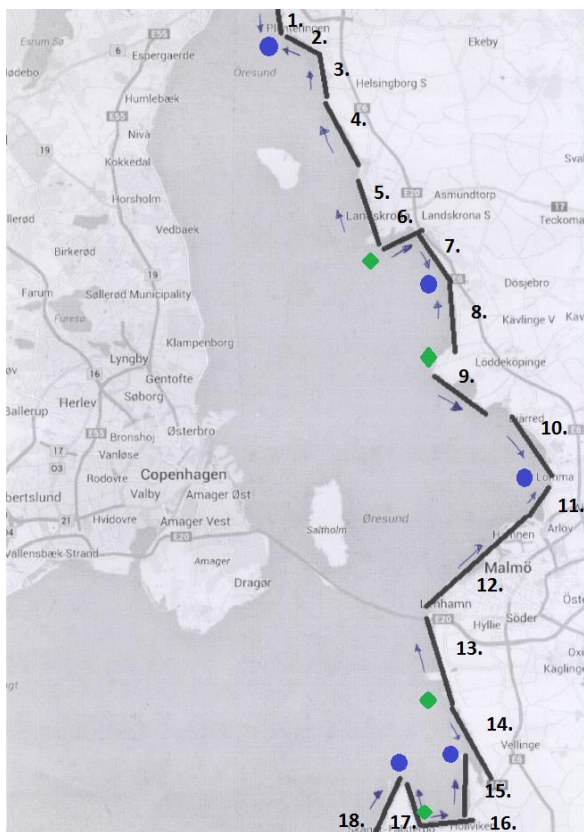


Figure 41. Map over the potential sediment transport. Calculation based on WAM results. Blue circles represent potential accumulation points, green diamonds represent potential erosion points.

With these results, it is easy to draw a conclusion about where sediment could be accumulating or where erosion might occur. These points correspond to a change from negative to positive (or vice-versa) in Figure 40. The result in Figure 40 can be interpreted as the forces acting on the coast line.

Figure 41 shows a map of these schematic potential sediment movements. Note that the arrows only represent the directions of the potential movements and have no relationship with the amount of sediment actually transported (see Chapter 8.4.1).

The potential accumulation points would occur south of Helsingborg, in the center of Lundåkra bay and Lomma bay, at the horn of the bay outside of Vellinge and North of Falsterbo. On the contrary, erosion point could be found outside of Landskrona and Barsebäck, a location situated between Malmö and Vellinge and in the bay of Höllviken.

The modeled results in Bjärred are confirmed by another study conducted by De Mas and Södergren (2010). According to that study, approximately 20,000 $m^3/year$ of sediment is transported southward. For Falsterbo, the result coincides with what Hanson and Larson (1993) found. According to them, the potential sediment transport in the area of Falsterbo would be about 40,000 $m^3/year$ towards north.

It is worth noting that when the values of sediment transport shifts from a low value to a high value, or vice versa, within the same positive or negative half of the quadrants, there probably would be sediment transport as well. One example is for location 4 and 5 (on the map), location 5 has

significantly larger transport than location 4 (both of them had transport arrows indicating northward), which indicates that there is erosion at location 5 and accretion at location 4.

As mentioned in the previous chapter the cross-shore sediment transport is not taken into account, which means that there might be other patterns that are not visible in the results of this study.

One limitation of the results displayed in this chapter is that it does not consider that there might be a seasonal variation between the four seasons.

Roses of potential sediment transport for different locations can be found in the appendix, pages IX to XI.

8.5 Climate change

8.5.1 Input

Anthropogenic activities, such as the burning of fossil fuels, are expected to influence the climate over the coming centuries. According to IPCC (2007) an increase of 20 % in the wind speed could be expected, and the wind over Nordic countries could progressively become more dominated by wind coming from the West. Although in their new report, IPCC (2014) states that this is not an accurate assumption. This scenario was simulated anyway in order to test the sensitivity of the waves in the area to changes in wind speeds and directions.

To perform this test, a period of one year presenting a big storm was chosen. A wind speed of 28 m/s was observed in 1973 and this year was selected (from January to December).

West winds were at the present date of this study the most represented but this tendency was thought to become even more prominent during the next century.

In order to evaluate the evolution of the wave climate in respect to these climate changes, three test runs were conducted with adapted input parameters. The first run was completed with modifications in both wind speed and direction (ClimateB), then the effect of a wind direction (ClimateD) and a wind speed (ClimateS) modification were tested separately. For a few tested months all the wind speed were multiplied (or not, depending on the run) by a factor of 1.2 and the wind directions were modified (or not, depending on the run) by the following (arbitrary) formula:

$$d = d + (270 - d) / 2 \quad (17)$$

The effect of equation 5 on the wind direction can be seen by comparing Figure 42 and

Figure 43. Figure 42 shows the unchanged wind directions observed in 1973 (SMHI), and

Figure 43 shows the wind direction distribution after modification. The observed values were quite similar to the ones observed over the 50 years of available data (see Figure 4 in Chapter 5). It is worth noting that the modification excludes the directions from 0 to 135 degrees and from 315 to 360 degrees. This might seem like a dramatic overestimation of the effect that the climate change might cause, but the major focus with this test was to study extreme condition changes.

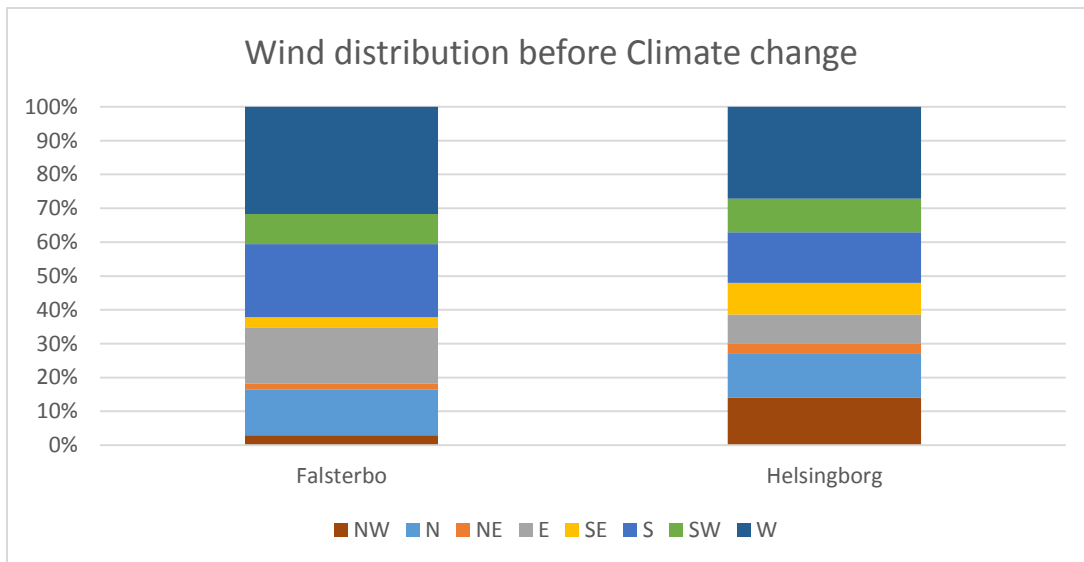


Figure 42. Wind distribution before climate change at meteorological stations Falsterbo and Helsingborg.

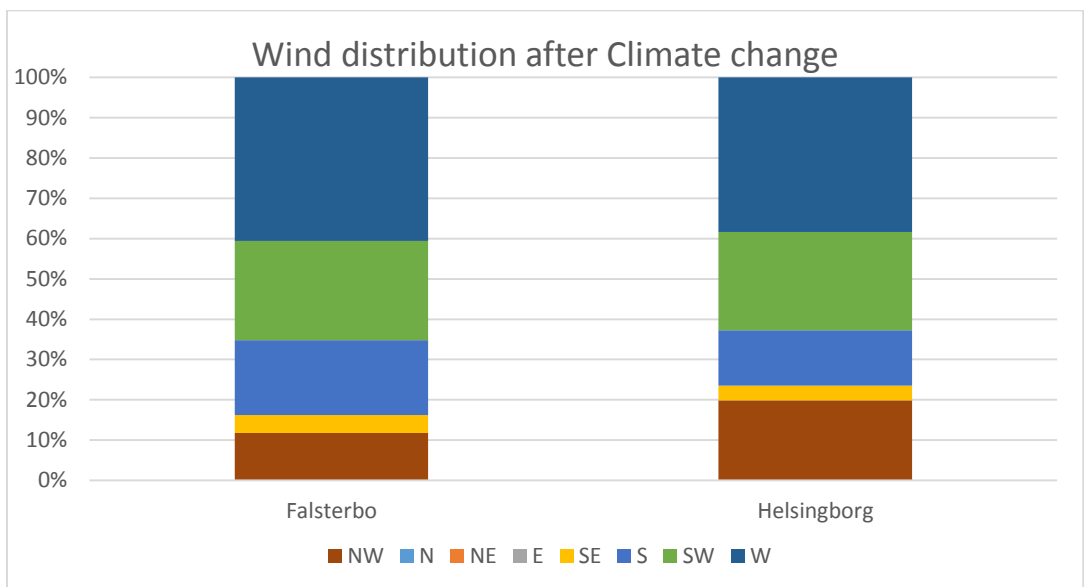


Figure 43. Wind distribution after climate change at meteorological stations Falsterbo and Helsingborg.

The effect of the increase in wind speed was rather straight forward. The average wind speed after changes was 10.9 and 9.0 m/s for Falsterbo and Helsingborg respectively, this should be compared with the unchanged wind speed averages of 9.1 and 7.5 m/s. The maximum wind speed was increased from 28 to 33.6 m/s for Falsterbo and from 24 to 28.8 m/s for Helsingborg.

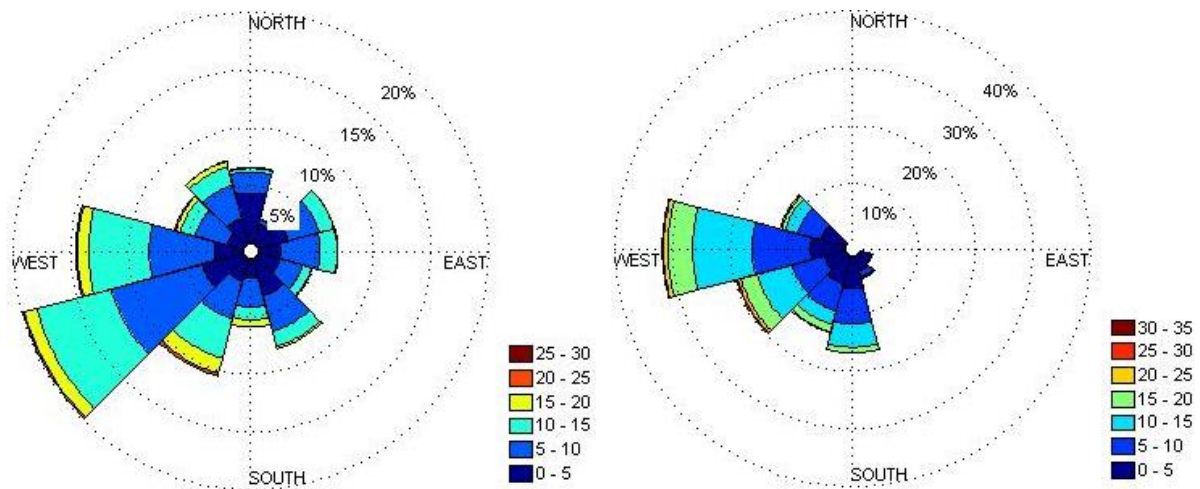


Figure 45. Wind rose for Falsterbo, before (left) and after (right) climate change. The scale is in m/s.

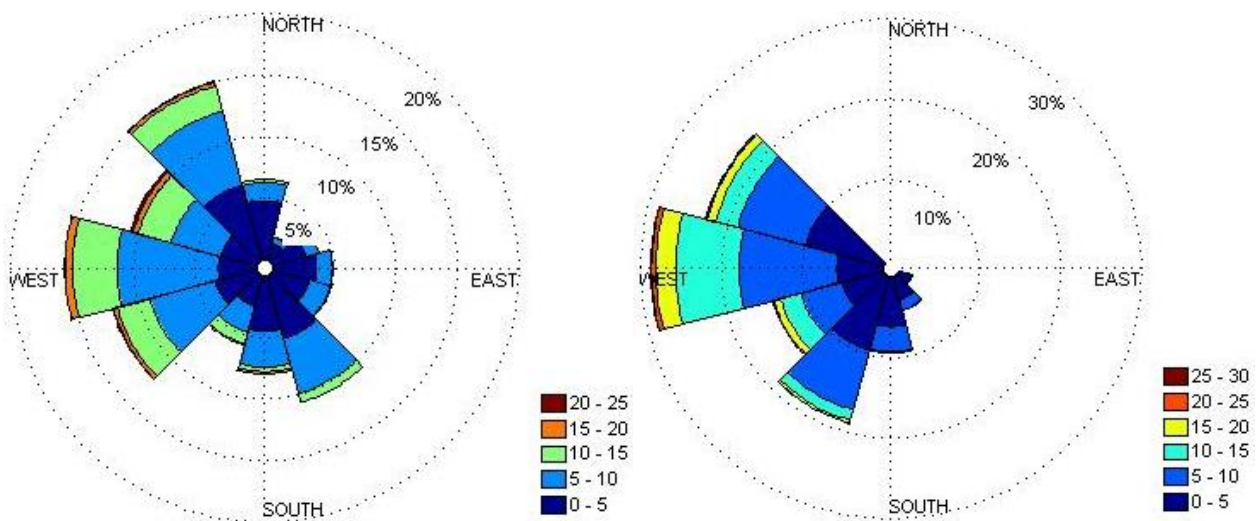


Figure 44. Wind roses for Helsingborg, before (left) and after (right) climate change. The scale is in m/s.

The transformation of the wind mentioned above can be seen easily in Figure 45 and Figure 44. These wind roses show how these modifications impact the distribution and strength of the winds, i.e. that the winds becomes more west-ward and that the percentage of the stronger winds increase at the cost of smaller ones.

8.5.2 Results

In this paragraph the results from this climate change simulation will be analyzed. Through the whole paragraph the results from the different runs will be referred to as follow: ClimateB refers to the run with both wind speed and direction modifications, ClimateD refers to the run corresponding to the

wind direction modifications, ClimateS refers to the run corresponding to the wind speed modifications, and the non-modified input run will be called ClimateN.

Figure 47 and Figure 46, although both displaying the wave direction distribution, each of them allow the reader to focus on a different aspect of the presented data.

Looking at Figure 46 one can easily see the main directions of propagation after modification for climate change, which were Westward directions. The same pattern can be noticed for the result before the modifications but not as pronounced. This increase in the waves coming from the west agrees with the change of wind setup.

In Figure 47 the focus was more on the proportions of each direction. It is easy to see the dramatic reduction of directions N to S, from representing 39% of the total directions they dropped down to 16%. At the same time, the opposite behavior was observed for the directions SW-W-NW.

Results from ClimateD and ClimateS are not displayed in Figure 47 and Figure 46 due to that they would only match the results from respectively ClimateB and ClimateN.

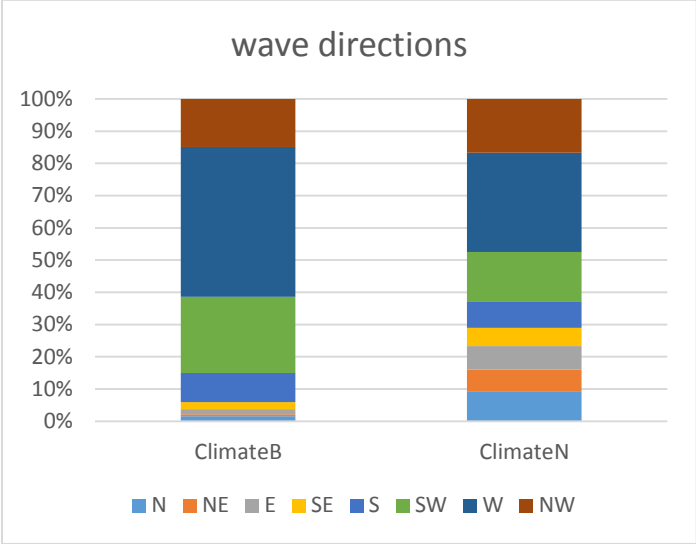


Figure 47. Wave direction of propagation distribution for both changed and unchanged conditions.

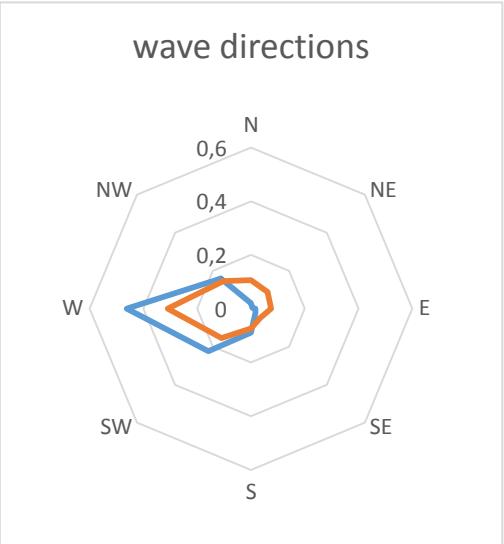


Figure 46. Wave direction distribution for both ClimateB (blue) and ClimateN (orange) conditions.

Figure 48 indicates that the area is more sensitive to an increase in wind speed regarding the average wave height. Of course the Climate run increases the average wave height of the western directions, but also decreases it for all the other directions. The ClimateD run does not increase the average wave height of western direction, it produces more waves in this direction but does not make them larger in average. Concerning the other directions, ClimateD decreases the average wave height.

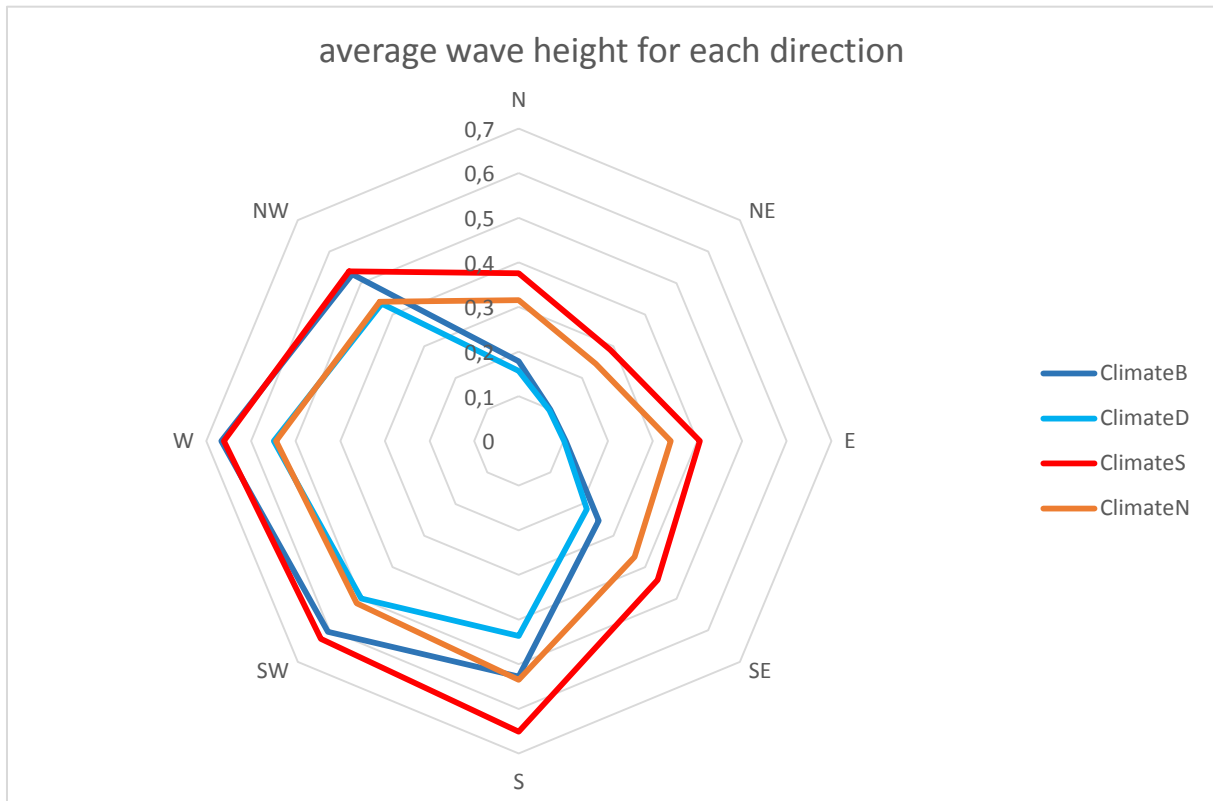


Figure 48. Average significant wave height (m) for each direction.

The resulting change in wave heights is seen in Figure 49. A decrease of smaller waves can be observed: waves smaller than 1 m decrease from 92% to 84% of the total waves. At the same time larger waves (greater than 1.5 m) appeared and represent up to 5% instead of 2% of the total waves.

Results from ClimateD and ClimateS are not displayed in Figure 49 due to that they would only match the results from respectively ClimateB and ClimateN.

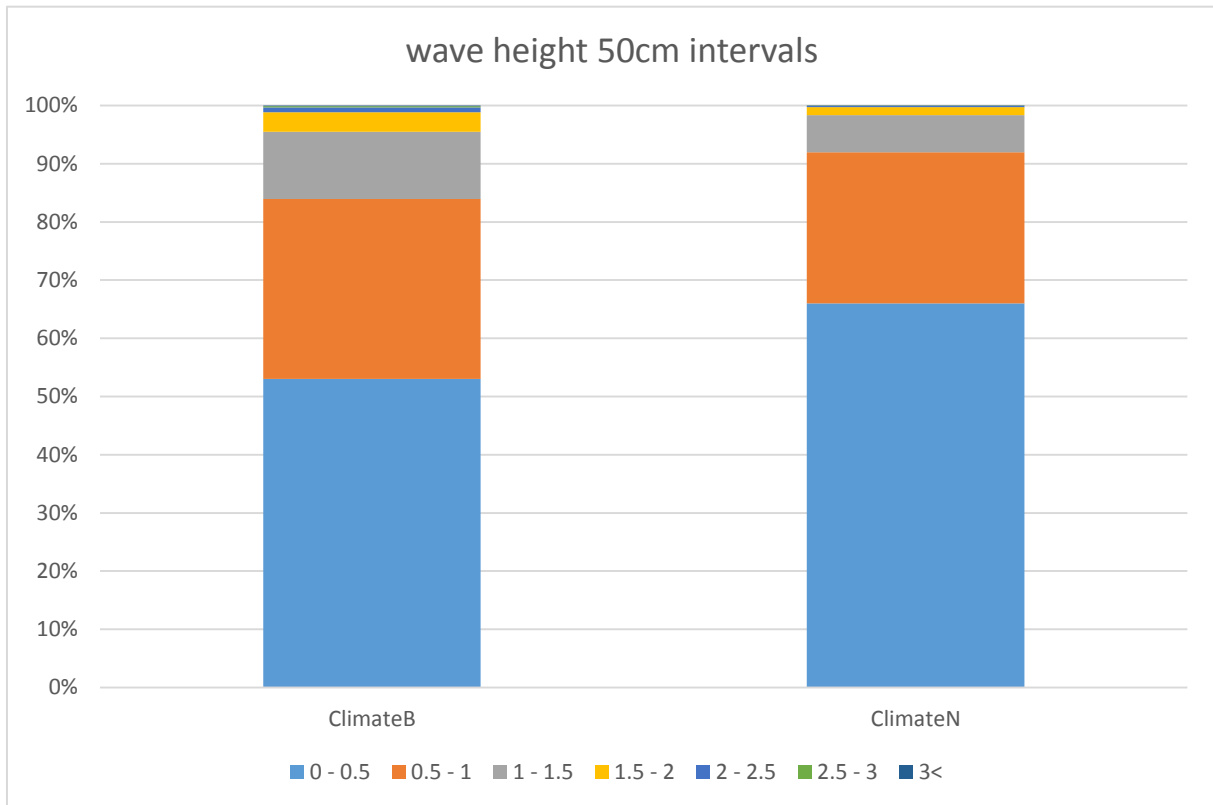


Figure 49. Proportion of wave height per 50 cm intervals.

In Figure 50 all changed (Wave height ClimateB) versus unchanged (Wave height ClimateN) waves for all time and locations were scatter-plotted. The linear regression indicates an overall of 1.2 multiplication factor for waves from unchanged to changed conditions. This means that if the climate change input setup is to happen in the future, larger waves would become more common and would have implication on present infrastructure and should be considered in future planning. This may seem contradicting to what have been mentioned in previous chapter 6.2 in regards to that a linear increase of the wind does not in general lead to linear increase of the wave height. This might be the result of that in some locations, especially at the Danish coastline, the waves might have been decreased as a result of the more westerly wind in this run.

Each wave height was coupled with its direction (color of the points) in order to get an overview of the relation between the change in wave height and the original direction of the waves. In other words, the color of each point corresponds to the direction where the wave before climate change comes from.

An unexpected pattern can be seen for smaller waves: wave height up to 1 m for one setup while the other setup gives in some cases almost a 0 m response. This was due to the modified distribution of wind directions that can produce great change of fetch length. Under the trend line the directions represented by the colors red, cyan and magenta are the most affected by this effect. Which was expected because the corresponding directions were the most modified (SE-E-NE wind were changed into more western winds).

Above the trend line the same pattern can be observed with the western waves (colored in blue, black and pink). These points correspond to waves created by western winds that were from other directions before climate change.

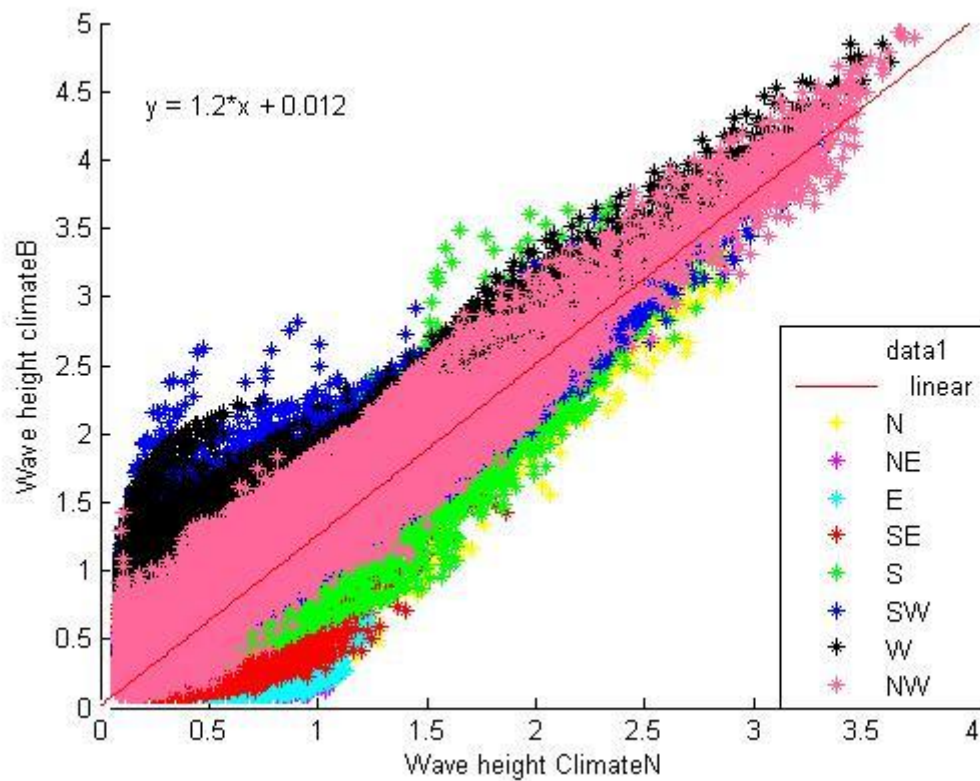


Figure 50. Significant wave height (m) comparison for all locations and all time.

Figure 51 displays the same results as Figure 50 but shows every direction of propagation in a separate figure. The advantage is that one can analyze easily the influence of the conditions change on the waves from every direction.

The trendline used in all the graphs is the same and is the global trendline. One can notice that all the westward directions are increased (above the trendline) whereas the eastward direction are reduced and present smaller waves.

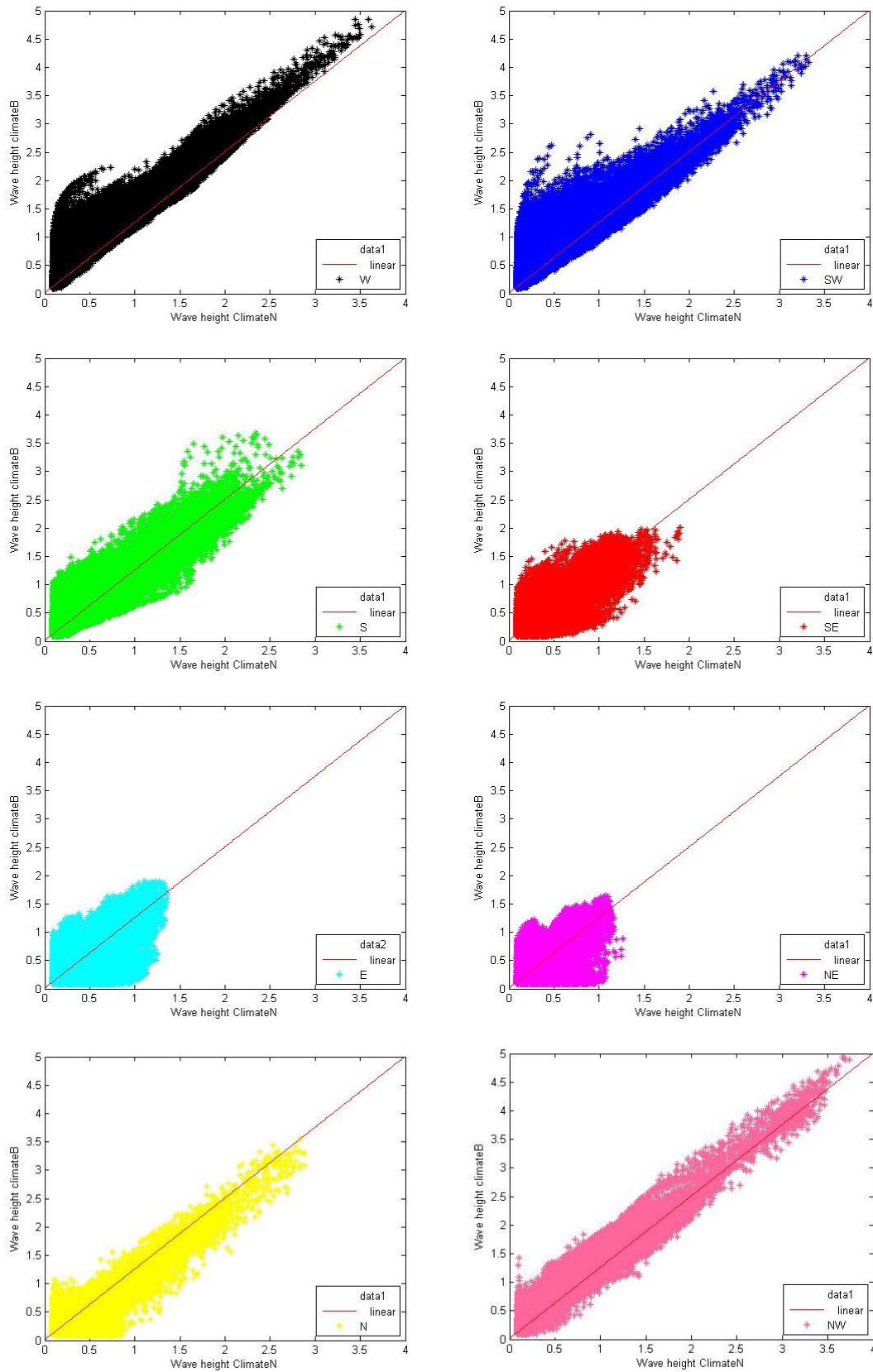


Figure 51. Significant wave height (m) comparison for all location and all time, separated by direction of propagation of climateN waves.

Figure 52 to Figure 53 displays a comparison of wave heights, before and after a change in climate conditions, for four specific locations: Helsingborg, Copenhagen, Malmö and the southern midpoint of Öresund. In Figure 52 the percentage of increase in wave height were 22, 15, 20 and 30% for respectively Helsingborg, Copenhagen, Southern midpoint and Malmö. The fact that Malmö present the largest increase can be linked to the larger fetch length of this location for the dominating direction (SW-W). This behavior has already been discussed in Chapter 5. The R^2 value indicates that the increase in wave height was consistent for all four locations and time.

Figure 54 shows that a change in wind direction alone does not affect the wave height much. Depending on the location, the waves can be larger or smaller, this effect can be explained by the modification of the fetch length resulting from the wind direction change. Here, Malmö is the location presenting an increase, which is due to the open sea area on the South-West direction (one of the dominant directions after modifications of the wind).

Figure 53 presents results from the ClimateS run. The analysis is rather simple, all locations have almost the same sensitivity to a 20% increase in wind speed: a 23% increase of the wave height.

The result from this simulation should be considered as an indication rather than an exact representation of type of scenarios that could occur in the future.

This simulation indicates that the wind speed modification affects the results significantly more than the wind direction modification. Alone, a change in wind direction does not seem to have a strong effect on the wave climate, but it can increase the effect of a wind speed modification if coupled with it.

Overall, the wind speed should be considered as the most influential parameter.

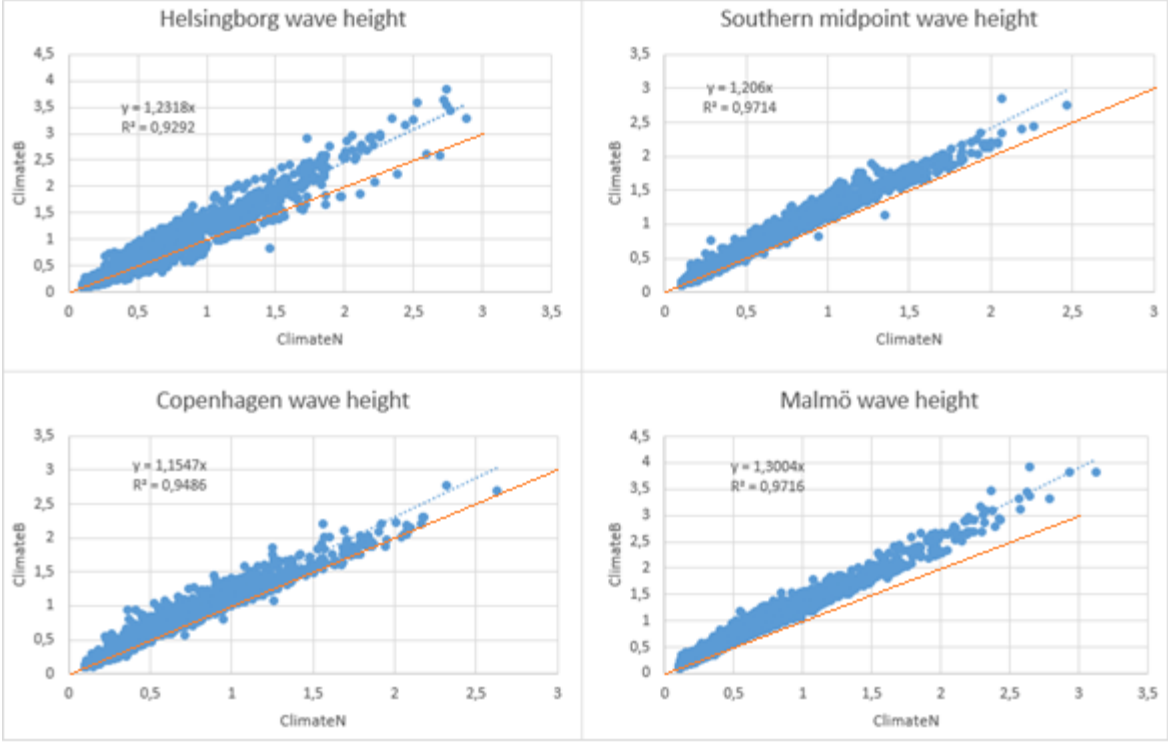


Figure 52. Significant wave height (m) comparison between ClimateB and ClimateN. The 1-1 line is in orange.

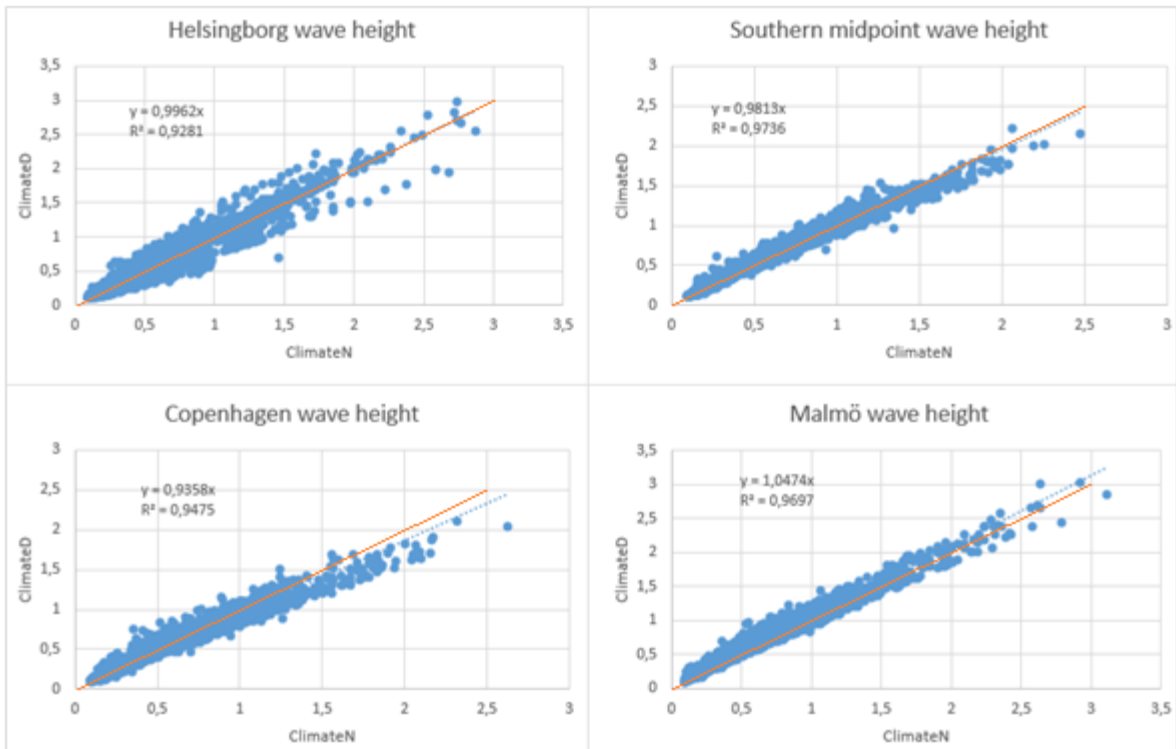


Figure 54. Significant wave height (m) comparison between ClimateD and ClimateN.

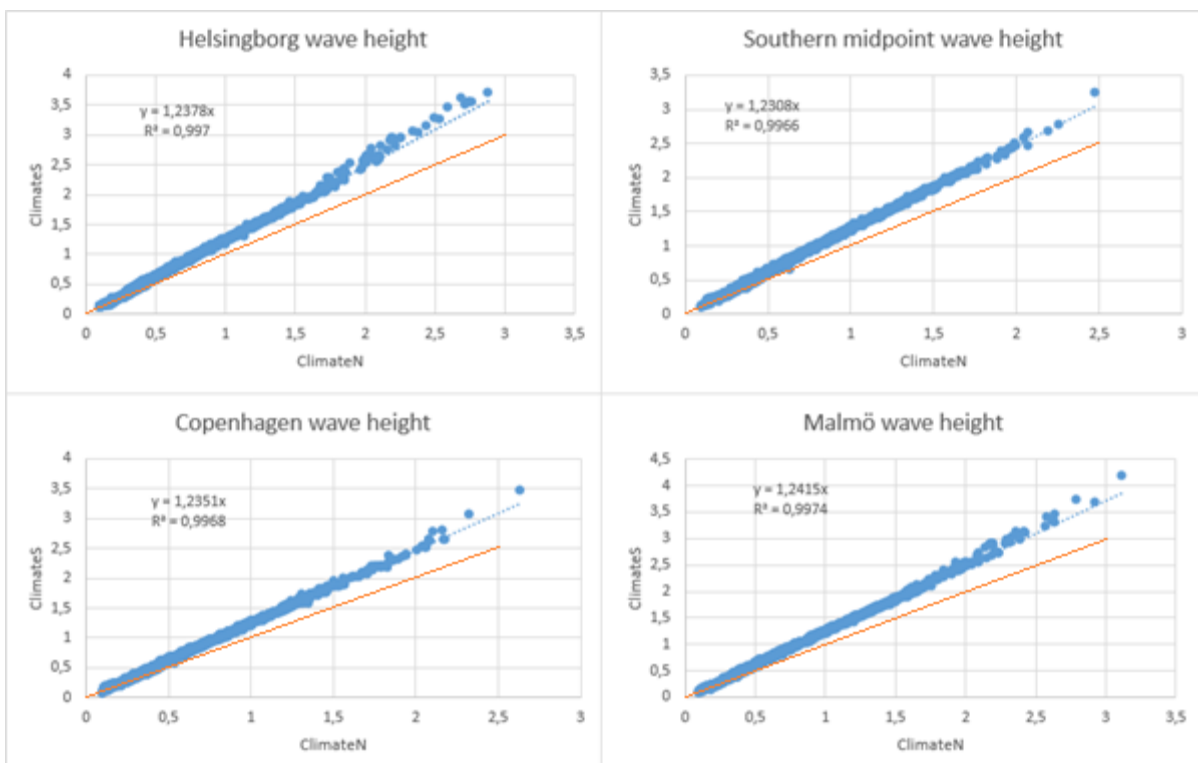


Figure 53. Significant wave height (m) comparison between ClimateS and ClimateN.

9 Discussion and Conclusion

During the study, a sensitivity analysis was performed in order to test the response of the model to different changes in the input. Multiple parameters and conditions were tested, here is a short summary of the conclusions drawn from the sensitivity analysis. A change in the time step used for the calculation does not have a significant impact on the precision of the model but increases the computation time so one should use the longest time step possible without encountering stability problems. The relation between wind speed and wave height is not linear but cubic so storm conditions can create surprisingly large waves compare to calm period. And the wave direction has a direct impact on the fetch length thus it can also influence the wave height, but has a different effect depending on the location. By examining the grid it could be thought that the strait was closed between Helsingborg and Helsingör, so a test was performed where the land cell in Helsingör was replaced by a water cell. The results did not show that the change had a significant effect on the wave climate. It was then concluded that WAM can model wave passing through the corners of two diagonal touching cells. The area of Kattegat was of concern as well. Two runs were conducted, one including and one excluding the area. The conclusion was that this change did not have a strong effect on the results so it was decided to exclude the area in order to reduce the computation time. The last test performed in this sensitivity analysis was concerning the cell size of the grid. A coarse and a fine grid were assessed, they gave almost indistinguishable results and precision when compared to measurements.

The calibration of the model was conducted by analyzing the influence of the bottom friction and the wind input. The bottom friction coefficient was increased by values from 1 to 400 and the increasing of this coefficient did not give the desired improvements of the results, i.e. reducing the wave height of especially smaller waves. Thus the bottom friction was kept at its default value. Concerning the wind speed, three different set ups were assessed; one with unmodified wind, a second with an increase of 20% of every wind speed value and a third one using a logarithmic increase of wind speeds. The best results were obtained using the set up three and therefore this one was chosen. It was noticed that the wind speed in Falsterbo meteorological station was in average 50% higher than in Malmö and 60% higher than in Helsingborg. Thus multiple options were considered. The use of Helsingborg alone lead to a decrease of precision, specifically underestimating the wave height in comparison to measured data. Using the meteorological station in Malmö coupled with Helsingborg was reconsidered but gave no better results than using Helsingborg alone. Last, wind speed in Falsterbo was divided by 1.5 (in order to match the average in Malmö) before applying the logarithmic growth to the whole wind climate. This option gave the best results and was considered to result in a good precision when compared to measurements at both tested time periods (1999 and 2013).

The generally small fetch length in the Öresund region results in a wave climate dominated by smaller waves, i.e. less than 1 m. Studying the accumulative probability, it could be seen that 60% of the waves are 0.5 m or smaller and that around 5% of the waves are larger than 1 m in coastal areas. Although, storms might give significantly larger waves, e.g. the storm in November 1973. Due to its unsheltered conditions Falsterbo presents in general larger waves than the rest of the strait. The return periods of a 2 m wave in most of the coastal areas are around 10 years and a typical 1 year wave is 1.3 m. When studying the monthly average significant wave height it can be concluded that the summer months tend to result in lower averages compared to the winter months, although the differences are in the tens of centimeters. Similar pattern can be observed for the monthly average mean period. The monthly average peak period does not seem to vary over the year.

The calculation of the run-up height was greatly simplified in order to obtain comparable values along the Swedish coast line. Examining the monthly average it was observed that April had significantly lower averages compared to the other months, the underlying reason seemed to be a coupled effect of directions of the propagation of the waves and the water levels in the strait of Öresund. The global average run-up level appears to be around 0.4 m at the studied locations, although storm conditions can produce combination of run-up heights and water levels around 2.5 m. Interestingly enough, of the studied locations Falsterbo has the lowest maximum value, this could be due to the water levels being low during storm conditions. Similar behavior was observed by Dahlerus and Egermayer (2005) at the nearby location Ystad.

A simplified assessment of the sediment transport along the Swedish coast was conducted in order to gain an overview picture of the potential sediment transport, i.e. the forces acting on the coast line. The results show that Helsingborg, the center of Lundåkra bay and Lomma bay, the horn of the bay outside of Vellinge and North of Falsterbo do appear to be locations where accumulation of sediment are occurring. According to these calculations erosion would take place outside of Landskrona and Barsebäck, at a location situated between Malmö and Vellinge and in the bay of Höllviken. This seems to coincide at the two locations Falsterbo and Bjärred (Hanson and Larson, 1993, respectively De Mas and Södergren, 2010), due to lack of research for comparison, the results at the other locations cannot be assessed properly. The results were obtained without regards to the grain size at the locations and thus it only represents the sediment transport that would occur if sand was present. Still, they can be used as a schematic guide for the sediment movement in the strait.

The tested setup for assessing potential climate change scenarios are based on the IPCC report of 2007: an increased wind speed of 20% and more Westward directions for the wind. This assumption is outdated, however this modeled scenario gives an indication of how sensitive the wave climate in Öresund is to changes in the wind climate. The conclusion was that the wave height would be more influenced by an increase in wind speed, and that a wind direction change would mainly be an aggravating factor but not significant by itself. Overall, a 20% increase in wind speed produces an increase in significant wave height around 23%. If the change in wind direction is included the percentage of increase in wave height ranges from 15 to 30%. These differences of increases are due to the potential fetch lengths at the different locations. Which means that the average wave in Malmö is from ... to ... etc.

When hindcasting the wave climate there are multiple potential uses of the results. In this thesis a few of them have been presented and were mainly concerning coastal processes. These results can be used as a first guideline when trying to choose the right type of protection because different types of protections work for different types of erosion processes. During the construction or renovation of piers in harbors, it is important that they are optimized in terms of wave protection and sand transport, which is also something that could be extracted from wave climate modeling. Also, the analysis of the combination of water levels and wave run up heights can be useful for an analysis of flood risks. And another application of this thesis results could be an investigation of natural coast protections (i.e. sand dunes) – if they are capable of withstanding an extreme storm today and in the future. For all these different applications the results from this thesis can give a general idea of the wave climate and wave conditions on the shore.

Reference list

Publications

F. Ardhuina, L. Bertottib, V. Filipettob, J.R. Bidlotc, J.M. Lefevred, L. Cavalerib, P. Wittmanne, *Comparison of wind and wave measurements and models in the western Mediterranean Sea*, Ocean Engineering 34 (2007) 526–541

S. Blomgren, H. Hanson, M. Larson, 1999, *Numerical modeling of the wave climate in the southern Baltic sea*, Journal of Coastal Research, 2001, 17(2):342-352

CEM, 2002a. *Coastal sediment properties (Part III, Chapter 1)*. In: *Coastal Engineering Manual (CEM)*. Washington DC: US Army Corps of Engineers.

CEM, 2002b. *Water wave mechanics (Part II, Chapter 1)*. In: *Coastal Engineering Manual (CEM)*. Washington DC: US Army Corps of Engineers.

CEM, 2003, *Surf Zone Hydrodynamics (Part II, Chapter 4)*. In: *Coastal Engineering Manual (CEM)*. Washington DC: US Army Corps of Engineering.

CEM, 2006. *Meteorology and Wave Climate (Part II, Chapter 2)*. In: *Coastal Engineering Manual (CEM)*. Washington DC: US Army Corps of Engineering.

COWI/DHI/LIC, 1990. *Miljökonsekvensbeskrivning för fasta förbindelser över Öresund. Underlagsrapport 1, Östersjöns vattenmiljö*, Malmö: SVEDAB.

C. De Mas De Mas, J. Södergren, 2010. *Modeling coastal erosion in Bjärred, Lomma municipality - Long-term evolution and protective measures*. Division of Water Resources Engineering, Department of Building and Environmental Technology. Lund University.

Den svenska Öresundsdelegationen, 1987. *Miljökonsekvensbeskrivning för fasta förbindelser över Öresund. Underlagsrapport 10, Hydrografiska undersökningar i Öresund: mätningar och modellberäkningar*, Malmö: SVEDAB

Engineering Geology Department at Lund University

Gunther, H., K. Hasselmann and P.A.E Janssen, 1992: Report NO.4, *the WAM Model Cycle 4*, Edited by Modellberatungsgruppe, Hamburg.

H. Hanson, M. Larson, 1993, *Strandtransport och Kustutveckling Vid Skanör/Falsterbo*, Institutionen för Teknisk Vattenresurslära, Raport 3166.

H. Hanson, M. Larson, 2008, *Implications of extreme waves and water levels in the southern Baltic Sea*

K. Hasselmann, 1962: *On the nonlinear energy transfer in a gravity-wave spectrum. 1. General theory*, JFM, vol. 12, 481-500.

S. Iriminger-Street, 2011, *Wave atlas along the south - eastern coast of Sweden*, Examensarbete, TVVR 11/5007, Division of Water Resources Engineering, Department of Building and Environmental Technology, Lund University

P.D. Komar, 1998. *Beach processes and sedimentation*. Upper Saddle River: Prentice Hall Inc.

G.J. Komen, L. Cavaleri, M. Donelan, K. Hasselmann, S. Hasselmann, P.A.E.M Janssen. *Dynamics and Modeling of Ocean Waves*, Cambridge University Press, 1994.

M. Larson, L. Xuan Hoan, H. Hanson 2011, *Direct Formula to Compute Wave Height and Angle at Incipient Breaking*, Journal of Waterway, Port, Coastal, and Ocean Engineering.

Miljöförvaltningen Landskronakommun / Toxicon AB, 1998. Landskrona havsmiljö, Toxicon AB rapport 1998:8

H. L. Tolman, 1996, *Source Terms in a Third-Generation Wind Wave Model*, Journal of oceanography, American, Metrological Society.

Van Vledder, G. P., and Holthuijsen, L. H. 1993. "The Directional Response of Ocean Waves to Turning Winds," J. Phys. Oceanogr., Vol 23, pp 177-192.

WAMDI Group, 1988, *The WAM Model - A Third Generation Ocean Wave Prediction Model*, Journal of oceanography, American, Metrological Society.

WMO *Guide to Wave Analysis and Forecasting*, Revised Edition, July, 1995

Electronic sources

Link 1: SWAN: <http://www.swan.tudelft.nl/>(available 2014-05-30)

Link 2: WAVEWATCH III

Link 3: National Encyklopedi (available 2014-05-27):

<http://www.ne.se/lang/v%C3%A4stvindsb%C3%A4lten>(available 2014-05-30)

Link 4: IOW <http://www.io-warnemuende.de/topography-of-the-baltic-sea.html>(available 2014-05-30)

Link 5: SMHI Wind data, water level data and wave data: <http://opendata-download-ocobs.smhi.se/explore/>(available 2014-05-30)

SMHI, 2014. *Inflöden till Östersjön*: <http://www.smhi.se/kunskapsbanken/oceanografi/infloden-till-ostersjon-1.4203>(available 2014-05-30)

Appendix

Strait opening test

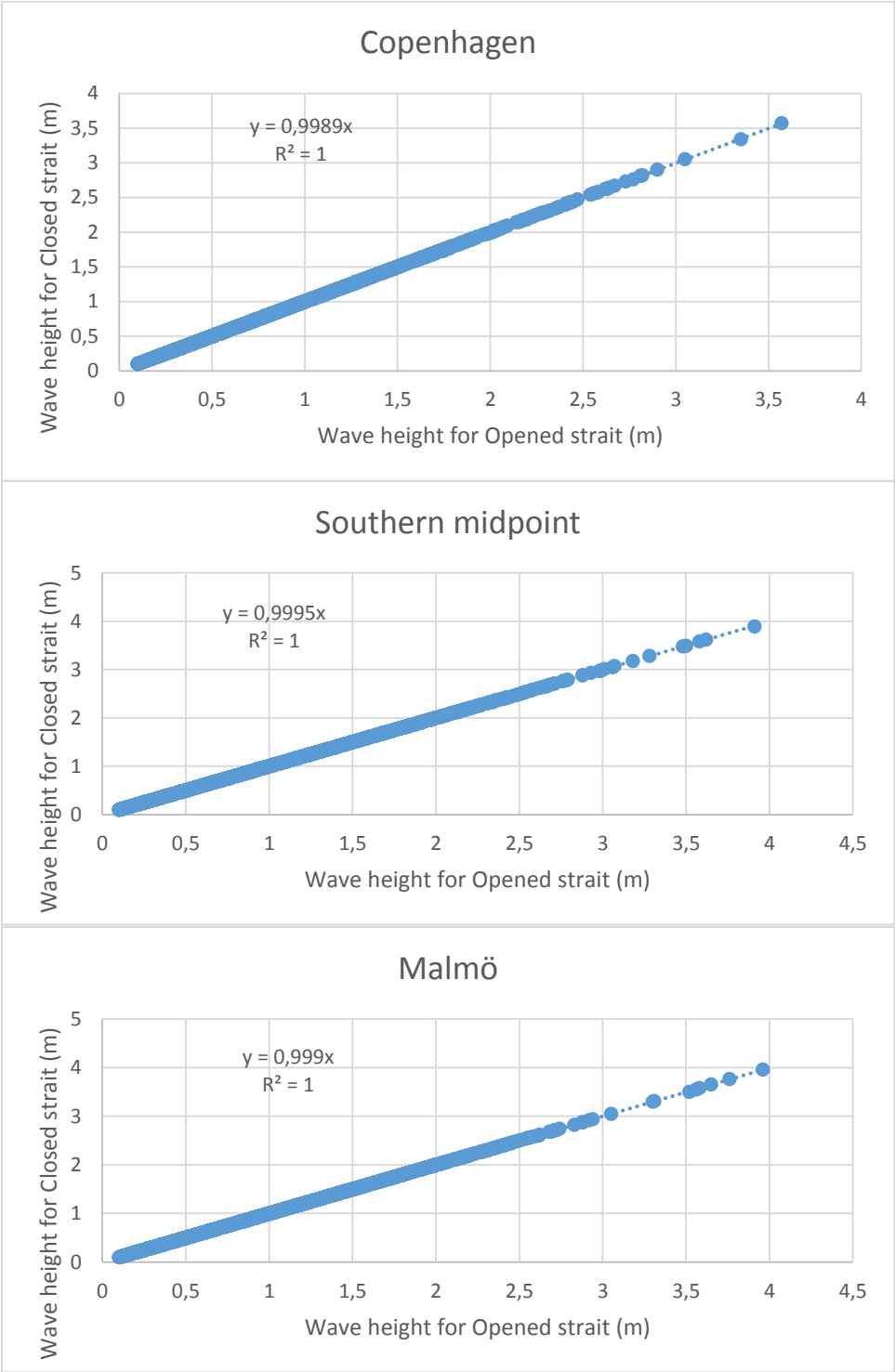


Figure 55. Scatter plot of H_s (m) before and after opening the strait between Helsingör and Helsingborg, at locations Copenhagen, Southern midpoint and Malmö.

Calibration

For all following graphs, both x and y-axis represent Hs given in meters. EGD means Engineering Geology Department, and the measurements from it are the values on the x-axis, WAM results being on the y-axis.

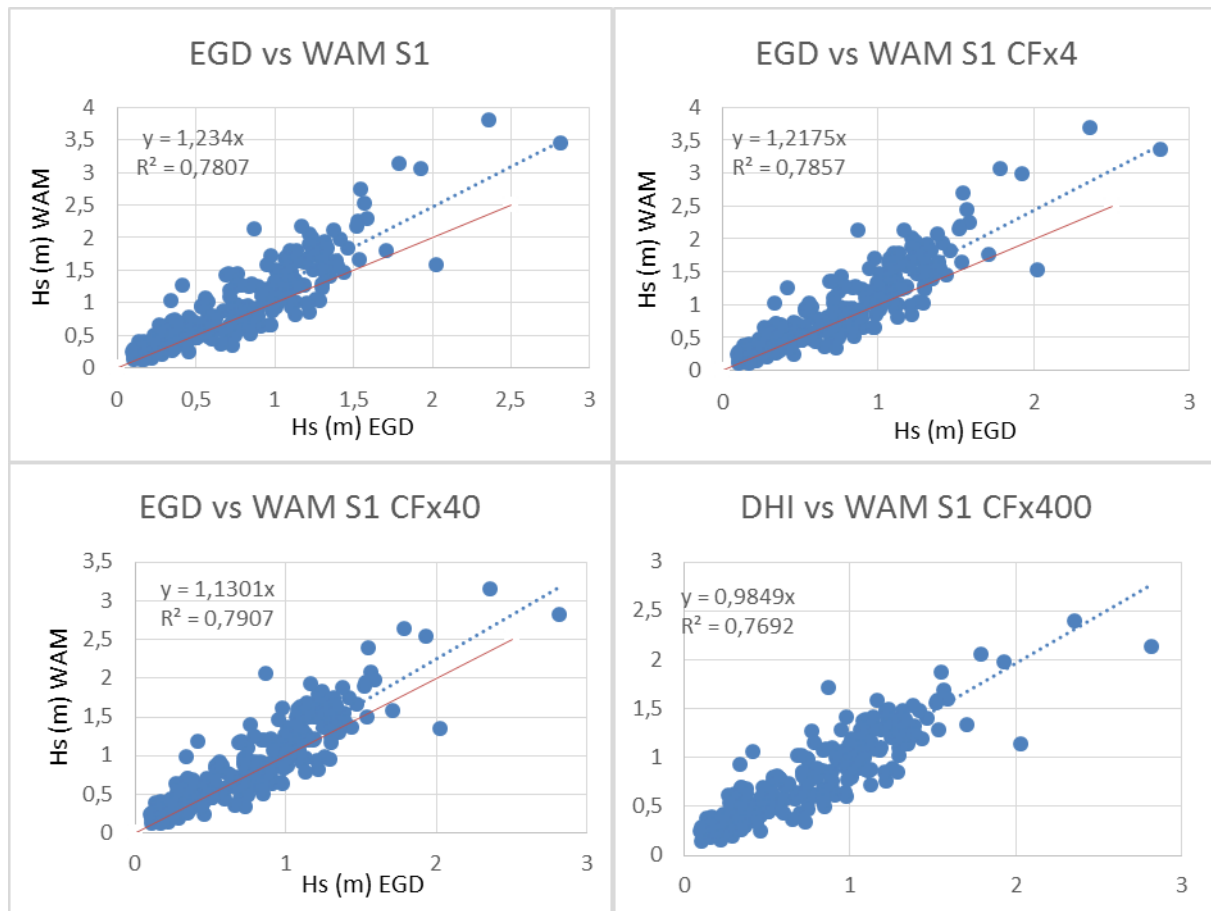


Figure 56. Significant wave height (m) comparison between Engineering Geology Department at Lund University measurements and modeled value from WAM with setup 1 and changing bottom friction coefficient. Location Drogden, 1999.

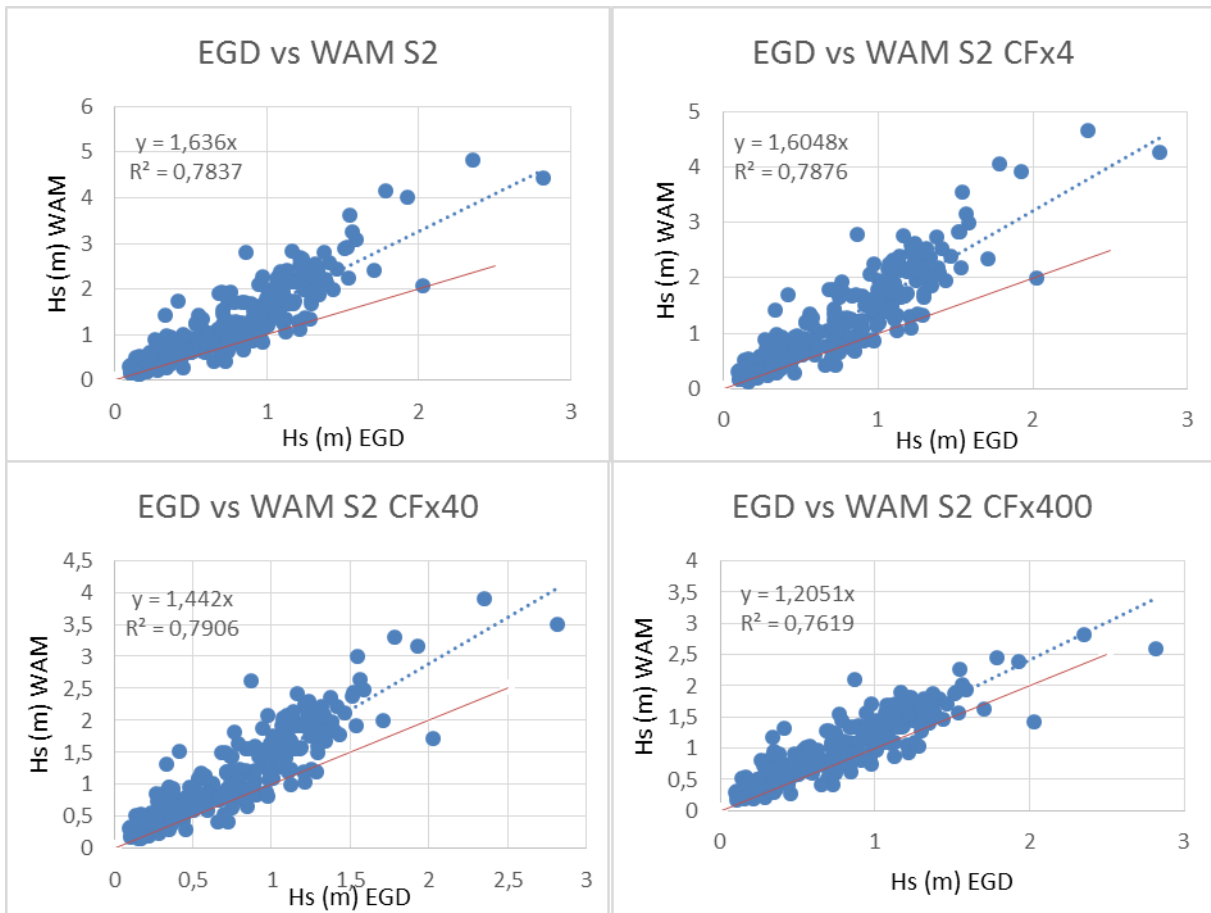


Figure 57. Significant wave height (m) comparison between Engineering Geology Department at Lund University measurements and modeled value from WAM with setup 2 and changing bottom friction coefficient. Location Drogden, 1999.

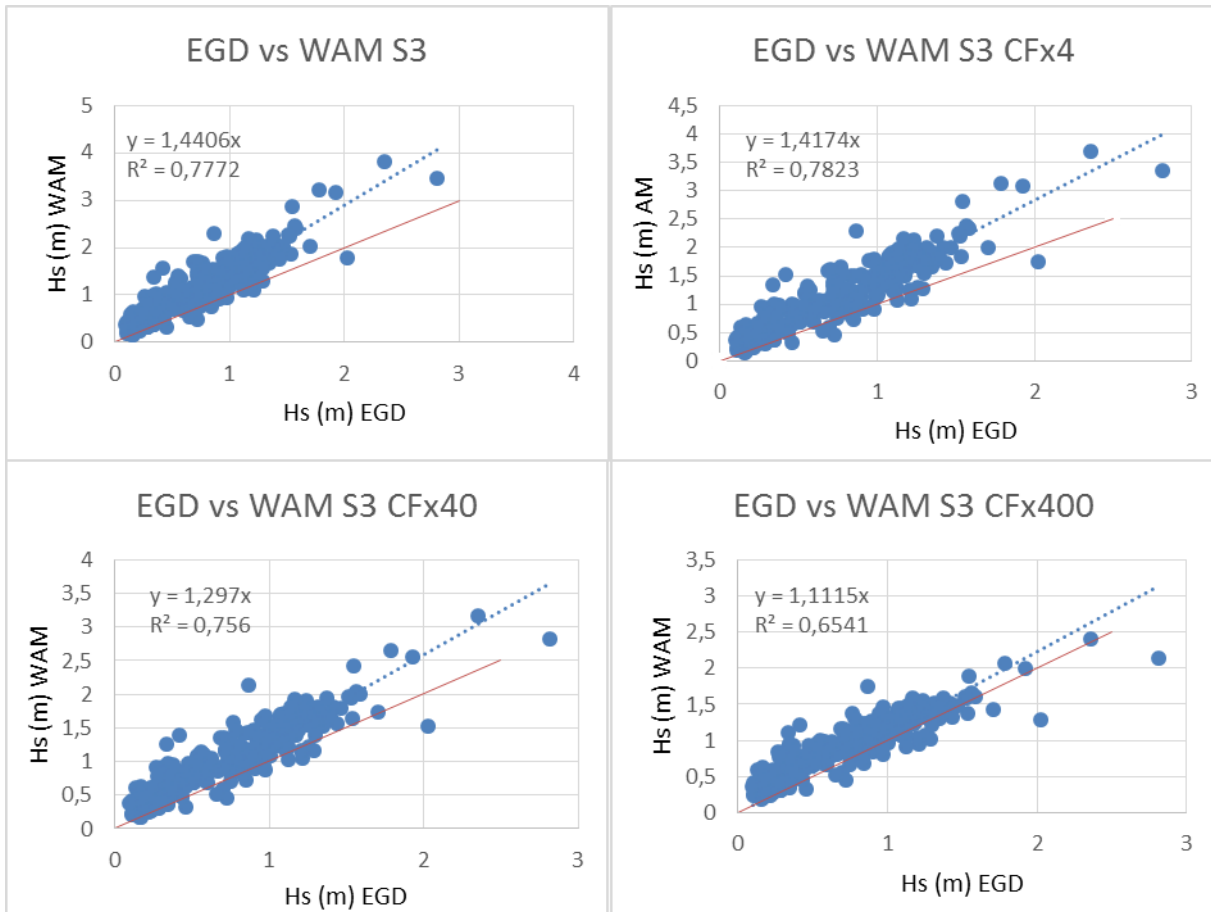


Figure 60. Significant wave height (m) comparison between Engineering Geology Department at Lund University measurements and modeled value from WAM with setup 3 and changing bottom friction coefficient. Location Drogden, 1999.

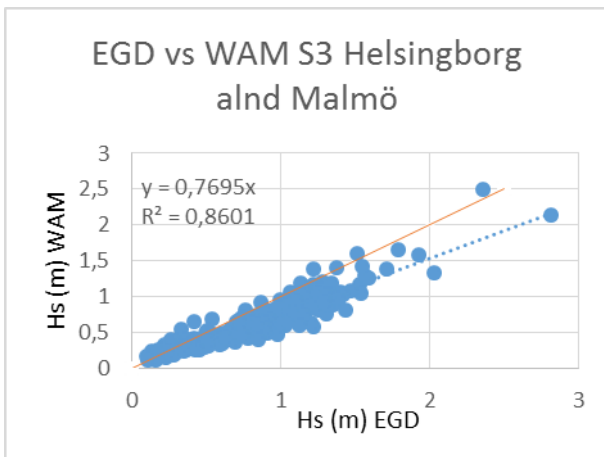


Figure 59. Significant wave height (m) comparison between EGD measurements and modeled value from WAM using wind from Helsingborg and Malmö MET. Location Drogden, 1999.

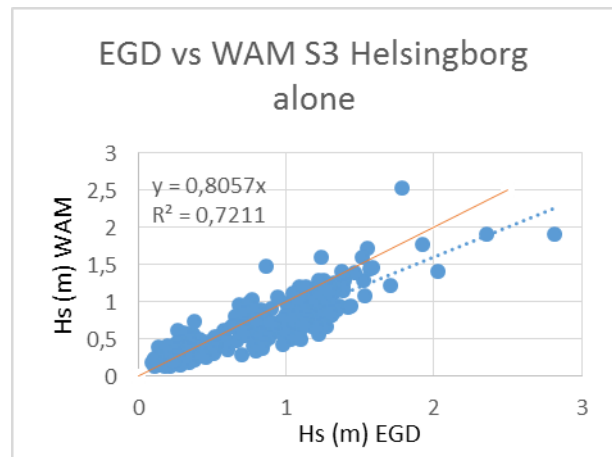


Figure 58. Significant wave height (m) comparison between EGD measurements and modeled value from WAM using wind from only Helsingborg MET. Location Drogden, 1999.

Wave roses

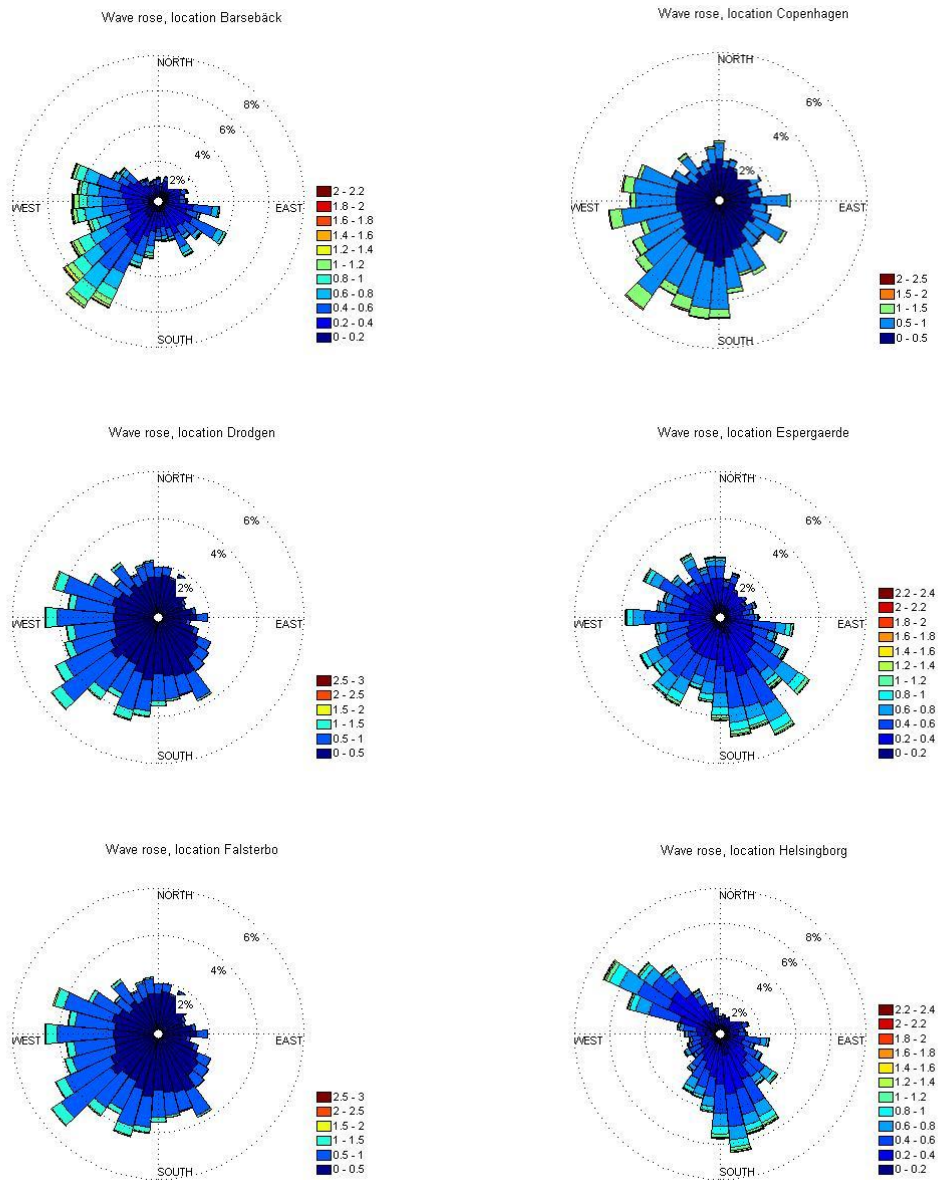


Figure 61. Wave roses for locations: Barsebäck, Copenhagen, Drogden, Espergearde, Falsterbo and Helsingborg. The scale is in meters.

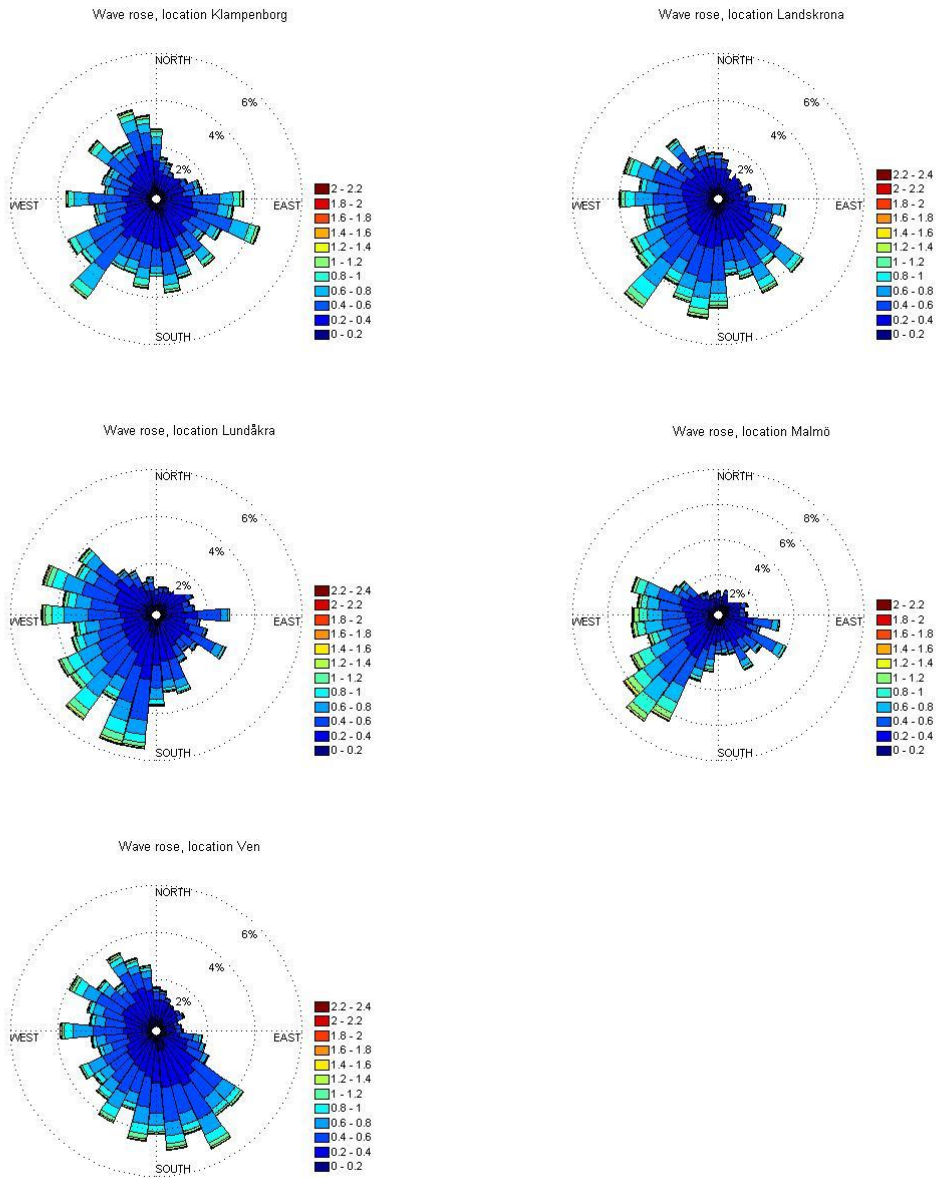


Figure 62. Wave roses for locations: Klampenborg, Landskrona, Lundåkra, Malmö, Ven. The scale is in meters.

Return period diagrams

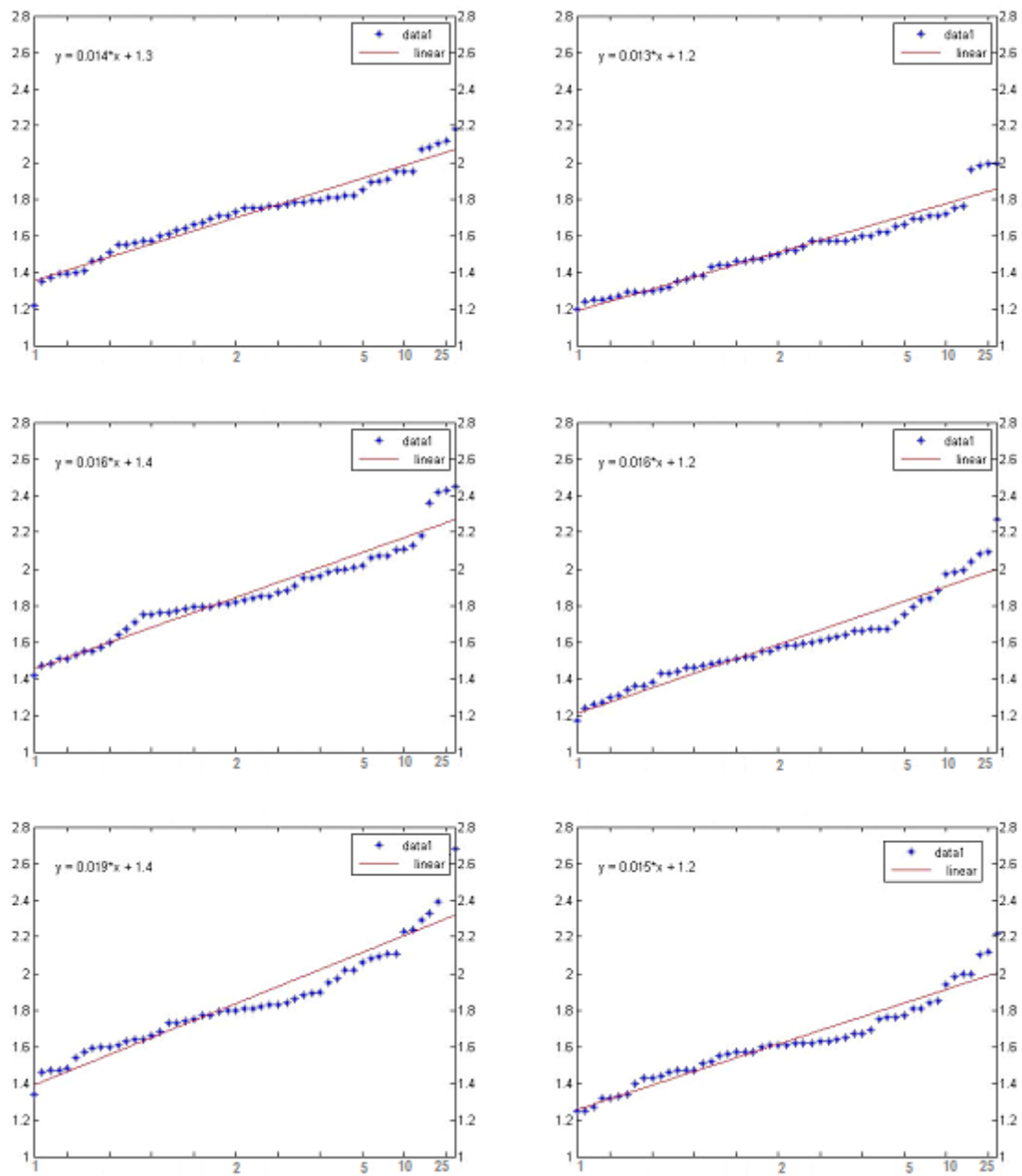


Figure 63. Return period diagram for H_s (m) for locations: Barsebäck, Copenhagen, Drogden, Espergearde, Falsterbo and Helsingborg.

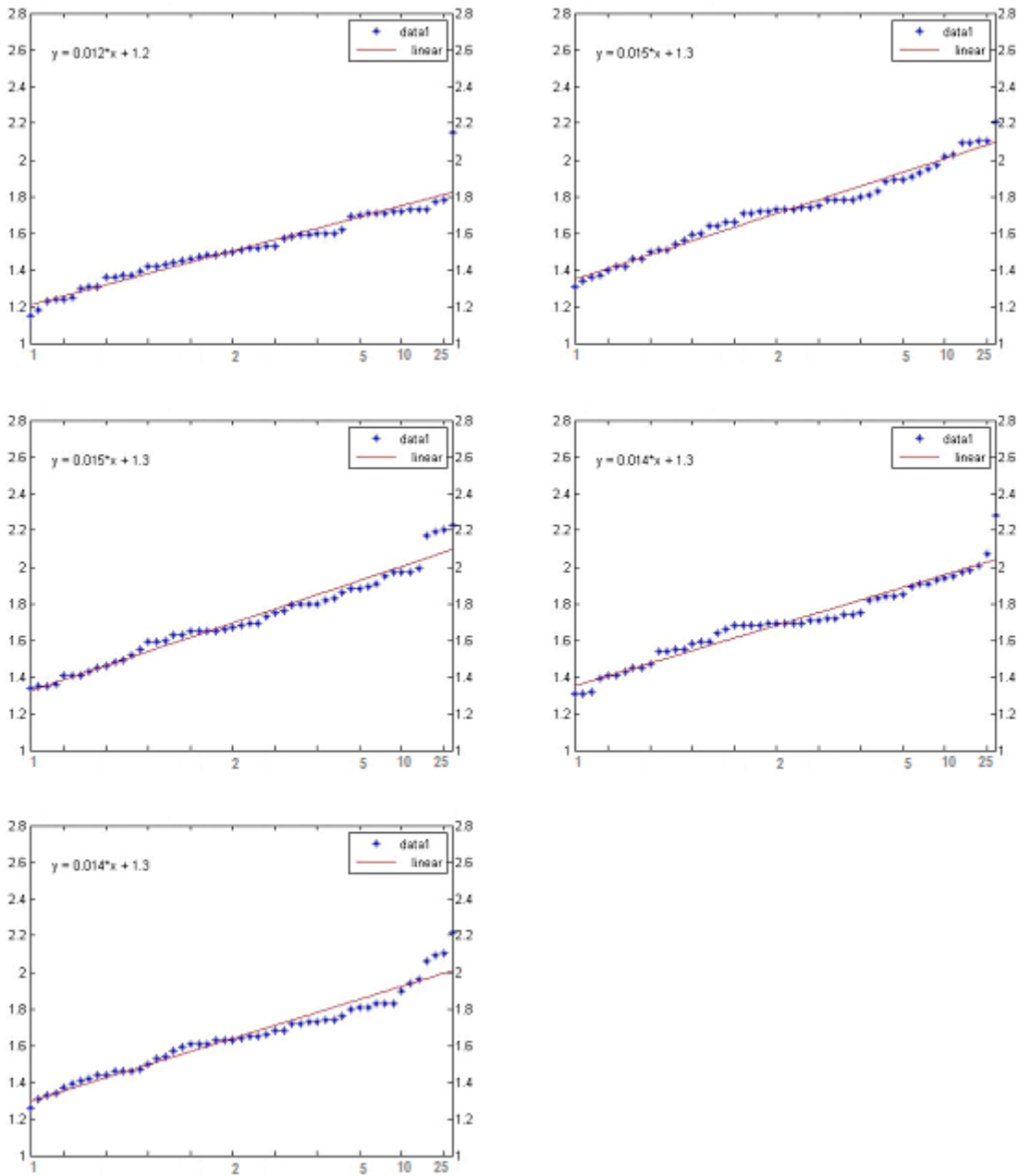


Figure 64. Return period diagram for H_s (m) for locations: Klampenborg, Landskrona, Lundåkra, Malmö, Ven.

Potential sediment transport roses

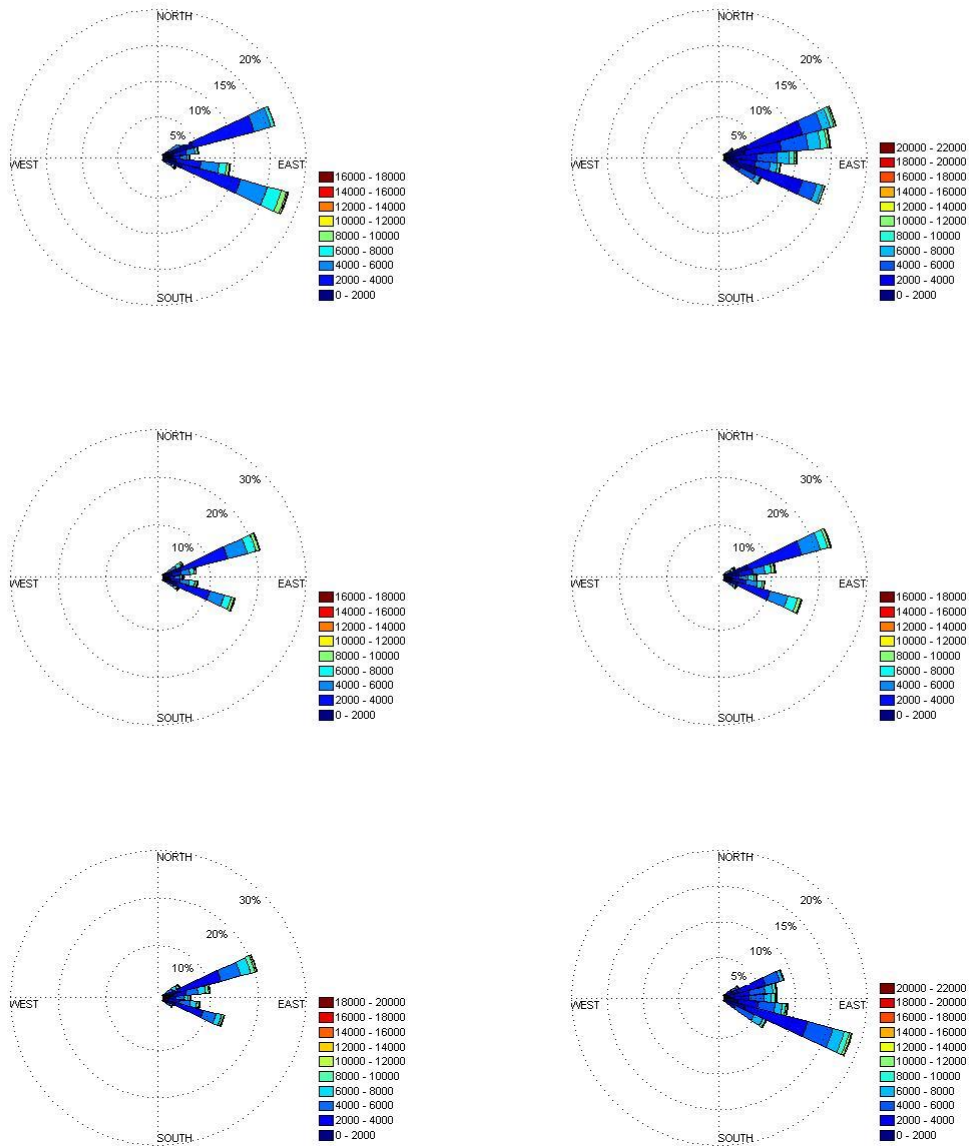


Figure 65. Potential sediment transport for locations 1 to 6. The scale is in m³/year.

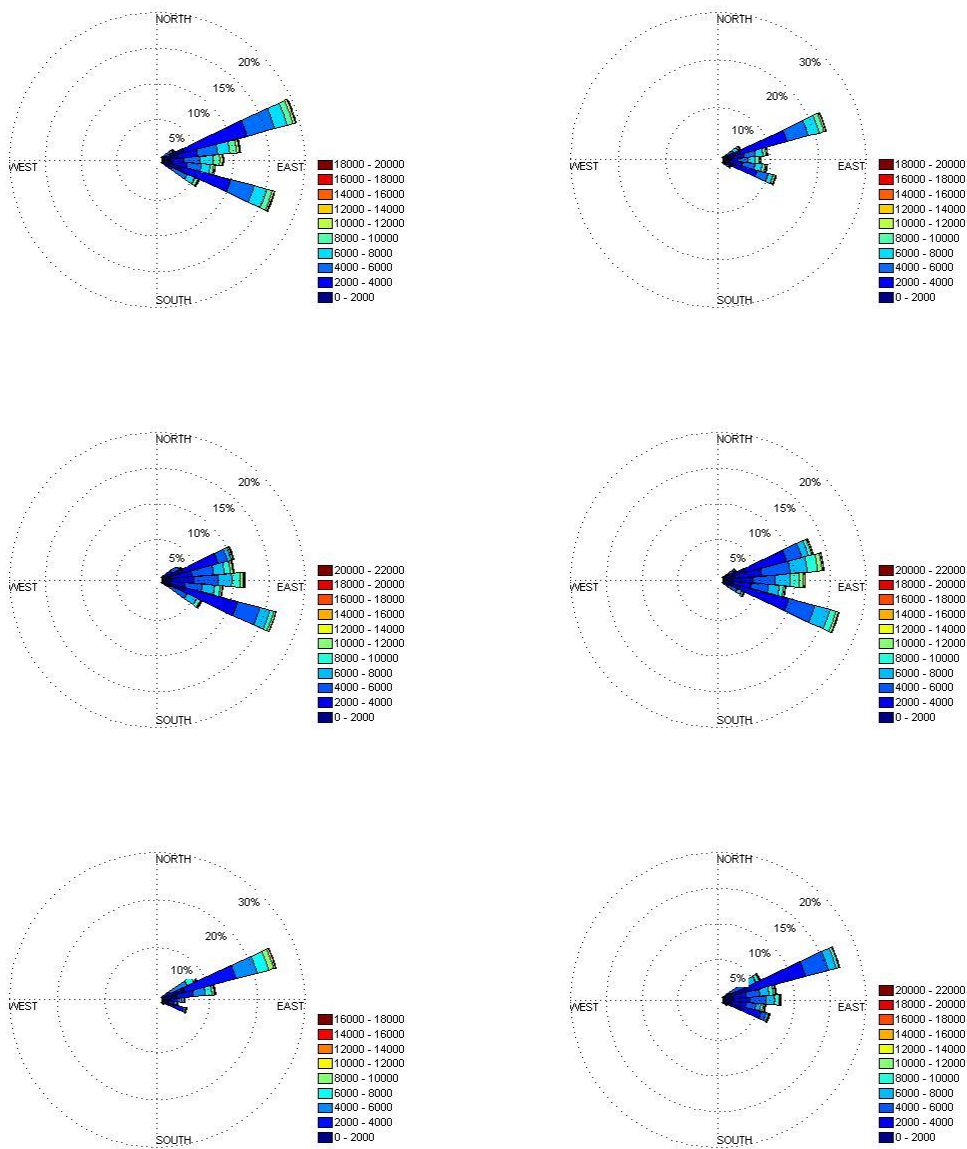


Figure 66. Potential sediment transport for locations 6 to 12. The scale is in $m^3/year$.

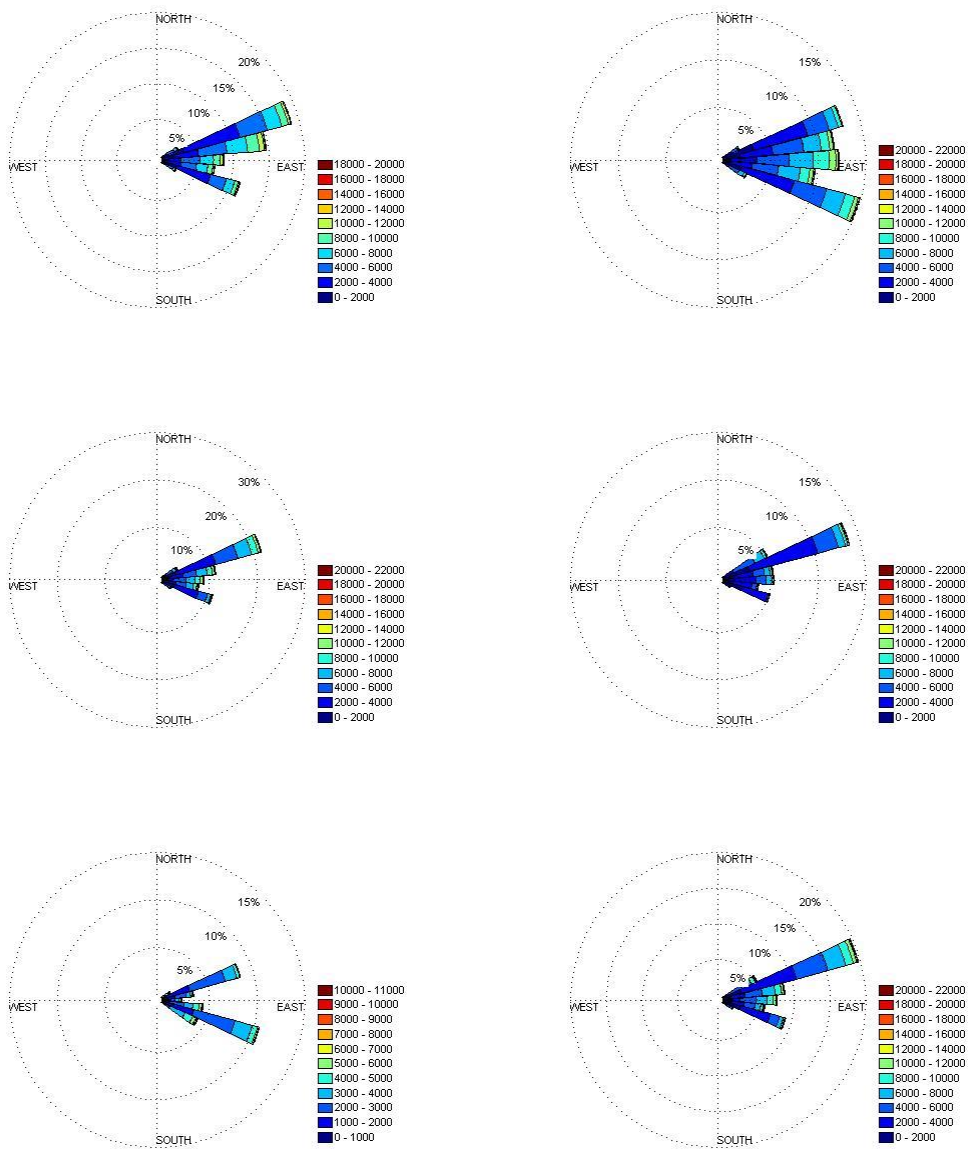


Figure 67. Potential sediment transport for locations 13 to 18. The scale is in $m^3/year$.

MatLab code:

height_extract

```
%% extract values from original significant wave height file: fort.30
fid = fopen('fort.30');
Theight = textscan(fid,'%f','CollectOutput',1); %read the file and put the
values in a cell array
fclose(fid);

%% create vector of wave height for all time and locations
height=cell2mat(Theight); % transform the cell array into a matrix
height (height>=400) = []; %remove the date and time lines of the matrix
height

%% create time/map matrix of wave height
ngx=39; %number of values on x direction
ngy=34; %number of values on y direction
t = 488; %number of time steps
l = ngx*ngy;
Mh = zeros(t,ngy,ngx);
Nh = zeros(ngy,ngx,t);
for i = 1:t
    for j = 1:ngy
        Mh(i,j,1:ngx)=          height((i-1)*l+(ngy-j)*ngx+1:(i-1)*l+(ngy-
j)*ngx+ngx); %creates a map-matrix of the wave height for each time step
        Nh(j,1:ngx,i)=          height((i-1)*l+(ngy-j)*ngx+1:(i-1)*l+(ngy-
j)*ngx+ngx); %same but not ordered in the same way
    end;
end;

%% play the video
implay(Nh) %displays a video of the evolution of the wave heights
```

direction_extract

```
%% extract strings from original fort.40 file
fid = fopen('fort.40');
Tdirection = textscan(fid, '%s', 'delimiter', '\n'); %read the file and put
the values as string in a cell array
Tdirection=char(Tdirection{:}); %transform Tdirection into a character
array
fclose(fid);

%% create vector of wave directions for all time and locations
ngx=39; %number of values on x direction
ngy=34; %number of values on y direction
l=ngx*ngy;
t=488; %number of time steps

Tdirection(1:l+1:end,:) = []; %remove the date and time lines

direction = str2num(Tdirection(:,12:18)); %extract the values of direction
from each string, convert it into a number, and put it in a matrix

%% convert the wave direction into meteorological system
directionfinal = direction;

direction (direction<0.1) = NaN ;
directionfinal (directionfinal<0.1) = NaN ; %replace the 0 by NaN to avoid
the land values
%actual 0 values for direction are assumed to be negligeable considering
%the number of values treated.

directionfinal (directionfinal<=180) = direction (direction<=180) - 180;
%all the values below 180 are lowered by 180 (range now from -180 to 0)
directionfinal (directionfinal>180) = direction (direction>180) - 180; %all
the values above 180 are lowered by 180 (range now from 0 to 180)
directionfinal (directionfinal<=0) = direction (direction<=180) + 180; %all
the values below 0 are shifted above 180 (range now from 180 to 360)

%% create time/map matrix of wave directions
Md = zeros(t,ngy,ngx);
Nd = zeros(ngy,ngx,t);
for i = 1:t
    for j = 1:ngy
        Md(i,j,1:ngx)= direction((i-1)*1+(ngy-j)*ngx+1:(i-1)*1+(ngy-
j)*ngx+ngx); %creates a map-matrix of the wave directions for each time
step
        Nd(j,1:ngx,i)= direction((i-1)*1+(ngy-j)*ngx+1:(i-1)*1+(ngy-
j)*ngx+ngx); %same but not ordered in the same way
    end;
end;

%% play the video
implay(Nd) %displays a video of the evolution of the wave heights
```

```

extract
%% extract wave height from specific points
%this can be done by a subroutine with fortran in postproc, but if height
%is not too big that can be useful to extract directly with matlab,
%especially if WAM is in the middle of a run.

%it is assumed that height_extract and direction_extract have been run
%before.

%location 14 4 Helsingborg
X = 14;
Y =4;
H_14_4 = zeros(t,1);

for i = 1:t
    H_14_4(i) = height((i-1)*l+X+(Y-1)*ngx); %select the values in height
                                                %corresponding to a location
end;

%location 20 13 Malmö
X = 20;
Y =13;
H_20_13= zeros(t,1);

for i = 1:t
    H_20_13(i) = height((i-1)*l+X+(Y-1)*ngx);
end;

%location 15 16 Southern midpoint
X = 15;
Y =16;
H_15_16 = zeros(t,1);

for i = 1:t
    H_15_16(i) = height((i-1)*l+X+(Y-1)*ngx);
end;

%location 15 12 Copenhagen
X = 15;
Y =12;
H_15_12 = zeros(t,1);

for i = 1:t
    H_15_12(i) = height((i-1)*l+X+(Y-1)*ngx);
end;

%% extract wave direction from specific point
%location 14 4 helsingborg
X = 14;
Y =4;
D_14_4 = zeros(t,1);

for i = 1:t
    D_14_4(i) = directionfinal((i-1)*l+X+(Y-1)*ngx); % select values in
                                                %directionfinal corresponding to a location
end;

%location 20 13 Malmö
X = 20;

```

```

Y =13;
D_20_13 = zeros(t,1);

for i = 1:t
    D_20_13(i) = directionfinal((i-1)*l+X+(Y-1)*ngx);
end;

%location 15 16 Southern midpoint
X = 15;
Y =16;
D_15_16 = zeros(t,1);

for i = 1:t
    D_15_16(i) = directionfinal((i-1)*l+X+(Y-1)*ngx);
end;

%location 15 12 Copenhagen
X = 15;
Y =12;
D_15_12 = zeros(t,1);

for i = 1:t
    D_15_12(i) = directionfinal((i-1)*l+X+(Y-1)*ngx);
end;

%% extract map of wave height for a specific time step
time=1;
maph = flipud(Nh(1:ngy,1:ngx,time));

%% extract map of wave direction for a specific time step
time=1;
mapd = flipud(Nd(1:ngy,1:ngx,time));

%% extract percentage of wave for each interval of 50cm
allheight = height;
allheight (allheight<=0.00001) = []; % remove land from allheight

percenth =zeros(1,7); %it is assumed here that no wave height are above 3 m
for i=0:0.5:2.5

percenth(2*i+1)=length(allheight((i+0.5>=allheight)&(allheight>i)))/length(
allheight);
    %assign each element of percenth its value
end
percenth(7)=length(allheight(allheight>3))/length(allheight);

bar(0:0.5:3,percenth) %plot the distribution in a histogram

%% extract percentage of wave for each interval of 45°
alldirections = directionfinal;
alldirections (isnan(alldirections)) = []; %remove all NaN lines i.e. land
corresponding lines

percentd=zeros(1,8);
percentd(1)=length(alldirections((337.5<=alldirections)))/length(alldirecti
ons)+length(alldirections((alldirections<22.5)))/length(alldirections);
for i=1:7

```

```

    percentd(i+1)=length(alldirections((22.5+(i-
1)*45<alldirections)&(alldirections<=67.5+(i-
1)*45)))/length(alldirections);
end

%% Wave height / Wave direction combination
heightdirection = zeros (1*t,2);
heightdirection(:,1) = height(:);
heightdirection(:,2) = directionfinal(:); %put wave height and direction in
the same matrix

selected_h=zeros(1,8);
selected_h(1)=
(sum(heightdirection((337.5<=heightdirection(:,2))))+sum(heightdirection((h
eightdirection(:,2)<22.5)))) /
(length(heightdirection((337.5<=heightdirection(:,2))))+length(heightdirect
ion((heightdirection(:,2)<22.5))));
for i=1:7
    selected_h(i+1) = (sum(heightdirection((22.5+(i-
1)*45<heightdirection(:,2))&(heightdirection(:,2)<=67.5+(i-1)*45)))) /
(length(heightdirection((22.5+(i-
1)*45<heightdirection(:,2))&(heightdirection(:,2)<=67.5+(i-1)*45))));
end
%calculate the average height of the waves for each direction
%(45° intervals)

%% Create a scatter plot of wave heights colored in function of wave
direction

%this run needs two different couples of height and direction matrices.
%here used for the Climate change analysis

heightdirection1 = zeros (1*t,2);
heightdirection1(:,1) = heightclimate(:);
heightdirection1(:,2) = directionfinal(:); %put wave height and direction
from ClimateB in the same matrix

heightdirection2 = zeros (1*t,2);
heightdirection2(:,1) = heightclimateN(:);
heightdirection2(:,2) = directionfinalN(:); %put wave height and direction
from ClimateN in the same matrix

color_heightdir1{1} = [heightdirection1((337.5<=heightdirection2(:,2))) ;
heightdirection1((heightdirection2(:,2)<22.5))];
for i=1:7
    color_heightdir1{i+1} = heightdirection1((22.5+(i-
1)*45<heightdirection2(:,2))&(heightdirection2(:,2)<=67.5+(i-1)*45));
end %regroup the wave heights corresponding to same direction in a vector.
All eight vector are together in a cell array. For ClimateB

color_heightdir2{1} = [heightdirection2((337.5<=heightdirection2(:,2))) ;
heightdirection2((heightdirection2(:,2)<22.5))];
for i=1:7
    color_heightdir2{i+1} = heightdirection2((22.5+(i-
1)*45<heightdirection2(:,2))&(heightdirection2(:,2)<=67.5+(i-1)*45));
end %regroup the wave heights corresponding to same direction in a vector.
All eight vector are together in a cell array. For ClimateN

```



```

hold all %specify to matlab that all the following plot will be displayed
on the same figure
plot(heightdirection2(:,1),heightdirection1(:,1),'*','color','white')
%plot all the wave heights from ClimateB against all the wave heights from
%ClimateN in white. This set of data will be used in the plot tool to
produce a
%global linear trendline.
plot(color_heightdir2{1},color_heightdir1{1},'*', 'color', 'yellow')
plot(color_heightdir2{2},color_heightdir1{2},'*', 'color', 'magenta')
plot(color_heightdir2{3},color_heightdir1{3},'*', 'color', 'cyan')
plot(color_heightdir2{4},color_heightdir1{4},'*', 'color', 'red')
plot(color_heightdir2{5},color_heightdir1{5},'*', 'color', 'green')
plot(color_heightdir2{6},color_heightdir1{6},'*', 'color', 'blue')
plot(color_heightdir2{7},color_heightdir1{7},'*', 'color', 'black')
plot(color_heightdir2{8},color_heightdir1{8},'*', 'color', [1,0.4,0.6])
%plot the wave height from ClimateB corresponding to a certain direction
%against the wave height from ClimateN corresponding to this same direction
xlabel('Wave height ClimateN')
ylabel('Wave height climateB')
legend('','N','NE','E','SE','S','SW','W','NW')

```

direction_height_movie

```
%This routines needs results from the routines height_extract and
%direction_extract.

writerObj = VideoWriter('direction_height.avi');
open(writerObj); %create and open a video object

maximum = max(height()); %select the maximum of all wave heights
M (t) = struct('cdata', {1}, 'colormap', {1}); %create the structure that
will be needed to produce the video
for i=1:t
    maph = Nh(1:ngy,1:ngx,i); %at each time step extract a map of the wave
height from Nh
    maph(1,1) = maximum; %set the top left corner of the map to the global
maximum
    % to ensure that the scale of all the time steps are uniform: from 0 to
global maximum
    imagesc(maph); %create an image of the map
    colormap(hot); %using the colorscale type 'hot' [black red yellow
white]
    hold on; %keep the image and will put above the quiver

quiver(1:39,1:34,cos(Nd(1:ngy,1:ngx,i)*pi/360),sin(Nd(1:ngy,1:ngx,i)*pi/360
),'color','blue');
    %create the quiver i.e. map of arrows of directions

    M(i)= getframe; %put the image in the structure M
    writeVideo(writerObj,M(i)); %produce the video from M step by step
    clf %clear the image before the new iteration of the loop
end

close(writerObj);
```

Fill_in

%% From a non-regular set of data (missing values or extra values), creates a regular timeserie.

```
fid = fopen('Untitled.txt'); %open file
T = textscan(fid, '%s %s %f %f %f'); %extract data to cellarray
fclose(fid);
datestring = strcat(T{1},T{2}); %concatenate date and time into one string
and put it in a vector

date = zeros(1,length(datestring)); %create blank vector, size of
datestring
formatIn = 'yyyymmddHH'; %set the format use to read date and time
for i = 1:length(datestring)
    DateString = datestring(i); %set input of datenum function
    date(i) = datenum(DateString,formatIn); %fill in date with matlab
version of date and time
end

startValue = datenum(1995,1,1,0,0,0); %starting observation
endValue = datenum(1995,07,31,21,0,0); %ending observation
increment = datenum(1995,1,1,3,0,0)-datenum(1995,1,1,0,0,0); %3h
increments
timeserie = startValue:increment:endValue; %desired time points

data = cat(2,timeserie',NaN(length(timeserie),3)); %matrix of time + blank
values

j=1;
for i = 1:length(date)
    while date(i)~= data(j,1) %find the appropriate place for date(i)
        j=j+1;
    end
    data(j,2) = T{3}(i); %fill the values in data
    data(j,3) = T{4}(i);
    data(j,4) = T{5}(i);
end

%final = mat2cell(data,length(timepoints), [1 1 1 1]); %transform to cell
array, maybe not necessary
dlmwrite('data.txt',data); % create the .txt file
```

fort_extract

```
%values from specific points defined in the INPUT file in WAM.

%one should not use this routine in the same workspace than height_extract
%or direction_extract, first the applications are different. But also
%variable names could be in conflict.

%the example below uses fort.50 (height) for 11 locations in Öresund. In
%this order: Helsingborg, Landskrona, Lundakra, Barsebäck, Malmö,
%Faslterbo, Drogden, Copenhagen, klampenborg, Ven, Espergærde.

%% extract values from original file
fid = fopen('fort.50');
T = textscan(fid, '%f', 'CollectOutput', 1); %open and read the file
fclose(fid);

%% create vector of wave height for all time and locations
out=cell2mat(T); %transform the cell array into a matrix

height=zeros(12,length(out)/13); %create a matrix of 12 columns that
%will be the timeserie and the 11 locations' values

height(1,:) = out ((1960000000<=out)); %fill in the timeserie as first
column
out (out>=100000000) = []; %remove the dates an time lines of the matrix
out

%directionfinal = out;
%directionfinal (directionfinal<=180) = out (out<=180) - 180;
%directionfinal (directionfinal>180) = out (out>180) - 180;
%directionfinal (directionfinal<=0) = out (out<=180) + 180;
%out=directionfinal+180;

%this part can be used to transform the output direction from WAM into
%meteorological style direction.

for i = 0:length(out)/11-1 %fill in all the other columns of height
    height(2,i+1) = out(1+i*11); %hbg
    height(3,i+1) = out(2+i*11); %lkn
    height(4,i+1) = out(3+i*11); %ldk
    height(5,i+1) = out(4+i*11); %bbk
    height(6,i+1) = out(5+i*11); %mlm
    height(7,i+1) = out(6+i*11); %ftb
    height(8,i+1) = out(7+i*11); %dgd
    height(9,i+1) = out(8+i*11); %cph
    height(10,i+1) = out(9+i*11); %kbg
    height(11,i+1) = out(10+i*11); %ven
    height(12,i+1) = out(11+i*11); %egd
end
    height=height'; %tanspose hieght
%% Create the return period diagram

X = -log(-log(1-(51:-1:1)/52)); %x-axis for the return period diagram
X2 = 1:1:51; %second x-axis showing the number of the sample
max_year_location = zeros(51,1);
for i=0:50
    max_year_location (i+1) = max(height(floor(i*2922+1):floor((i+1)*2922-
7),2)); %calculate the maximum value for each year, here for Helsingborg
```

```

end
max_year_location = sortrows(max_year_location); %sort the values from
highest to lowest

scatter(X2,max_year_location, '*') %plot has to be with points or stars
(no lines)
%and should have for x-axis: X at the
bottom,
%X2 at the top

h_axes_1 = gca; %find handle for axis this
%is to call that axis later
h_axes_1_position = get(h_axes_1, 'Position'); %find axis position
y_axis_limits = [1 2.8]; %set the limits wanted
ylim ([y_axis_limits(1) y_axis_limits(2)]) %for the plot
x_axis_limits = [1 51];
xlim ([x_axis_limits(1) x_axis_limits(2)])
Bottom_ticks = get(gca, 'XTick'); %Find what values of
%x are been displayed by the figure.
%here create the SAME axis but at the top.
h_axes_2 = axes('Position',h_axes_1_position,...
'XAxisLocation','top',...
'YAxisLocation','right',...
'Color','none');
%make sure that they have the same limits
ylim ([y_axis_limits(1) y_axis_limits(2)])
xlim ([x_axis_limits(1) x_axis_limits(2)])
%what is wanted is to find what is the
%relationship between the x values displayed at the bottom with those that
%are wanted at the top. by looking at the equations:
%
% X = -log(-log( 1-( (52-X2)/52 ) ))
%
%Using that relationship, one can calculate the value of the top axis, and
then
%change it to a string, and finally add it to a cell array to be used as
%new label for the top axis.
for i=1:length(Bottom_ticks)
i_label_num = -log(-log( 1-( (52-Bottom_ticks(i))/52 ) ));
i_label_str = num2str(i_label_num,2);
Top_Label{i} = i_label_str;
end
set(gca, 'XTickLabel',Top_Label)

%% extract percentage of wave for each interval of 10cm
height_at_location = height(:,2); %example done with Helsingborg

percent_location=zeros(1,23);
for i=0:1:21

percent_location(i+1)=length(height_at_location((i/10+0.1>=height_at_locati
on)&(height_at_location>i/10)))/length(height_at_location);
% for each interval, calculate the percentage of wave in it
end
percent_location(23)=length(height_at_location(height_at_location>2.2))/len
gth(height_at_location);
%all the waves above 2.2 m are together (not separated by interval)

percent_location = percent_location'; %transpose the vector

```

```
% Wave height duration for each interval of 10cm

height_at_location = height(:,12);

duration_location=zeros(1,23);
for i=0:1:22

duration_location(i+1)=length(height_at_location(height_at_location>i/10))*
3;
    %calculate the number of hours spent above each height value
end
duration_location = duration_location'; %transpose the vector
```

run_up

```
%This routine calculates the run-up heights and run-up levels.

%height_run-up, direction_runup and peakF have been adapted to the time
%period: from Jan 2001 to Dec 2011.

%% Set global parameters

R = zeros(32136,4); %R will be the run-up heights. 32136 is the number of
                    %time steps between Jan 2001 and Dec 2011
beta = 0.15;       %actually here it is tan(beta)
g = 9.81;
d = [13 24 10 7]; %water depth from the bathymetry file

%% Helsingborg
H0 = height_runup(:,1); %get H0 from the file "fort_extract"
D = direction_runup(:,1); %get D from the file "fort_extract"
teta = cos((D-90-355)*pi/180); %calculate the angle between direction of
%propagation and shoreline
teta (teta<0)= 0; %replace negative values by 0
H0 = sqrt(teta).*H0; %modification of H0 because of the angle
period = 1./peakF(:,1); %get T from the file "fort_extract"
L0 = sqrt(g*d(1)).*period; %calculate the wave length
z = water_level(:,1)./100; %from excel
R(:,1) = beta.*H0./sqrt(H0./L0); %calculate the run-up height
R (isnan(R)) = 0; % replace all the NaN by 0
Rz(:,1) = R(:,1)+z; %create Rz: run-up levels
%% Landskrona
H0 = height_runup(:,2); %get H0 from the file "fort_extract"
D = direction_runup(:,2);
teta = cos((D-90-342)*pi/180);
teta (teta<0)= 0;
H0 = sqrt(teta).*H0;
period = 1./peakF(:,2); %get T from the file "fort_extract"
L0 = sqrt(g*d(2)).*period;
z = water_level(:,2)./100; %from excel
R(:,2) = beta.*H0./sqrt(H0./L0);
R (isnan(R)) = 0;
Rz(:,2) = R(:,2)+z;
%% Malmö
H0 = height_runup(:,3); %get H0 from the file "fort_extract"
D = direction_runup(:,3);
teta = cos((D-90-50)*pi/180);
teta (teta<0)= 0;
H0 = sqrt(teta).*H0;
period = 1./peakF(:,3); %get T from the file "fort_extract"
L0 = sqrt(g*d(3)).*period;
z = water_level(:,3)./100; %from excel
R(:,3) = beta.*H0./sqrt(H0./L0);
R (isnan(R)) = 0;
Rz(:,3) = R(:,3)+z;
%% Falsterbo
H0 = height_runup(:,4); %get H0 from the file "fort_extract"
D = direction_runup(:,4);
teta = cos((D-90-25)*pi/180);
teta (teta<0)= 0;
H0 = sqrt(teta).*H0;
period = 1./peakF(:,4); %get T from the file "fort_extract"
L0 = sqrt(g*d(4)).*period;
z = water_level(:,4)./100; %from excel
```

```
R(:,4) = beta.*H0./sqrt(H0./L0);  
R(isnan(R)) = 0;  
Rz(:,4) = R(:,4)+z;
```


nearshore

```
%This routine calculates the potential sediment transport for specific
%locations.
%The input comes from fort_extract

%% set global parameters
angles = [355 299 350 332 342 244 326 356 306 325 48 50 343 330 1 84 162
25];
%angles of the shore. Pointing: north=0, east=90, south=180, west=270
H = height(:,7); %wave height at location
T = 1./meanf(:,7); %wave period at location
D = direction(:,7); %direction of waves moving toward (angle=0 means the
%wave is moving to the north), at location
angle = angles(18); %angle of the coastline at location
s = 2.6; %sand density/water density

%% Angle creation

teta0 = 360 - (D - (angle+90)); %difference between wave angle and shore
%angle at location
teta0 (cos(teta0*pi/180)<0)= NaN; %replace all the cases where the waves
%are not moving toward the shore by NaN values

%% deepwater conditions
C = 1.56 * T; %calculate the wave speed
L = 1.56 * T.^2; %calculate the wave length
Cg = C / 2; %calculate the group speed
gamma = 0.78; %is arbitrary

alpha = (C./sqrt(9.81*H)).^4 .* (C ./ Cg) * gamma^2;
lambda_a = (cos(pi*teta0/180)./alpha).^(2/5);
epsi = lambda_a .* sin(teta0*pi/180).^2;
delta = 1 + 0.1649 * epsi + 0.5948 * epsi.^2 - 1.6787 * epsi.^3 + 2.8573 *
epsi.^4;
lambda = delta .* lambda_a;

hb = lambda .* C.^2 / 9.81; %compute water depth at breaking
Hb = gamma * hb; %wave height at breaking
teta_b = asin(sin(teta0*pi/180).* sqrt(lambda))*180/pi; %wave angle at
%breaking

hb(isnan(hb))=0; %replace all NaN values by 0
Hb(isnan(Hb))=0; %replace all NaN values by 0

sediment{1,1}(:,18) = Hb(:); %store results in a cell array
sediment{1,2}(:,18) = hb(:);
sediment{1,3}(:,18) = teta_b(:);
%% CERC formula for the transport
%calculate the potential sediment transport using the CERC formula
sediment{1,4}=(sediment{1,1}.^(5/2)).*sin(2*sediment{1,3}*pi/180)*0.023/(s-
1)*9.81^0.5;
sediment{1,4}(isnan(sediment{1,4}))=0;
```

